ABSTRACT

Analysis of Deposition, Erosion, and Landscape Stability during the Late Quaternary Using Multi-Proxy Evidence from Owl Creek, Central Texas, USA

Holly A. Meier, Ph.D.

Mentor: Lee C. Nordt, Ph.D.

Episodes of fluvial deposition and incision preserved in Quaternary sediments are valuable archives of environmental change, but have been understudied in low order streams in central Texas, USA. An exposure along Owl Creek a tributary of the Brazos River was examined using geological and pedological approaches, including stratigraphic and soil description and characterization. Eight stratigraphic units were identified, described, and constrained in time based on relative stratigraphy and optically stimulated luminescent (OSL) ranging in age from ~120 ka to <8 ka. Despite the dynamic nature of fluvial systems, the Owl Creek record has uniquely preserved sediment spanning the late Quaternary with major erosional events that may reflect the advance and retreat of the Laurentide ice sheet and the southward displacement of the jet stream and ensuing wetter conditions as recorded by regional climate proxies. Compilation of the proxies presented shows evidence for a cooler and wetter late Pleistocene climate, followed by a warmer and drier climate dominating during the Holocene. Regional proxies become more

abundant into the Holocene with Owl Creek and other local stream preserving sediment of different ages and are likely responding to intrinsic variables.

Buried soils formed in association with low-order tributary streams are valuable archives of past climates, but have not been studied extensively in central Texas, USA. Four buried soils exposed along Owl Creek, within the larger Brazos River drainage basin, were examined using soil morphology and micromorphology, optically stimulated luminescence (OSL) dating, soil characterization, whole-soil geochemical and stable isotope analyses of soil organic matter and pedogenic carbonate. These buried soils provide a record of changes in paleoecological and paleo-alluvial conditions spanning ~14 ky. Morphological and geochemical differences between buried soils reflect changes in landscape attributable to climate, with a distinct 5‰ increase in δ13C values of soil organic matter corresponding to the onset of drier conditions during the Holocene. Paleoecological reconstructions coupled with depth to Bk horizon suggest possible amounts of erosion of ~1 m for each of the buried soils.

Analysis of Deposition, Erosion, and Landscape Stability during the Late Quaternary Using Multi-Proxy Evidence from Owl Creek, Central Texas, USA

by

Holly A. Meier, B.A., M.A.

A Dissertation

Approved by the Department of Geology

____
Lee C. Nordt, Ph.D., Chariperson

Submitted to the Graduate Faculty of
Baylor University in Partial Fulfillment of the
Requirements for the Degree
of
Doctor of Philosophy

Approved by the Dissertation Committee

____
Lee C. Nordt, Ph.D, Chairperson

____
Steve G. Driese, Ph.D.

____
Stephen I. Dworkin, Ph.D.

____
Peter M. Allen, Ph.D.

____
Gattett W. Cook, Ph.D.

Accepted by the Graduate School
May 2014

____
J. Larry Lyon, Ph.D., Dean

Page bearing signatures is kept on file in the Graduate School.

TABLE OF CONTENTS

LIST OF FIGURES

Figures Page

LIST OF TABLES

ACKNOWLEDGEMENTS

I would like to thank my committee, family, and friends. Special thanks to: Dr. Steven Forman; Dr. Brit Bousman; and to Paulette Penney. Thank you to Quaternary International and Catena, both Elsevier Journals, for permission to include Chapter 2 (Meier at al., 2013) and Chapter 3 (Meier et al., 2014) in this dissertation.

"In the temple of science are many mansions…and various indeed are they that dwell therein and the motives that have led them there."

—Albert Einstein

CHAPTER ONE

Introduction

The analysis of the alluvial history along modern fluvial systems has proven to be a viable option for the understanding of the periods of environmental stability and flux during the late Quaternary (Bettis and Mandel, 2002; Holliday 1989a, 1989b; Knox, 1996, 2000; Mandel, 1995; Nordt, 1992, 1993, 2004; Waters and Nordt, 1995). Periods of environmental fluctuation are characterized by deposition, erosion, and landscape stability and used to interpret environments of deposition, episodes of soil formation, and changing climates.

Owl Creek, a low-order stream in central Texas, has provided to be an ideal natural laboratory for this purpose. The stratigraphy and depositional chronology interpreted for Owl Creek has helped to decipher climate shifts and environments of deposition in central Texas spanning the past ~120 ka (Meier et al., 2013). Dynamic fluvial environments, such the Owl Creek study site, can be reconstructed using multi-proxies and to partion extrinsic from intrinsic forcing mechanisms (Meier et al., 2014). The unique location of Owl Creek, on the Fort Hood Military Reservation, provides an opportunity to examine the human-landscape interaction by drawing upon the previous research (excavations and surveys) during the Prehistoric periods in central Texas.

The purpose of the research is to chronicle the depositional history of Owl Creek as detailed in Chapter Two “Late Quaternary alluvial history of the middle Owl Creek drainage basin in central Texas: A record of geomorphic response to environmental change.” Additional goals are presented in Chapter Three “Interpretation of Late Quaternary climate and landscape variability based upon buried soil macro- and micromorphology, geochemisty, and stable isotope of soil organic matter, Owl Crek, central Texas, USA” and presents archives preserved in the buried soils at Owl Creek. Chapter Four presents the composite alluvial history of Owl Creek in “Late Quaternary alluvial history of Owl Creek, central Texas USA: Aggradation and degradation in the past 50 ka.”

CHAPTER TWO

Late Quaternary alluvial history of the middle Owl Creek drainage basin in central Texas: A record of geomorphic response to environmental change

This chapter published as: Meier, H.A., Nordt, L.C., Forman, S.L., Driese, S.G., 2013. Late Quaternary alluvial history of the middle Owl Creek drainage basin in central Texas: a record of geomorphic response to environmental change. Quat. Int. 306, 24–41.

Abstract

Episodes of fluvial deposition and incision preserved in Quaternary sediments are valuable archives, but have been understudied in low order streams in central Texas, USA. An exposure along Owl Creek a tributary of the Brazos River was examined using geological approaches and pedological, including stratigraphy and soil description and characterization. Eight stratigraphic units were identified, described, and constrained in time based on relative stratigraphy and optically stimulated luminescent (OSL) ranging in age from ~120 ka to <8 ka. Despite the dynamic nature of fluvial systems, the Owl Creek record has uniquely preserved sediment spanning the late Quaternary with major erosional events that may reflect the advance and retreat of the Laurentide ice sheet and the southward displacement of the jet stream and ensuing wetter conditions. Regional proxies become more abundant into the Holocene with Owl Creek and other local stream preserving sediment of different ages and are likely responding to intrinsic variables.

1. Introduction

There is a rich record of late Quaternary environmental change in fluvial terrace sequences of river systems in Texas (Blum and Valastro, 1989, 1992; Blum et al., 1994;

Waters and Nordt, 1995; Nordt et al., 2002; Nordt, 2004; Mandel et al., 2007; Hall et al., 2012). These rivers are hypothesized to have responded to a combination of changes in global sea-level, varying sediment supply, and discharge during glacial to interglacial climate changes in the past ca. 22 ka. Records of deposition prior to this time are typically based on relative chronological order of sedimentary units and degree of soil formation. Consequently, there is limited under- standing of the geomorphic response of river systems in central Texas during the late Pleistocene. There were large climate changes in North America with the advance and retreat of the Laurentide ice sheet and associated sea level changes (Kutzbach and Guetter, 1986; Bromwich et al., 2004, 2005) that may have variably affected fluvial systems (Schumm, 1999). Owl Creek is an ideal drainage basin in central Texas to study because it is a first-order tributary within the larger Brazos River drainage basin, and it contains alluvial exposures that span the late Pleistocene. Previously Nordt (1992) identified 5 alluvial stratigraphic units in the Owl Creek drainage basin. The deposits were bracketed by radiocarbon ages and by correlation to radiocarbon- dated deposits along Cowhouse Creek (Nordt, 2004). Identified alluvial units are the Jackson (~15,000 BP), Georgetown (~11,000-9000 BP), Fort Hood (8000-4800 BP), West Range (4300-600 BP) and Ford (<400 years). This study provided a general spatial and temporal fluvial interpretation, but did not address older alluvial deposits along Owl Creek.

The focus of this study is to provide new insights on a late Pleistocene landscape evolution preserved in an expansive exposure of alluvial deposits along Owl Creek (Red Bluff). The objectives were to: (1) map and describe the sequence of unconformable stratigraphic units, (2) chronologically constrain the units using stratigraphic relationships and optically stimulated luminescence (OSL) dating, (3) reconstruct environments of deposition, (4) infer possible extrinsic and intrinsic factors that effected fluvial deposition and erosion, and (5) compare the interpreted record to other fluvial time-series within the region. The data from Owl Creek coupled with other Pleistocene and Holocene fluvial records provide an a framework to further evaluate regional stream erosion and depositional events in the past ca. 120 ka and reference to changes in sea level, ice sheet configuration and changing climate conditions.

2. Regional setting

The upper and middle Owl Creek drainage basin is located on the Fort Hood Military Reservation and covers approximately 72 km^2 of surface area (Fig. 1). The Owl Creek channel has a gradient of 3.4 m km-1 with a sinuosity of 1.1 and is interpreted as a bedload-dominated, straight to meandering stream (Nordt, 1992).

One expansive outcrop is studied along Owl Creek, referred to as Red Bluff. Red Bluff is approximately 14 m high and 80 m wide on the southern bank of Owl Creek (Fig. 2). The adjacent uplands on the south side of the valley average 250 m elevation, with the study site at 214 m elevation and the active floodplain at 200 m elevation.

The oldest geologic unit exposed in the area is the Cretaceous- aged Walnut Clay Formation, which occurs in the low lands and is incised by Owl Creek (Barnes, 1970). The Edwards Limestone forms the uplands within the Owl Creek basin. There are a series of alluvial terraces previously identified, but undated in the study area (Nordt, 1992).

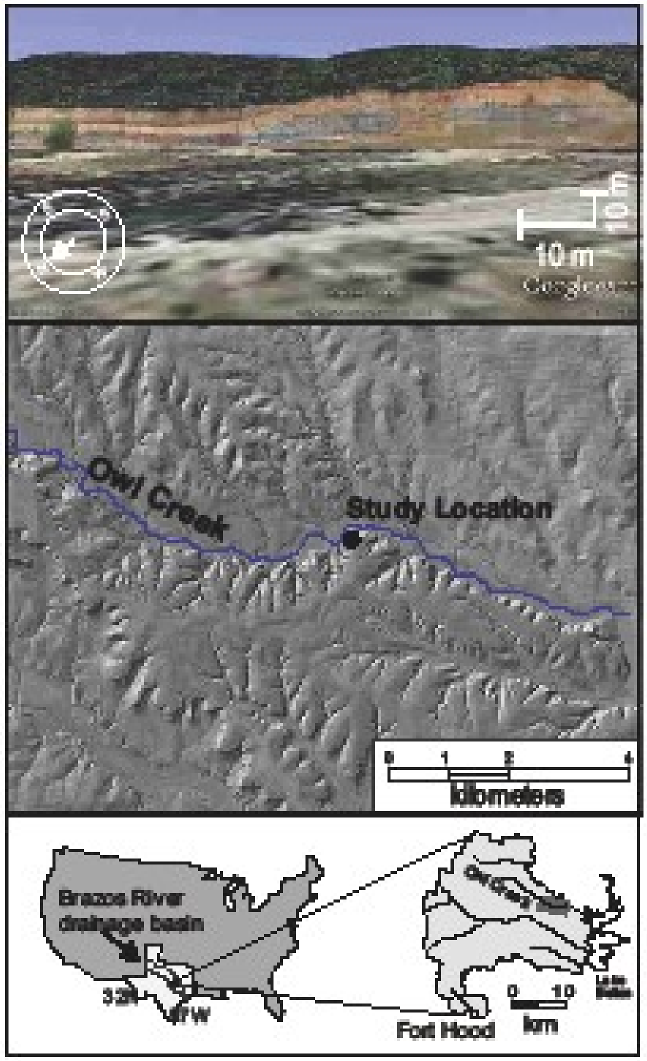

Fig. 2.1. Google Earth image of the Owl Creek with a photo overlay of the outcrop. Note the major unconformity between the Walnut Clay (greyish) and the overlying alluvium and modern channel flow is from south to east. The geographical location of the study site in the Brazos River drainage basin and the digital elevation model (DEM), show the location of study site along Owl Creek on the Fort Hood Military Reservation in central Texas.

The modern climate of the area is subhumid with hot summers and short and dry winters (Huckabee et al., 1977; Bomar, 1983). The mean annual precipitation is approximately 86 cm, with peak rain- fall occurring in the late spring and early fall (Huckabee et al., 1977). The average maximum August temperature is 40 ºC with a January maximum monthly average of 25.5 ºC (Huckabee et al., 1977). The area is dominated by grasslands and motts of trees along hillslopes bisected by alluvial valleys (Bomar, 1983). The upland soils in the Owl Creek drainage basin are mapped as the Real-Rock and Eckrant-Rock series and are classified as loamy-skeletal, carbonatic, thermic, shallow Typic Calciustolls and clayey-skeletal, smectitic, thermic Lithic Haplustolls. The active floodplain soils are mapped as the Topsey and Lewisville series and are classify as fine-loamy, carbonatic, thermic Udic Calciustolls and fine-silty, mixed, active, thermic Udic Calciustolls (Soil Survey Staff, 2012). These soils are carbonate-rich and appear to have formed under grasslands with mollic epipedons.

3. Methods

3.1. Facies and depositional units

Six vertical profiles were selected from the Owl Creek study area to capture all of the observed depositional units and buried soils. Lithologic characteristics described in the field include grain size, grain and cement type, sedimentary structures, stratal thickness, and bounding relations. These data were used to characterize facies and interpret depositional style and environments (cf. Miall, 1992) (Table 2.1).

Table 2.1. Facies codes, sediment texture, and diagnostic features identified at Owl Creek (based upon Miall, 1978).

Facies Code	Sediment	Features
Gm	Gravels	unstratified; subrounded poorly sorted gravels; matrix supported
Gt	Gravels	trough cross-beds; poorly to moderately well- sorted gravels; clast-supported
Gs	Gravels	broad, shallow gravel lense scours
Gl	Gravels	low-angle (<10^{o}) cross-beds; moderately well-sorted pebbles to gravels; matrix-supported
Ss	Sands	broad, shallow, fine sand lens scour fills
St	Sands	trough cross-beds; fine- to medium sand; well- sorted
Fm	Fines	massive to bioturbated fines
Fh	Fines	horizontally laminated; fines with few pebbles

Depositional units are defined for strata at Owl Creek using a non-genetic and scale-independent methodology. These units are identified at the study site according to bounding sedimentary unconformities and are partitioned by interpreting episodes of deposition, erosion, and soil formation. The units at Owl Creek are ordered, from oldest to youngest (Q1 through Q8, respectively), based on cross-cutting relationships and the law of superposition, and then by OSL ages (Fig. 2.3).

3.2. Paleosol description and analysis

Soil and buried soil profiles were described according to USDA- NRCS (U.S. Department of Agriculture-Natural Resource Conservation Service) standards noting horizon designation, texture, structure, color, redoximorphic features, reaction to HCl, pedogenic calcium carbonate segregations, and roots (Soil Survey Staff, 1996; Schoeneberger et al., 2002). Bulk samples were collected from each profile and associated parent materials for laboratory analysis. The pipette method (Soil Survey Staff, 2010) was used to determine particle size distributions with texture modifies, such as gravelly, following the USDA-NRCS criteria (Schoeneberger et al., 2002). The pipette method (Soil Survey Staff, 2010) was used to determine particle size distributions and the Shimadzu carbon analyzer was employed for measuring organic carbon (OC) and inorganic carbon (IC) content (See Table 2.4).

Relative maturity of the surface and buried soils was estimated using horizon development based on pedogenic carbonate morphology (Table 2.2) (e.g. Cleveland et al., 2007). Horizon thickness was not considered for buried soil maturity due to the possibility of profile truncation. Buried soil development was used in this study to estimate intervals of non-deposition and soil formation, and to determine the associated depositional hiatus. Surface soils were classified to the taxonomic subgroup level, whereas buried soils were not because of possible soil truncation of surface horizons (Soil Survey Staff, 2010).

Table 2.2. Soil and buried soil relative maturity index. Soils have A horizons while buried soils were classified with AB horizons due to possible erosion during burial.

Relative Soil Maturity Index	Horizon Sequence	Other Comments
1	A or AB-Bw -BC	development of subsurface horizon with ped structure (Bw) and no calcium carbonate accumulation; poorly developed.
2	A or AB-Bk	development of carbonate-rich horizon with pedogenic filaments and nodules (stage I and/or stage II); may have associated Bw, may have weak to distinct slickensides (Bss) and/or multiple associated Bk horizons; moderately developed.
3	A or AB-Bkm	presence of a indurated horizon with laminar cap (stage IV); well-developed.

Stages of calcium carbonate development were classified ac- cording to Gile et al. (1966) where: stage I consists of thin filaments or discontinuous coatings on clasts; stage II contains both soft and hard carbonate nodules or thick clast coatings; stage III consists of a continuous and lithified layer of carbonate nodules; and stage IV consists of a massive carbonate-enriched zone with a laminar cap (Gile et al., 1966). Stage I and II are typically described as Bk horizons in the field and Stage III and IV as Bkm horizons. Non- pedogenic carbonate is present in the fine-earth fraction (<2 mm diameter) as detritus deposited during flooding.

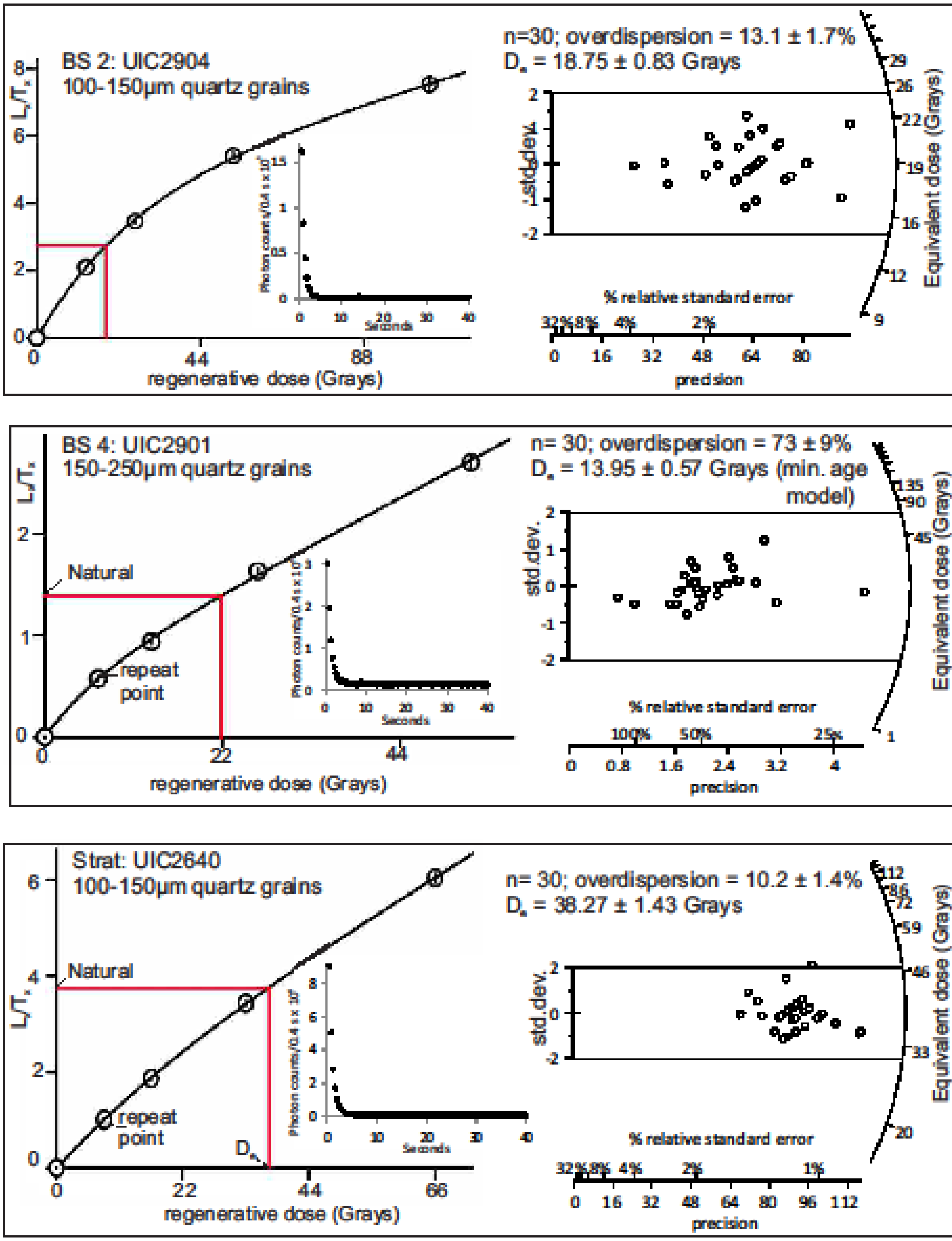

Fig. 2.2. Single aliquot regeneration (SAR) dose response curve, with inset figure showing representative shine down curve and radial plot of equivalent dose values for samples UIC2640, 2649 and 2647.

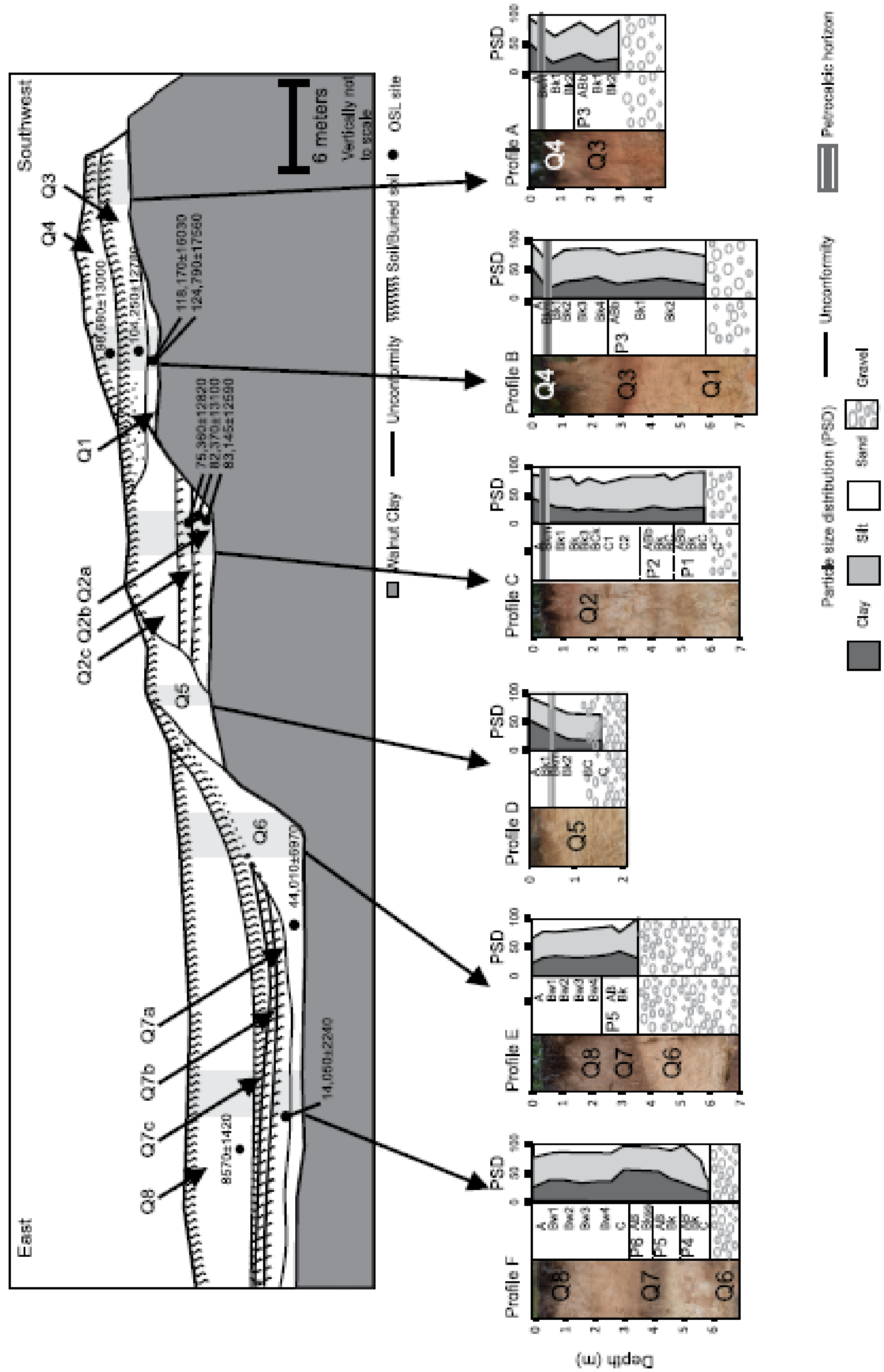

Fig. 2.3. Measured panoramic cross-section of Red Bluff along Owl Creek showing distribution of depositional units, profile locations, and OSL ages. Profiles show soil horizonation and particle size distribution (PSD). (For interpretation of the references to colour in this figure legend, the reader is referred to the web version of this article.)

3.3. OSL dating

Recent advances in optically-stimulated luminescence (OSL) dating (Murray and Wintle, 2003; Wintle and Murray, 2006; Rittenour et al., 2007) for carefully selected fluvial sediments, usually low-energy facies, that yield numerical ages that are well beyond limits of radiocarbon dating, making Owl Creek ideal. Ten samples for OSL dating were taken from non- or mildly pedogenically modified sediments to avoid specifically bioturbated soils. Samples were taken from a freshly cleaned surface using copper tubes 15 cm long and 2.5 cm in diameter driven into the pit face with a hammer, accompanied by the collection of associated bulk samples for geochemical analysis and processed at the Luminescence Dating Research Laboratory at the University Illinois at Chicago. In this study, single aliquot regenerative (SAR) protocols yielded individual OSL ages by averaging ~30 separate, equivalent doses from respective aliquots of quartz grains (Murray and Wintle, 2003). This is followed by the application of central age and minimum age models (Galbraith et al., 1999). The soil water content (by weight) is estimated for the cumulative period of burial of these samples and partially reflects the presence of fine-grained sediments in an alluvial setting. Optical ages are reported in years prior to AD 2010 (See Table 2.3).

Single aliquot regeneration (SAR) protocols (Murray and Wintle, 2003) were used in this study to estimate the apparent equivalent dose of the 63-100, 100-150 or 150-250 mm quartz fraction for 25-30 separate aliquots (Table 2.3). Each aliquot contained approximately 100-500 quartz grains corresponding to a 2.0 mm circular diameter of grains adhered (with silicon) to a 1 cm diameter circular aluminum disc. This aliquot size was chosen to maximize light output for the natural with excitation; smaller aliquots often yielded insufficient emissions (<400 photon counts/s). The sands analyzed were mineralogically mature with SiO_2 content of 78%-95% of the non-carbonate fraction and are predominantly (>80%) well-sorted quartz grains. The quartz fraction was isolated by density separations using the heavy liquid Naepolytungstate, and a 40-min immersion in HF (40%) was applied to etch the outer ~10 mm of grains, which is affected by alpha radiation (Mejdahl and Christiansen, 1994). Quartz grains were rinsed finally in HCl (10%) to remove any insoluble fluorides. The purity of quartz separate was evaluated by petrographic in- spection and point counting of a representative aliquot. Samples that showed >1% of non-quartz minerals were retreated with HF and rechecked petrographically. The purity of quartz separates was tested by exposing aliquots to infrared excitation (1.08 W from a laser diode at 845 ± 4 nm), which preferentially excites feldspar minerals. Samples measured showed weak emissions (<200 counts/s), at or close to background counts with infrared excitation, and ratio of emissions from blue to infrared excitation of >20, indicating a spectrally pure quartz extract (Duller et al., 2003).

An Automated Risø TL/OSL-DA-15 system (Botter-Jensen et al., 2000) was used for SAR analyses. Blue light excitation (470 ± 20 nm) was from an array of 30 light-emitting diodes that deliver ~15 mW/cm^2 to the sample position at 90% power. Optical stimulation for all samples was completed at an elevated temperature (125 ºC) using a heating rate of 5 ºC/s. All SAR emissions were integrated over the first 0.8 s of stimulation out of 40 s of measurement, with background based on emissions for the last 30- to 40-s interval. The luminescence emission for all quartz sands showed a dominance of a fast component (cf. Murray and Wintle, 2003) with >90% diminution of luminescence after 4 s of excitation with blue light.

Table 2.3. Optically stimulated luminescence (OSL) ages on quartz grains from fluvial sediments Owl Creek, Texas. Ages are shown with two-sigma error and calculated using the central age model with Q7 & Q8 ages calculated using the minimum age model (Galbraith et al., 1999).

Sample #	Depth (m)	Laboratory number	Aliquots	Grain size (µm)	Equivalent dose (Gray) [a]	Over-dispersion (%) [b]	U (ppm) [c]	Th (ppm) [c]	K_2O (%) [c]	H_2O (%)	Cosmic dose (mGray/yr) [d]	Dose rate (mGray/yr)	OSL age (yr) [e]
Q8	1.9	UIC2900	25	150-250	11.94 ± 0.46	86.5 ± 10.4	2.6 ± 0.1	3.7 ± 0.1	0.49 ± 0.01	5 ± 2	0.18 ± 0.02	1.20 ± 0.06	8570 ± 1420 [f]
Q7	4.7	UIC2901	30	150-250	13.95 ± 0.57	72.9 ± 9.5	2.6 ± 0.1	4.0 ± 0.1	0.30 ± 0.01	25 ± 5	0.12 ± 0.01	1.09 ± 0.05	14,050 ± 2240 [f]
Q6	5.0	UIC2640	30	100-150	38.27 ± 1.43	10.2 ± 1.4	2.3 ± 0.1	3.5 ± 0.1	0.23 ± 0.01	25 ± 5	0.11 ± 0.01	0.97 ± 0.05	44,010 ± 6970
Q4	4.0	UIC2649	30	63-100	143.30 ± 6.50	15.5 ± 2.0	2.5 ± 0.1	5.1± 0.1	0.65 ± 0.01	10 ± 3	0.13 ± 0.01	1.52 ± 0.08	94,245 ± 13678
Q4	4.0	UIC2649b	30	63-100	147. 25 ± 5.33	9.0 ± 1.4	2.5 ± 0.1	5.1± 0.1	0.65 ± 0.01	10 ± 3	0.13 ± 0.01	1.52 ± 0.08	98,680 ± 13000
Q3	2.2	UIC2638	30	150-250	169.32 ± 8.61	17.8 ± 2.3	2.8 ± 0.1	5.7± 0.1	0.75 ± 0.01	10 ± 3	0.16 ± 0.01	1.66 ± 0.08	102,095± 15420
Q3	2.2	UIC2638b	24	150-250	172.90 ± 4.39	10.2 ± 1.8	2.8 ± 0.1	5.7± 0.1	0.75 ± 0.01	10 ± 3	0.16 ± 0.01	1.75 ± 0.08	104,250 ± 12780
Q2	5.0	UIC2645	30	63-100	125.49 ± 7.18	21.1 ± 2.8	2.5 ± 0.1	6.0± 0.1	0.66 ± 0.01	10 ± 3	0.11 ± 0.01	1.57 ± 0.08	79,710 ± 12820
Q2	6.5	UIC2643	30	63-100	118.43 ± 7.08	19.1 ± 2.5	2.3 ± 0.1	5.0± 0.1	0.53 ± 0.01	5 ± 2	0.12 ± 0.01	1.44 ± 0.07	82,370 ± 13100
Q2	6.0	UIC2646	28	63-100	137.48 ± 7.59	22.0 ± 3.0	2.6 ± 0.1	5.8± 0.1	0.64 ± 0.01	5 ± 2	0.11 ± 0.01	1.65 ± 0.08	83,145 ± 12590
Q1	6.5	UIC2647	30	63-100	202.12 ± 8.85	22.6 ± 3.0	2.5 ± 0.1	6.0 ± 0.1	0.73 ± 0.01	5 ± 2	0.10 ± 0.01	1.71 ± 0.08	118,170 ± 16030
Q1	6.5	UIC2650	30	63-100	165.99 ± 7.62	17.7 ± 2.3	2.0 ± 0.1	4.0 ± 0.1	0.59 ± 0.01	5 ± 2	0.10 ± 0.01	1.42 ± 0.07	124,790 ± 17560

[a]Quartz fraction analyzed under blue-light excitation (470 ± 20 nm) by single aliquot regeneration protocols (Murray and Wintle, 2003). Each aliquot contained between 100 and 500 grains in a 2 mm plate diameter.
[b]Values reflect precision beyond instrumental errors; values of ≤ 25% indicate low dispersion in equivalent dose values.
[c]U, Th and K_20 content analyzed by inductively coupled plasma-mass spectrometry analyzed by Activation Laboratory LTD, Ontario, Canada.
[d]From Presott and Hutton (1994).
[e]Ages calculated using the central age model of Galbraith et al. (1999).
[f] Ages calculated using the minimum age model of Galbraith et al. (1999).
All errors are at two-sigma and include systematic and random errors.
Ages are from the reference year AD 2010.

A series of experiments was performed to evaluate the effect of preheating at 180, 200, 220, 240 and 260 °C on isolating the most robust time-sensitive emissions and thermal transfer of the regenerative signal prior to the application of SAR dating protocols (cf. Murray and Wintle, 2003). These experiments entailed giving a known dose (20 Gy) and evaluating which preheat resulted in recovery of this dose. There was concordance with the known dose (20 Gy) for preheat temperatures above 200 ºC with an initial preheat temperature used of 220 ºC for 10 s in the SAR protocols. A "cut heat" at 160 ºC for 10 s was applied prior to the measurement of the test dose and a final heating at 280 º C for 40 s was applied to minimize carryover of luminescence to the succession of regenerative doses. A test for dose reproducibility was also performed following procedures of Murray and Wintle (2003) with the initial and final regenerative dose of 9.8 Gy yielding concordant luminescence responses (at one-sigma error).

Calculation of equivalent dose by the single aliquot protocols was accomplished for 30 to 25 aliquots (Table 2.3). For most samples all aliquots were used for the final (De) distribution and age determination; only seven aliquots (out of 300) were removed from analysis because the recycling ratio was not between 0.90 and 1.10 or the zero dose was >5% of the natural emissions. Equivalent dose (De) distributions, except for samples UIC2900 and UIC2901, were log normal and exhibited overdispersion values $\leq$20% (at one-sigma errors) (Table 2.3). An overdispersion percentage of a De distribution is an estimate of the relative standard deviation from a central De value in context of a statistical estimate of errors (Galbraith et al., 1999; Galbraith and Roberts, 2012). A zero overdispersion percentage indicates high internal consistency in De values with 95% of the De values within 2s errors. Overdispersion values $\leq$20% are routinely assessed for quartz grains that are well solar reset, like eolian sands (e.g., Olley et al., 2004; Wright et al., 2011) and this value is considered a threshold metric for calculation of a De value using the central age model of Galbraith et al. (1999). Overdispersion values >20% indicate mixing or grains of various ages or partial solar resetting of grains; the minimum age model (three parameters) may be an appropriate statistical treatment for such data and weights for the youngest De distribution (Galbraith et al., 1999), and this model was used for quartz extracts for UIC2900 and UIC2901 with over- dispersion values of >70% (Table 2.3). One apparent OSL age was also determined using ultra-small aliquots (3-6 grains) for quartz grains from UIC2900 to evaluate the accuracy of ages by larger aliquots using the minimum age model (e.g., Duller, 2008). OSL ages from units Q2, Q3, and Q4 (UIC2646, UIC2643, UIC2645, UIC2638, UIC2638b, UIC2649, UIC2649b) are derived from a regenerative dose response that is at or below 20% of the saturation dose and may be near the upper limit of the technique. OSL ages for these units overlap at two-sigma and may indicate deposition within ca. 15-20 ka.

A determination of the environmental dose rate is a needed to render an optical age, which is an estimate of the exposure of quartz grains to ionizing radiation from U and Th decay series, 40K, and cosmic sources during the burial period (Table 2.3). The U and Th content of the sediments, assuming secular equilibrium in the decay series and 40K, were determined by inductively coupled plasma-mass spectrometry (ICP-MS) analysed by Activation Laboratory LTD, Ontario, Canada. The beta and gamma doses were adjusted according to grain diameter to compensate for mass attenuation (Fain et al., 1999). A significant cosmic ray component between 0.10 and 0.18 mGy/yr was included in the estimated dose rate taking in to account the current depth of burial (Prescott and

Hutton, 1994). A moisture content (by weight) of 5 ± 2%, or 25 ± 5 was used in dose rate calculations, which reflects the variability in current field moisture conditions. Fig. 2.2 shows representative SAR dose response curves and corresponding radial plots for samples UIC2640, UIC2649, and UIC2647.

4. Depositional units and chronostratigraphy

The stratigraphic profiles from Owl Creek represent a complex history of erosion, sedimentation, and landscape stability followed by soil formation. Field observations indicate the presence of eight fluvial/colluvial units (Fig. 2.3; Table 2.4) chronologically constrained using OSL ages (Table 2.3).

OSL ages for the Owl Creek sequence are determined predominantly on very fine sand (63-100 mm) aliquots of quartz from thin (<20 cm) channel infill (Table 2.3). This sedimentary facies was selected based on the inferred environment of deposition of ripple bed accretion in shallow water (<20 cm) enhanced solar resetting of luminescence of quartz grains (cf. Berger, 1990; Forman, 1990). Low overdispersion values (<20%) for older samples, >30 ka indicate a single equivalent dose population, with negligible inheritance of luminescence, well within the error in measurement. Younger sediments ca. <10 ka old yielded significant higher overdispersion values (>70%), indicating a mixed population of grains of various ages, reflecting partial solar resetting. OSL ages are calculated using the minimum age model (Galbraith and Roberts, 2012) with such elevated overdispersion values that weight for the youngest population, though definition of this youngest component is data dependent.

4.1. Depositional unit Q1

4.1.1. Description

Unit Q1 is the oldest sediment exposed at Red Bluff, which rests unconformably on a bedrock strath terrace into the Walnut Clay Formation approximately 9 m above the modern thalweg (Fig. 2.3). The unit ranges in thickness from 0.5 m to 2.6 m with a lower boundary marked by an erosional unconformity into underlying bedrock (Fig. 3, Profile B). The surface of this unit is unconformably overlain by unit Q3 and is laterally truncated by unit Q2. Unit Q1 is comprised of trough cross-bedded (Gt) to broad and shallow gravel and sand lenses (Gs, Ss) infilling basal scours (Table 2.1). The gravels are ne to cobble size, poorly sorted, massive to trough cross- bedded, and both matrix- and grain-supported. The gravels consist of limestone and chert clasts, with carbonate cementation (Table 2.4). This unit may have been weakly modified by pedogenesis prior to burial as evidenced by ped structure and lack of bedding. The OSL ages from Q1 were taken from a sand lense near the bedrock contact indicating that deposition was ongoing by approximately ca. 120 to 125 ka (UIC2650 124,790 ± 17,560; UIC2647 118,170 ± 16,030) (Fig. 2.3, Table 2.3).

4.1.2. Interpretation

The sedimentary structures and facies assemblage suggest that the Q1 formed by colluvial deposition (cf. Dietrich and Dunne, 1978; Blair and McPherson, 1994; Blikra and Nemec, 1998; Harvey, 2012). The massive, poorly modern flow, apparently derived from the adjacent uplands on the sorted matrix-and grain-supported gravels and sand scour infill are south side of the valley inferred from geomorphic preservation of characteristic of debris-flow (Table 2.5) (cf. Dietrich and Dunne, 1978; Blair and McPherson, 1994; Blikra and Nemec, 1998; Harvey, 2012). Possible ‘toe-cutting’, distal erosion, and later deposition at Owl Creek may have truncated the Q1 and prevent unequivocal interpretation of this facies (cf. Harvey, 2012). Cross-bedded gravels occur in Q1 and probably represent a channel facies in a fan-head trench (cf. Stanistreet and McCarthy, 1993). The 2-3 m diameter gully channels suggest run-off with paleoflow perpendicular to modern flow, apparently derived from the adjacent uplands on the south side of the valet inferred from geomorphic preservation of the paleochannel (cf. Blair and McPherson, 1994). The low organic carbon value from the horizon is consistent with minor amounts of organic matter accumulating at depth and the corresponding higher inorganic carbon values reflecting the pedogenic and non-pedogenic carbonate within the horizon (Table 2.4).

4.2. Depositional unit Q2

4.2.1. Description

The Q2 unit is a 7 m-thick deposit unconformably bound by the lower Walnut Clay Formation and the surface soil, 8 m above the modern channel thalweg. Unit 2 is laterally inset to unit Q1 and is partly unconformably overlain by unit Q3 and unit Q5 to the east (Fig. 3). Unit Q2 is comprised of laterally extensive massive gravels (Gm) and fines (Fm) with scours. Two buried soils (P1 and P2) and a surface soil are developed in Unit Q2 (Table 2.4). Unit Q2 is divided into sub-units based on paraconformable surfaces defined by buried soils. OSL ages from the base of unit Q2 near the bedrock contact suggest deposition was ongoing by ca. 80-85 ka (UIC2646 83,145 ± 12,590; UIC2643 82,370 ± 13,100; UIC2645 79,710 ± 12,820) (Fig. 2.3, Table 2.3).

Table 2.4. Depositional units and soil/buried soil characteristics, including horizon designation, thickness, structure, and lower boundary conditions are detailed. Organic carbon (OC) and inorganic carbon (IC) content, along with sediment texture and selected features are also presented. Clast supported C horizons and Bkm horizons were not measured for OC and IC. All of the sediments are strongly effervescent.

	Horizon	Depth (cm)	Structure	Boundary	OC wt %	IC wt %	Texture and selected features
Depositional Unit Q8							
	A	0-43	3, f, sbk	C, W	5.25	5.50	GR CL; dark grayish brown (10YR 4/2); common fine to coarse roots; common coarse to very coarse fragments, matrix supported, well sorted limestone and cherts.
	Bw1	43-81	2, m, sbk	G, W	1.20	7.20	SiCL; brown (10YR 4/3); common medium roots; common coarse snail shells; very few calcium carbonate filaments (stage I); common coarse fragments, matrix supported well sorted limestone and cherts.
	Bw2	81-132	1, co, pr	G, W	0.52	8.16	GR SiCL; grayish brown (10YR 5/2); very few coarse sediment in-filled burrows; very few calcium carbonate filaments (stage I); common coarse fragments, matrix supported, poorly sorted limestone and cherts.
	Bw3	132-202	M	C, S	0.56	8.19	GR SiCL; brown (7.5YR 5/3); common coarse snail shells; many coarse fragments, matrix supported, poorly sorted, limestone and cherts.
	Bw4	202-248	1, co, sbk	C, S	0.40	5.50	GR SiCL; brown (7.5YR 5/3); Few coarse snail shell fragments; very few calcium carbonate filaments (stage I); common coarse fragments, matrix supported, poorly sorted limestone and few cherts.
	Cb	248-300	M	G, S	0.38	4.10	GR SiCL; brown (7.5YR 5/3); common coarse snail shell fragments; very few fine calcium carbonate filaments (stage I); common coarse fragments, matrix supported, poorly sorted limestone and cherts.
Depositional Unit Q7							
Q7c	ABb	300-343	3, co, pr	G, S	0.45	1.90	SiC; dark yellowish brown (10YR 3/4); common coarse granular infilled burrows; common medium calcium carbonate filaments (stage I); common coarse calcium carbonate nodules (stage II).
	Bkss	343-393	3, m, pr w	C, W	0.39	1.20	SiC; Brown (10YR 4/3); common fine faint calcium carbonate filaments (stage I); common coarse calcium carbonate nodules (stage II).
Q7b	ABb	393-423	3, f, sbk	G, S	0.24	1.70	SiC; dark yellowish brown (10YR 4/4); few coarse calcium carbonate rhizoliths; few fine calcium carbonate filaments (stage I); common medium calcium carbonate nodules (stage II); common coarse fragments, matrix supported, well sorted limestone and cherts.
	Bk	423-453	3, f, sbk	C, S	0.17	4.00	SiCL; dark yellowish brown (10YR 4/4); common calcium carbonate rhizoliths common fine calcium carbonate filaments (stage I); common fine calcium carbonate nodules (stage II); few coarse fragments, matrix supported, well sorted limestone and cherts.
Q7a	ABb	453-510	3, m, sbk	G, S	0.80	6.70	SiCL; yellowish brown (10YR 5/6); common fine calcium carbonate filaments (stage I); common calcium carbonate nodules (stage II).
	Bk	510-540	3, f, sbk	D, S	0.53	6.62	SiC; very pale brown (10YR 7/4); few fine calcium carbonate filaments (stage I); few coarse fragments, matrix supported, well sorted limestone and cherts.
	C	540-560	3, m, sbk	C, S	0.49	6.58	L; white (10YR 8/1); very few very fine to fine rootlets; few coarse clasts, clast supported, well sorted limestone and cherts; finer and sandier facies within horizon.
Depositional Unit Q6							
		560-624	-	A, W	-	-	G C; Common calcium carbonate pendants (stage I); clast supported, poorly sorted limestone and cherts.

		624-694	-	V, W	-	-	G C; trough cross-bedded clast supported, poorly sorted limestone and cherts; common carbonate pendants (stage I).
Depositional Unit Q5							
	A	0-10	3, m, gr	G, S	3.23	4.02	CL; dark grayish brown (10YR 4/2); many coarse modern roots; common medium burrows; very few coarse fragments, matrix supported, poorly sorted limestone and cherts.
	Bk1	10-27	2, f, sbk	C, S	2.47	5.60	CL; brown (10YR 4/3); many coarse modern roots; common medium burrows; common fine calcium carbonate filaments (stage I); common medium soft calcium carbonate nodules (stage II); few coarse fragments, matrix supported, well sorted limestone and cherts.
	Bkm	27-33	M	A, S	-	-	White (7.5YR 8/1); laminar in the upper 2 to 3 cm; strongly cemented.
	Bk2	33-132	2, m, sbk	A, W	0.84	7.04	L; reddish yellow (7.5YR 6/6); very few fine roots; common fine calcium carbonate filaments (stage I); common very coarse soft calcium carbonate nodules (stage II); few coarse fragments, matrix supported, well sorted very coarse limestone and cherts.
	BC	132-152	M	C, S	0.52	5.14	GR L; very pale brown (10YR 8/2); few fine roots; common medium burrows; common coarse fragments, matrix supported, well sorted very coarse limestone and cherts.
	C	152-237	-	C, W	-	-	G C; trough cross bedded gravels with laminated sands; common calcium carbonate pendants (stage I); abundance thickness clasts with calcium carbonate pendants on gravel bottoms (stage I); common coarse fragments, clasts supported, poorly sorted limestone and cherts.
Depositional Unit Q4							
	A	0-27	2, f, sbk	A, S	2.43	3.99	GR SiCL; very dark grayish brown (10YR 3/2); Common medium roots; common medium hard calcium carbonate nodules (stage II); common, matrix supported, well sorted limestone and cherts.
	Bkm	27-32	M	A, S	-	-	Pinkish white (7.5YR 8/2); laminar petrocalcic; strongly cemented.
	Bk1	32-62	2, f, sbk	G, S	0.32	6.82	L; reddish yellow (7.5YR 7/6); heavily cemented calcium carbonate; few fine modern roots; few coarse fragments, matrix supported, well sorted limestone and cherts with calcium carbonate pendants (stage I).
	Bk2	62-154	2, f, sbk	G, S	0.26	10.55	VGR SiCL; reddish yellow (7.5YR 7/6); Very few fine roots; few calcium carbonate pendants (stage I); many coarse fragments, matirix supported, well sorted limestone and cherts.
	Bk3	154-204	2, f, sbk	G, S	0.34	7.02	SiCL; strong brown (7.5YR 4/6); very few fine roots; few medium sediment in filled burrows; common medium hard calcium carbonate nodules (stage II); few coarse fragments, matrix supported, well sorted limestone clasts.
	Bk4	204-227	2, f, sbk	C, S	0.43	5.82	SiCL; strong brown (7.5YR 4/6); common fine soft and hard calcium carbonate nodules (stage II); few coarse fragments, matrix supported, well sorted limestone clasts.
Depositional Unit Q3							
	ABb	227-267	3, m, sbk	G, S	0.56	4.01	SiCL; strong brown (7.5YR 4/6); very few fine to medium roots; few fine sediment infilled burrows; common medium soft calcium carbonate nodules (stage II); few coarse , matrix supported, well sorted limestone clasts.
	Bk1	267-310	3, f, sbk	C, W	0.19	4.89	SiL; strong brown (7.5YR 4/6); very few fine sediment infilled burrows; common coarse soft calcium carbonate nodules (stage II) and few fine hard calcium carbonate nodules (stage II); few coarse fragments, matrix supported, well sorted limestone clasts.
	Bk2	310-562	3, m, sbk	C, W	0.08	10.68	VGR SiCL; strong brown (7.5YR 5/8); common coarse soft calcium carbonate nodules (stage II); common medium hard calcium carbonate nodules (stage II); common coarse fragments, matrix supported, poorly sorted limestone and few cherts.
Depositional Unit Q2							
Q2c	A	0-34	1, m, sbk	G, S	0.57	9.24	GR CL; very dark grayish brown (10YR 3/2); many fine to medium roots; common medium calcium carbonate nodules (stage II); common coarse fragments, matrix supported, well

							sorted limestone and cherts.
	Bkm	34-37	M	C, S	-	-	Pinkish white (7.5RY 8/2); laminar in the upper 2 to 3 cm; strongly cemented.
	Bk1	37-121	1, f, sbk	D, S	0.53	7.29	CL; strong brown (7.5YR 5/6); common fine roots; common fine soft and hard calcium carbonate nodules (stage II); few coarse limestone and cherts gravel stringers, matrix supported, well sorted limestone and cherts.
	Bk2	121-131	1, f, sbk	G, S	0.61	8.77	SiL; brown (7.5YR 4/3); few fine roots; common fine soft and hard calcium carbonate nodules (stage II); few coarse limestone and cherts gravel stringers, matrix supported, well sorted limestone and cherts.
	Bk3	131-166	M	G, S	0.35	9.15	SiL; yellowish brown (10YR 5/4); common coarse fragments, well sorted limestone and cherts cemented with calcium carbonate pendants (stage I).
	BCk	166-205	M	A, S	0.21	10.19	GR L; yellow (10YR 7/6); common calcium carbonate pendants (stage I); common coarse fragments, matrix supported, poorly supported limestone and cherts cemented with calcium carbonate (stage I).
	C1	205-267	M	C, S	0.23	8.84	SiL; brownish yellow (10YR 6/6); common coarse fragments, matrix supported, poorly sorted limestone and cherts.
	C2	267-387	M	G, S	0.33	7.69	L; pinkish white (7.5YR 8/2); lenticular sand lenses; few fine distinct yellowish brown (10YR 5/6) dendritic redox concentrations; common coarse fragments, grain supported, well sorted limestone and angular cherts.
Q2b	ABb	387-422	1, f, sbk	G, S	0.30	8.84	SiCL; strong brown (7.5YR 5/6); common medium soft calcium carbonate nodules (stage II); few coarse fragments, matrix supported, well sorted limestone and cherts.
	Bk	422-457	2, m, sbk	C, S	0.22	8.70	SiL; very pale brown (10YR 7/4); common coarse hard calcium carbonate nodules (stage II); few coarse fragments, matrix supported, poorly sorted limestone and cherts.
	BC	457-467	M	C, S	0.18	8.62	GR SiL; very pale brown (10YR 7/3); common coarse fragments, matrix supported, well sorted limestone and cherts.
Q2a	ABb	467-492	2, m, sbk	G, S	0.26	8.50	SiL; Light yellowish brown (10YR 6/4); common coarse hard calcium carbonate nodules (stage II); common coarse fragments, matrix supported, poorly sorted limestone and cherts.
	Bk	492-535	2, f, sbk	G, S	0.28	8.40	SiL; yellow (10YR 7/6); common coarse hard calcium carbonate nodules (stage II); few coarse fragments, matrix supported, well sorted limestone and cherts.
	BC	535-613	M	C, S	0.20	9.20	GR SiL; white (10YR 8/1); well sorted, rounded to subrounded, matrix supported limestone and cherts.
	C	613-678	-	C, W	0.19	9.52	G C; massive grain supported well sorted limestone and cherts.
Depositional Unit Q1							
	C1	678-715	2, m, sbk	G, W	0.19	4.89	SiCL; common coarse hard calcium carbonate nodules (stage II); common medium soft nodules (stage II); few coarse fragments, matrix supported, well sorted limestone and few cherts.
	C2	715-850	-	V, S	-	-	G C; high calcium carbonate cementation; trough cross-bedded and massive, grain supported, poorly sorted limestone and cherts and sands.

Unit Q2a is approximately 2 m thick and unconformably overlies the Walnut Clay, with a clear and smooth upper boundary between the buried soil forming the surface of this unit and the overlying subunit (Fig. 2.3). Unit Q2a is comprised of massive gravel and gravel stringers (Gm) interbedded with laterally continuous massive fines (Fm) modified by pedogenesis (P1) (Table 2.1). The coarse to very coarse gravels are well-sorted and rounded to sub-rounded grain supported clasts consisting of limestone and chert. The 1 m thick buried soil consists of an ABb-Bk-BC-C profile (Fig. 2.3, Profile B; Table 2.4). The P1 buried soil profile is a very pale brown with silt loam textures, subangular blocky structure, and common distinct soft iron-oxide masses. Pedogenic calcium carbonate in the form of stage I filaments and stage II hard nodules occur in the Bk horizon.

The Q2b unit overlies unit Q2a with a clear and smooth upper boundary to the overlying Q2c unit. Q2b is comprised of approximately 1 m of pedogenically modified (P2) loamy sands with massive gravels (Gm) in the lower 40 cm. The gravels are rounded limestone and chert grains. The buried soil has an ABb-Bk-BC profile with subangular blocky structure, strong brown colors, silty clay loam textures (Fig. 2.3, Profile C; Table 2.4). A relative maturity index of 2 suggests the soil is moderately developed based on the presences of a Bk horizon, with stage II carbonate nodules (Table 2.2).

The Q2c is an approximately 4 m thick subunit overlying Unit Q2b, with the surface soil as its upper boundary (Fig. 2.3). The unit is comprised of scour fills (Ss) and massive fines (Fm) in the lower 2 m with a surface soil in the upper 2 m. The basal sands form discrete, lenticular and horizontally bedded (Fh) bodies with interbedded with massive fines (Fm) (Table 2.1). The surface soil has an A-Bkm-Bk profile and developed in fine-grained alluvium comprising the upper 2 m of Q2c (Fig. 2.3, Profile D; Table 2.4). The A horizon is very dark grayish-brown, with common coarse limestone fragments, overlying an indurated Bkm horizon that grades downward to a series of Bk horizons with stage I calcium carbonate pendants and stage II nodules. The modern surface soil is classified as a Petrocalcic Paleustoll based on the presence of a mollic epipedon, ustic soil moisture regime, and the petrocalcic horizon.

4.2.2. Interpretation

The dominantly fine facies and laterally extensive architecture of Q2 is interpreted as overbank fluvial sedimentation (Table 2.5). The fining-upward deposit with occasional gravel stringers and horizontally bedded fines reflect fluctuation in sediment supply or stream flow (cf. Germanoski and Schumm, 1993; Miall, 2006). P1 and P2 buried soils are moderately developed reflecting the formation of a Bk horizons and have a relative maturity index of 2 (Table 2.2). The presence of a Bkm suggests that the surface soil is well-developed with a relative maturity index of 3, but is still actively undergoing pedogenesis. Increase in the organic carbon values and dark color confirm the presence of the P1 and P2 buried soils within the unit (Table 2.4). The inorganic carbon content increases in identified carbonate rich horizons and with minor detrital carbonate redistribution at depth (Table 2.4).

4.3. Depositional unit Q3

4.3.1. Description

Unit Q3 ranges in thickness from 0.5 to 3 m and unconformably buries unit Q1 and is unconformable with the overlying unit Q4. The unit partly truncates the underlying bedrock and is inset to unit Q2 (Fig. 2.3). The depositional facies consist of massive gravels (Gm) and fines (Fm) and shallow sand scour infill (Ss) (Table 2.1). The sands form discrete, lenticular, concave-up bodies that transition to horizontally bedded sands. The P3 buried soil forms the upper boundary of the Q3 and consists of an ABb horizon over Bk horizons (Fig. 2.3, Profile A & B; Table 2.4). The P3 buried soil is a brown, silty clay loam with subangular blocky structure. Stage II soft pedogenic carbonate nodules occur throughout the profile and increase in abundance to the base of the solum at 3.7 m depth. OSL ages of 104,250 ± 12,780 and 102,095 ± 15,420 (UIC2638 and UIC2638b) on quartz grains from an infilled scour from beneath the P3 buried soil suggests deposition was ongoing at this time (Fig. 2.3, Table 2.3).

Table 2.5. Summary describing the environmental setting, facies code, architectural geometry and interpretation of the depositional units in the study area.

Depositional Unit	Environmental Setting	Facies code		Architectural geometry	Interpretation
		Dominant facies	Minor Facies		
Q8	Fluvial	Gm, Fm*		concave-up sediment body with an erosional base	bioturbated channel deposits
Q7	Fluvial	Gm, Fm*		laterally extensive depositional unit	overbank deposits distal to active channel
Q6	Fluvial	Gt, St, Gm		concave-up sediment body with an erosional base	lateral accretion bars associated with channel deposits
Q5	Fluvial	Gm, Fm*	Gt, Fh	concave-up sediment body with an erosional base	sediments associated with cut and fill channel deposits
Q4	Colluvial fan	Gm, Fm*		tabular sediment body with an erosive base	sediment debris flow sourced from the adjacent uplands
Q3	Fluvial	Gm, Fm*	Ss	concave-up sediment body with an erosional base	sediments associated with cut-and-fill channel deposits
Q2	Fluvial	Gm, Fm*	Ss, Fh	laterally extensive depositional unit	overbank deposits distal to active channel
Q1	Colluvial fan	Gm, Gt, Gs, Ss, Fm	-	sediment body with erosive base	sediment slope wash sourced from the adjacent uplands

* Denotes the presence of a soil or buried soils.

4.3.2. Interpretation

The Q3 unit was deposited following erosion and fine-grained fluvial infill preserving a concave-upward geometry typical of lateral accretion deposits and stream migration to the southwest. Changes in sediment texture have been attributed to a reduction of flow regime or change in sediment supply (Table 2.5). The relative maturity index of 2 for the P3 buried soil indicates moderate developed (Table 2.2). Organic content in the P3 buried soil decreases with depth with high inorganic carbon values attributed to pedogenic carbonate and secondary carbonate accumulation (Table 2.2).

4.4. Depositional unit Q4

4.4.1. Description

Unit Q4 is a sediment package that ranges in thickness from 1 to 3 m (Fig. 2.3, Profile A & B). This unit is unconformably bracketed by the underlying unit Q3 and the modern surface soil. The unit is comprised of massive gravels and fines (Gm, Fm). The limestone and chert gravels are pebble size, well-sorted, and matrix sup- ported (Table 4). The surface soil consists of an A-Bkm-Bk profile and is 2.3 m thick characterized by black to reddish-yellow, silty clay-loam with subangular blocky structure (Fig. 2.3, Profile A & B; Table 2.4). The A horizon has common coarse limestone fragments overlying the indurated and carbonate-rich Bkm horizon. The underlying Bk horizons have common pedogenic calcium carbonate nodules with gravel content peaking at 1.5 m and decreasing to the base of the solum. The modern surface soil is a Petrocalcic Paleustoll based the presence of a mollic epipedon in the ustic soil moisture regime and thin Bkm horizon (Soil Survey Staff, 2010). A relative maturity index of 3 suggests the surface soil is well- developed, but is still actively undergoing pedogenesis (Table 2.2). OSL ages of 98,680 ± 13,000 and 94,245 ± 13,678 ka (UIC2649 and UIC2649b) from the base of unit Q4 constrains deposition (Fig. 2.3, Table 2.3).

4.4.2. Interpretation

The facies assemblage suggests colluvial depositional environment consisting of massive, well-sorted, matrix supported, gravel- rich deposits (cf. Dietrich and Dunne, 1978; Blikra and Nemec, 1998; Harvey, 2012) (Table 2.5). The sediment, like the Q1 fan, was likely derived from the adjacent uplands on the south side of the valley (cf. Dietrich and Dunne, 1978; Blair and McPherson, 1994; Blikra and Nemec, 1998; Harvey, 2012). The unit Q4 debris-flow, like unit Q1, was likely truncated by 'toe-cutting' and later Owl Creek deposition (cf. Harvey, 2012). The well-developed soil in unit Q4 is actively undergoing pedogenesis (Table 2.2). The organic carbon content values are highest at the modern surface and generally decrease with depth (Table 2.4). High inorganic carbon values correspond to the presence of pedogenic carbonate with values in the Bk2 reflecting secondary carbonate accumulation (Table 2.4).

4.5. Depositional unit Q5

4.5.1. Description

Unit Q5 is approximately 2 m thick and is situated 5.5 m above the modern channel thalweg and is unconformably bound by the Walnut Clay Formation at the base with a surface soil developed in the top 1.5 m of the unit (Fig. 2.3). This unit onlaps on to the older unit Q2 to the southwest and is laterally bracketed by the younger units Q6 and Q7 to the east (Fig. 2.3). Unit Q5 is comprised of trough cross- bedded gravels (Gt), massive gravels (Gm), horizontally laminated fines (Fh), massive fines (Fm), and the surface soil (Table 2.4). The trough cross-bedded gravels form a clear wavy contact with the underlying Walnut Clay. These gravels are grain supported, angular to rounded limestone and chert with calcium carbonate pendants, overlain by horizontally bedded sands. The 1.5 m thick surface soil consists of an A-Bkm-Bk-BC profile (Fig. 2.3, Profile D; Table 2.4). The dark grayish-brown soil with silt loam textures and subangular blocky structure includes a 5 cm thick stage IV pedogenic calcium carbonate laminar horizon (Bkm). The Bkm horizon overlies a reddish-yellow Bk horizon with subangular blocky structure and pedogenic calcium carbonate filaments (stage I) and soft nodules (stage II).

The modern surface soil is s a Petrocalcic Paleustoll based a mollic epipedons, ustic soil moisture regime, and presence of a thin Bkm horizon (Soil Survey Staff, 2010). There are no direct OSL ages on unit Q5. However, the age of the unit is constrained by lower and upper bracketing OSL dates on units Q6 and Q4 of 94,245 ± 13,678 ka (UIC2649) and 44,010 ± 6970 ka (UIC2640)(Fig. 2.3, Table 2.3), respectively.

4.5.2. Interpretation

The fluvial cut-and-fill sequence of unit Q5 is interpreted as a lateral accretion deposit with later fine-grained sediments reflecting stream migration or fluctuation in sediment supply (cf. Miall, 2006). A relative maturity index of 3 demonstrates that the surface soil is well-developed based on the presence of a Bkm (Table 2.2). The surface soil, atop unit Q5, organic carbon content values steadily decrease with depth; inorganic carbon content values indicate the presence of only minor secondary carbonate at depth (Table 2.4).

4.6. Depositional unit Q6

4.6.1. Description

Unit Q6 is 1.3 m thick and overlies the incised Walnut Clay Formation. It is overlain by the younger unit Q7 and is laterally inset to unit Q5 (Fig. 2.3). The surface of this unit is approximately 2 m above the modern channel thalweg of Owl Creek. Deposition followed a major period of bedrock incision that removed a minimum of 4 vertical meters of Walnut Clay. The laterally extensive facies are characterized by trough cross-bedded (Gt) and massive (Gm) gravels with trough cross-bedded sand (St). The gravels are well sorted, grain supported, rounded, coarse limestone and chert clasts and with carbonate cementation (Fig. 2.3, Profile E & F; Table 2.4). Quartz grains from a sand lense at the base of the Q6 unit returned an OSL age of 44,010 ± 6970 ka (UIC2640) (Fig. 2.3, Table 2.3).

4.6.2. Interpretation

The trough-cross-bedded gravel facies of unit Q6 are indicative of a laterally migrating channel. The presence of the coarse-grained deposits and large volume of sandy alluvium is suggestive of a high competency stream or a shift in source from earlier and finer Owl Creek deposits, typical of a braided meandering stream (Table 2.5) (cf. Miall, 2006).

4.7. Depositional unit Q7

4.7.1. Description

Unit Q7 is a 2.6 m thick unit unconformably bound by Q6 and Q8 and partially onlaps unit Q5 (Fig. 2.3). Unit Q7 is comprised of gravels (Gm) and pedogenically modified alluvium (Fm) (Table 2.5). This unit is divided into sub-units based on paraconformable surfaces demarcated by buried soils.

The Q7a is a sub-unit with an abrupt, wavy lower contact with unit Q6, and a clear but smooth upper boundary. This sub-unit is weathered through its entire thickness by the P5 buried soil with an ABb-Bk-C profile (Fig. 2.3, Profile F & E). The P4 buried soil is a yellowish-brown, silty clay loam solum with subangular blocky structure and stage I pedogenic carbonate filaments that increase in abundance in the Bk horizon (Table 2.4). Quartz grains taken from the C horizon of the buried soil yielded an OSL age of 14,050 ± 2240 years ago (UIC2901) (Fig. 2.3, Table 2.3), by a minimum age model because of the high overdispersion value (73%). We have less con- fidence in this age compared to other analyses with overdispersion values of <20% (Table 2.3).

Sub-unit Q7b has a clear, wavy upper boundary to sub-unit Q7c. Sub-unit Q7b is 60 cm of pedogenically modified dark yellowish- brown sediment with an ABb-Bk profile (Fig. 2.3, Profile F & E). Buried soil P5 consists of silty clay to silty clay loam textures with subangular blocky structure (Table 2.4). The buried soil has stage I pedogenic calcium carbonate filaments and stage II hard nodules in the Bk horizon and distinctive carbonate-rich rhizocretions. The rhizoconcretions are probably remnants of roots of plants growing on the surface of the soil prior to burial.

The Q7c sub-unit is bound by the clear, wavy boundary to the overlying unit Q8. This sub-unit has preserved a hillslope that is continuous to unit Q5. The 1 m thick sub-unit is entirely pedogenically altered (P6) with an ABb-Bkss profile (Fig. 2.3, Profile E & F). The dark yellowish-brown P6 buried soil has a silty clay texture with prismatic to wedge shaped peds (Table 2.4). The Bkss horizon in the buried soil has stage I and stage II pedogenic carbonate filaments and nodules with prominent slickensides.

4.7.2. Interpretation

Unit Q7 consists of laterally extensive, fine-grained alluvium likely from overbank sedimentation distal to the channel. Pedogenic carbonate morphology suggests the P4, P5, and P6 buried soils are moderately developed. The P5 and P4 buried soils organic carbon values decrease with depth and inorganic carbon are attributed to redistribution with translocation (Table 2.4). The P6 buried soil preserves hillslope topography, overlies the Q5 and merges with the present surface. P6 buried soil has preserved high organic and inorganic carbon values consistent with redistribution at depth (Table 2.4). Relative maturity indices of 2, from the P6, P5, and P4, suggest moderate developed based on the degree of pedogenic carbonate formation (Bk horizon) (Table 2.2).

4.8. Depositional unit Q8

4.8.1. Description

Unit Q8 is a 3 m thick deposit, unconformably bound by the underlying unit Q7 and by its surface soil at the top (Fig. 2.3). The massive gravels (Gm) in the lower 1 m of unit Q8 are matrix-sup- ported and subangular, rounded and platy limestone and chert stringers (Table 2.1). The surface soil has an A-Bw-C profile (Fig. 2.3, Profile F & E). The very dark grayish-brown soil has a clay loam texture and fine, subangular blocky structure (Table 2.4). The present surface soil is a Cumulic Halpustolls based on an overthickened surface horizon of a Mollisol within an ustic soil moisture regime (Soil Survey Staff, 2010). Quartz grains from the C horizon at the base of Q8 returned an OSL age of 8570 ± 1420 ka (UIC2900) (Fig. 2.3, Table 2.3). We have less confidence in because of the high over- dispersion values (Table 2.3).

4.8.2. Interpretation

The concave-up geometry and a laterally extensive facies of unit Q8 are interpreted as fluvial channel deposits (Table 2.5) (Miall, 2006). The active channel scoured the underlying unit with sub- sequent deposition of fine and coarse grained sediments that indicate fluctuating stream capacity. The maturity index of the youngest soil suggests that the soil is poorly developed based on the presence of a Bw horizon (Table 2.2). The modern soil organic carbon values decreasing with depth. The inorganic carbon values reflect detrital carbonate with only few stage I filaments identified within the unit (Table 2.4).

5. Discussion

5.1. Depositional environments and landscape evolution

The paleoenvironmental reconstruction of Owl Creek reveals a complex history of erosion, deposition, and soil forming intervals. The sedimentary record extends from approximately 120 ka ago to the late Holocene and is dominated by alluvial deposition. The combined results of the stratigraphic record and OSL ages provide a chronologically-constrained depositional record for Owl Creek and a metric to compare to other areas of central Texas and beyond.

Table 2.6. Summary of the depositional unit with inferred depositional age, environmental setting, soil/buried soil, relative soil maturity index, and soil forming interval.

Depositional Unit: Unit	Sub-Unit	Inferred age[a]	Environmental setting [b]	Buried soil (P) or surface soil	Relative soil maturity index[c]	Inferred soil forming interval
Q8		<8 ka	Fluvial	surface soil	1	<3 ky[f]
Q7	Q7c Q7b Q7a	9 to 14 ka 9 to 14 ka 9 to 14 ka	Fluvial	P6 P5 P4	2 2 2	3 to 15 ky[g] 3 to 15 ky[g] 3 to 15 ky[g]
Q6		44 ka	Fluvial	-	-	
Q5		75 to 50 ka[d]	Fluvial	surface soil	3	70<100 ky[h]
Q4		95 to 75 ka[e]	Colluvial	surface soil	3	70<100 ky[h]
Q3		95 to 75 ka[e]	Fluvial	P3	2	3 to 15 ky[g]
Q2	Q2c Q2b Q2a	95 to 75 ka[d] 95 to 75 ka[d] 95 to 75 ka[e]	Fluvial	surface soil P2 P1	3 2 2	70<100 ky[h] 3 to 15 ky[g] 3 to 15 ky[g]
Q1		120 ka	Colluvial	-	-	

[a] Inferred age based on OSL dating (See Table 4), stratigraphic relations (See Fig. 2), and age-stratigraphic curve (See Fig. 3).
[b] Environment of deposition based on facies types and distributions.
[c] See Table 2 for explanation.
[d] Inferred age based on bracketing deposits.
[e] Based on OSL age from bracketing deposits and inferred soil forming interval.
[f] Soil forming interval based on Buck and Monger, 1999; Gile et al, 1981; Hall et al., 2012; Nordt, 1992.
[g] Soil forming interval based on Buck and Monger, 1999; Gile et al, 1981; Nordt, 1992; Water and Nordt, 1995.
[h] Soil forming interval based on Machette, 1985; Blum et al, 1994; Blum and Velastro, 1992; Candy et al., 2009.

Initial activity scoured the underlying Walnut Clay at Red Bluff, with subsequent infilling by colluvial slope wash (unit Q1), sourced from small gullies emanating from the upland hillslope to the south (Fig. 2.1). OSL ages indicate colluvial deposition began at ca. 120 ka (Tables 2.3 and 2.6). Discrete channels have been eroded into the gully deposits of unit Q1 and into the Walnut Clay. Unit Q1, a colluvial deposit, and the subjacent bedrock was partially eroded by incision of Owl Creek and subsequent infilling by overbank sediments of unit Q2, which yielded an OSL age of ca. 95 ka (Fig. 2.3, Table 2.6).

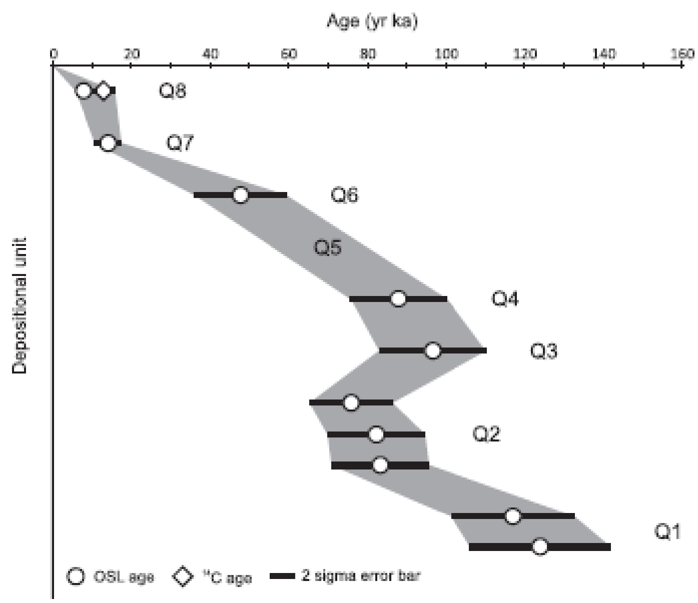

Fig. 2.4. Age-stratigraphic curve from Owl Creek showing the relationship between ages of the identified depositional units. Q5 has not been dated and Q8 shows both OSL and 14C ages. Black bars correspond to two-sigma error, circles to OSL ages, and the diamond to 14C age.

The deposition of units Q2, Q3, and Q4 at Owl Creek probably occurred in close succession in a fluvial environment sometime between ca. 95 and 75 ka. This inference is based on moderate to weak development of buried soils P1, P2, and P3 and associated similarity of OSL ages (Fig. 2.4, Table 2.2, 2.4 and 2.6).

The buried soils (P1 and P2) are moderately developed and with morphological characteristics indicate residence time of ca. 3-15 ky, although probably closer to the former based on the inferred depositional interval (Table 2.6). The estimated soil-forming interval is based on dated soils with similar properties from the southwest U.S. and central Texas, accounting for alluvial parent materials derived from limestone (Gile et al., 1981; Machette, 1985; Blum and Valastro, 1992; Nordt, 1992; Blum et al., 1994; Waters and Nordt, 1995; Buck and Monger, 1999; Nordt, 2004; Kraimer and Monger, 2009). The modern surface soil, in the T3 terrace, has a prominent Bkm horizon (stage IV) with a maturity index of 4 and development at sometime after deposition of unit Q2. However, a Bkm horizon with laminar cap may probably form in as little as ca. 70 ky in alluvial parent material derived from limestone in humid climates (Wright, 1990; Blum and Valastro, 1992; Blum et al., 1994; Nordt et al., 1998; Candy et al., 2004; Kraimer and Monger, 2009). The associated OSL ages of ca. 95-75 ka for these units are indistinguishable at two-sigma errors (Fig. 2.4) and are consistent with the inferred lapsed time from buried soil morphology.

Sediment supply after channel accretion of unit Q3 diminished and/or flooding eventually subsided, with ensuing surface stability and pedogenesis reflected by the P3 buried soil (Fig. 2.3; Table 6; see 4.3.2). The Bk horizon of the P3 buried soil suggests a residence time of 3-15 ky (Gile et al., 1981; Nordt, 1992; Waters and Nordt, 1995; Buck and Monger, 1999; Kraimer and Monger, 2009).

Colluvial deposits of unit Q4 overlie fluvial deposits of unit Q3, indicating destabilization of the adjacent uplands and expansion of a local colluvial fan, forming the T4 terrace. This terrace is higher in elevation, but younger than the T3 (associated with unit Q2) based on cross-cutting relationships and the law of superposition, with topographic inversion resulting from colluvial deposition (cf. Bryan, 1940; Mills, 1981). The surface soil developed in the top of unit Q4 and is characterized by a well-developed Bkm horizon. The soil is similar to the surface soil developed in unit Q2, and has an inferred development time of ca. 70-100 ky. The OSL age of ca. 89 ± 6 ka on fluvial quartz grains is consistent with rapid formation of a stage IV petrocalcic horizon (Table 6) (cf. Wright, 1990; Candy et al., 2004).

Fluvial erosion and deposition (unit Q5) resumed at Owl Creek sometime between ca. 75 and 50 ka (Table 2.6), with a cut and a fill sequence reflecting stream migration to the south and fluctuating sediment supply based on grain size. Unit Q5 forms the T2 terrace and stratigraphically younger than the older units and terraces. The surface soil modified unit Q5 and has a maturity index of 4, indicating a development interval of ca. 70-100 ky (Table 6) (cf. Wright, 1990; Candy et al., 2004). The morphology of the surface soil in units Q2, Q4, and Q5 suggests contemporaneous soil development. Unit Q5 deposits were subsequently eroded at which time at least 4 m of Walnut Clay was incised. Fluvial aggradation resumed by ca. 44 ka depositing unit Q6 by lateral accretion, possibly indicating the presence of a high-competency meandering river (Table 2.5; see 4.5.2). The uppermost portion of unit Q6 was scoured by renewed stream flow shortly before deposition of unit Q7, ca. 12 ka.

Deposition commenced again ca. 12 ka with fine-grained overbank sediments of unit Q7. However, the timing of this event is constrained by a single OSL age, with less accuracy than other ages, indicated by the high overdispersion values (Table 2.3). The pedogenically-modified overbank fines and buried soils within Q7 (P4, P5, and P6) are interbedded with thin gravel lenses, suggestive of variable stream discharge. Unlike buried soils P4 and P5, the P6 buried soil appears to have formed in colluvial parent material. This unit can be traced laterally along a hillslope and overlies unit Q5. The P4, P5, and P6 buried soils are all moderately developed. The minimum inferred residence time of each buried soil is ca. 3-15 ky, totaling to an inferred minimum time of formation of ca. 9 ky (Table 2.6). Later fluvial activity truncated the Q7 surface before fluvial deposition of unit Q8 at ca. 8 ka (Table 2.6). The fining-upward sedimentary sequence comprising unit Q8 indicates increasing isolation of the surface from fluvial processes, with eventual surface stabilization. The weakly developed modern surface soil on the T1 terrace indicates a maximum residence time of ca. 3 ky (Table 2.6).

5.2. Regional fluvial and climate trends

Changes in erosion, sedimentation, and pedogenesis in the sedimentary succession at Owl Creek reflect complex inter-related factors such as stream competency, climate, and vegetation (cf. Schumm, 1999). The Owl Creek succession probably preserves an incomplete record of fluvial aggradation and degradation due to the dynamic actions of fluvial systems. Though this record is incomplete, the studied fluvial deposits provide insights into the timing and nature of this tributary response to environmental and climatic variability during the past ca. 120 ka. A comparison of the Owl Creek succession with other records in the region provides a broader perspective on possible fluvial system response to climate variability during the Late Pleistocene (Fig. 2.5). However, the fluvial sedimentary records between central Texas (Blum and Valastro, 1989, 1994; Waters and Nordt, 1995; Nordt, 2004; Bongino and Nordt, 2007; Waters et al., 2011) and the Gulf Coast of Texas (Durbin et al., 1997; Blum and Price, 1998; Sylvia and Galloway, 2006;

Mandel et al., 2007) is limited to only a few localities with numeric ages limiting chronological comparison. The following discussion divides the depositional succession at Owl Creek into three temporal stages in reference to marine isotope stages (MIS) (Martinson et al., 1987).

5.2.1. MIS 5 (~130-74 ka)

MIS 5 is an interglacial period with sea level reaching levels of ~3-6 m above present at ca. 130 ka followed by a drop in sea level by ~30-40 m at ca. 110 and 90 ka (Waelbroeck et al., 2002; Thomas et al., 2009). However, there was a subsequent high stand equivalent to current sea level ca. 81 ka (Dorale et al., 2010), which was followed by a steep drop to ~-80 m by ca. 65 ka (Waelbroeck et al., 2002; Thomas et al., 2009). During this interglacial deltas extended on land by 30 m elevation from the Gulf of Mexico (Abdullah et al., 2004; Blum and Aslan, 2006). Coastal plain fluvial sediments for this interglacial are characterized by multiple, coarse-grained, cut- and-fill valley complexes, known as the Beaumont Formation (Blum and Valastro, 1992). The Beaumont Formation along coastal reaches of the Nueces (Durbin et al., 1997), Colorado (Blum and Price, 1998), and Brazos rivers (Sylvia and Galloway, 2006) may be coeval with Owl Creek deposits Q1 to Q4, spanning from ca. 75 to 120 ka (Fig. 2.5). Large regional fluvial systems in the lower Mississippi Valley were aggraded during the last interglacial (ca. 130 ka) possibly in response to a higher eustatic sea level and these systems degraded with subsequent fall in sea level (Rittenour et al., 2007; Shen et al., 2012).

There was rapid warming and disappearance of the Laurentide ice sheet in mid continental North America ca. 130 ka (Curry and Baker, 2000). However, low resolution d18O records from the Gulf of Mexico indicate possible meltwater excursions between

80 and 60 ka, indicating the re-growth of the Laurentide ice sheet into the Mississippi Valley drainage system (Joyce et al., 1993). This melt- water flux may have lead to cooling and/or stratification of the Gulf of Mexico, and broader effects to Atlantic Ocean circulation that possibly inhibited moisture flux into central Texas, particularly in the summer (Maasch and Oglesby, 1990; Pu et al., 2012). During late MIS 5, as the Laurentide ice sheet exceeded 75% of the Last Glacial Maximum volume, winter precipitation may have increased with the southward displacement of a consolidated jet stream (Bromwich et al., 2004). This may have steered cyclonic systems over the southern mid-continent and Texas (Kutzbach and Guetter, 1986; Bromwich et al., 2004; Asmerom et al., 2010). In turn, speleothem time series from Crevice Cave, Missouri (Dorale et al., 1998) and biostratigraphy from the Raymond Basin in southern Illinois (Curry and Baker, 2000) reveal high-frequency climate variability with the transition from MIS 5a to MIS 4. This inferred climate variability may be an important factor for the multiple aggradational/degradational events recorded in Owl Creek for this interval, although there may be direct effects of sea level change on this system (cf. Shen et al., 2012).

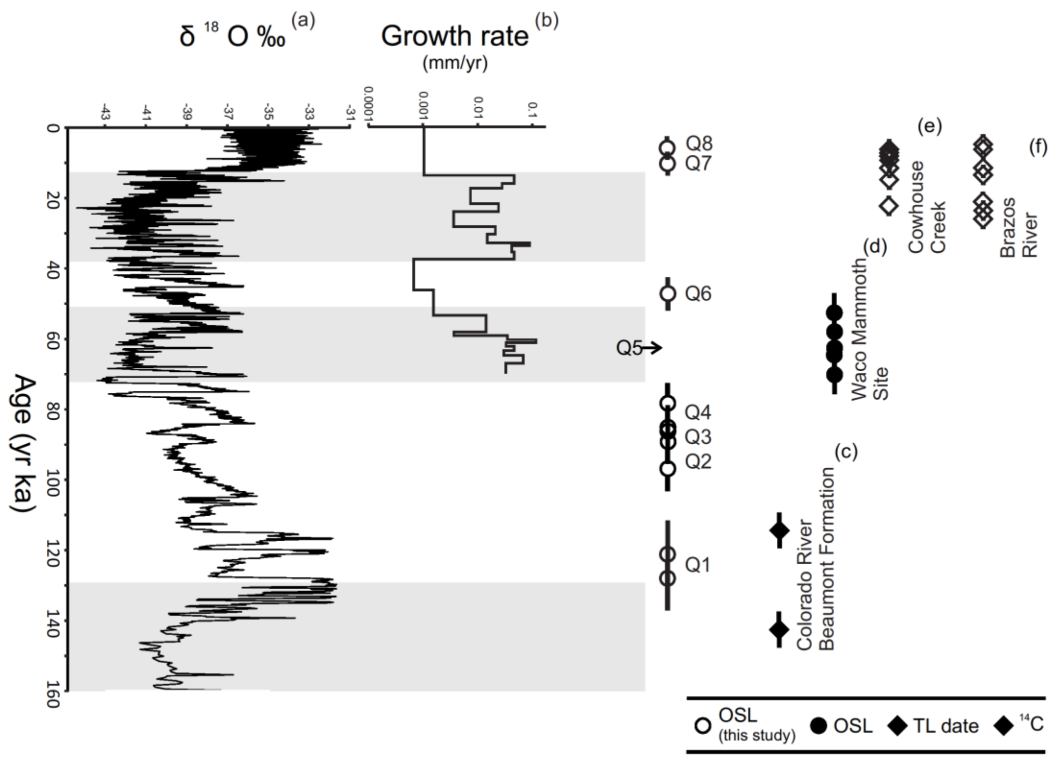

Fig. 2.5. Composite regional record compared to (a) GRIP oxygen isotopic profile in permil with respect to standard ocean water (SMOW) (Johnsen et al., 1997) and (b) record of speleothem growth rate (mm/yr) in central Texas (Musgrove et al., 2001). The central Texas fluvial record is compiled from Owl Creek (this study), (c) the Colorado River Beaumont Formation (Blum and Price, 1994), (d) Waco Mammoth Site (Bongino and Nordt, 2007) of the Bosque River, (e) Cowhouse Creek (Nordt, 2004), and the (f) Brazos River (Waters and Nordt, 1995). The gray intervals correspond to wet intervals as shown by correlating the (b) speleothem record and the (a) GRIP oxygen isotopic profile, with the 160 kae130 ka based only on the GRIP record.

5.2.2. MIS 4 to early MIS 2 (~74-20 ka)

This interval spans glacial and interstadial periods with sea level most likely 30-120 m below present sea level (Anderson et al., 2004; Siddall et al., 2009; Thomas et al., 2009; Lambeck et al., 2012). Previous research has identified valley fill complexes known as the Deweyville Formation, ranging from ca. 74 to 12 ka (Blum and Valastro, 1989, 1992; Blum and Price, 1998; Blum and Aslan, 2006; Sylvia and Galloway, 2006). Regional deposition at the confluence of the Brazos and Bosque rivers at the Waco Mammoth Site has preserved overbank sediments deposited between ca. 73 and 52 ka (Bongino and Nordt, 2007). An isotopic record of organic carbon for sediment and buried soils suggests a cool, wet environment spanning this interval (Bongino and Nordt, 2007). Interestingly, incision has been documented in the lower Mississippi Valley for the MIS 5 to 4 transition (Shen et al., 2012), linked to the w80 m fall in sea level (Waelbroeck et al., 2002; Thomas et al., 2009).

There appears to have been significant fluctuations in stream base level for Owl Creek between ca. 50 and 20 ka ago. Unit Q5 is not directly dated but was probably deposited early in this interval, ca. 50 ka based on bracketing OSL ages (Fig. 2.5, Table 2.6). During this time, the surface soils capping Q2, Q4, and Q5 at Owl Creek began to form similar pedogenic features, indicating isolation of these surfaces with stream degradation in close succession. The formation of a calcrete in these soils suggests a semi-arid climate, though with distinct wet and dry seasons (cf. Breecker et al., 2009). Sometime before ca. 44 ka there was a period of pronounced erosion removing over 4 m of bedrock and alluvium. Erosion of this magnitude would likely be accompanied by an increase in stream competency, possibly reflecting increased discharge. Deposition at Owl Creek resumed at ca. 44 ka (unit Q6), and may be broadly coherent with the initiation of aggradation at ca. 33 ka for other lower order streams in central Texas such as Buttermilk Creek (Waters et al., 2011), in west central Texas such as the Pedernales River (Blum and Valastro, 1989) and in south central Texas such as the Medina River (Mandel et al., 2007). Speleothem records from central Texas indicate wetter periods from ca. 39 to 33 ka and 24 to 13 ka (Musgrove et al., 2001). Generally, wet periods in central Texas during the Late Pleistocene correspond to glacial or stadial intervals that are usually concomitant with meltwater pluses entering the Gulf of Mexico and inferred ice sheet volumes >75% of the last glacial maximum (Joyce et al., 1993; Anderson et al., 2004; Tripsanas et al., 2007). Glacial cooling of sea surface temperatures in the North Atlantic would have suppressed moisture flux into central North American in the summer (Maasch and Oglesby, 1990; Bromwich et al., 2004; Pu et al., 2012); whereas winter conditions appear wetter with a southerly displaced consolidated Jet Stream (Kutzbach and Guetter, 1986; Bromwich et al., 2004; Asmerom et al., 2010). There is compelling evidence for the expansion of the Laurentide ice sheet into mid-continental North America ca. 53 and 31 ka from meltwater pulses entering the Gulf of Mexico at (Tripsanas et al., 2007) and other proxy records (Dorale et al., 1998; Bettis et al., 2003; Rittenour et al., 2007; Wood et al., 2010). Variable limits of the Laurentide Ice Sheet ca. 55e30 ka propagated hydrologic and vegetation changes in central Texas (e.g. Kutzbach and Guetter, 1986; Bromwich et al., 2004), which may have led to base level changes with prominent erosional event(s) preceding deposition for Owl Creek and other tributaries in central Texas (Mandel et al., 2007; Waters et al., 2011).

5.2.3. MIS 2 to present (~20 ka to present)

The last 20 ka corresponds to late in the last glacial maximum and the Holocene, with sea level rising from 120 m to present level by ca. 5 ka (Anderson et al., 2004). This period is characterized by coastal aggradation along the Nueces (Durbin et al., 1997), Colorado (Blum and Price, 1998), and Brazos rivers (Sylvia and Galloway, 2006; Taha and Anderson, 2008) with deposition of overbank fines and intermittent soil development, which were subsequently buried. There are numerous proxy climate records spanning the past 20 ka in from central Texas (Bousman, 1998; Musgrove et al., 2001; Ellwood and Gose, 2006) and fluvial records from the Brazos River valley in central Texas (Waters and Nordt, 1995; Nordt, 1995, 2004), which serve as metrics of comparison to the Owl Creek record (Fig. 2.6).

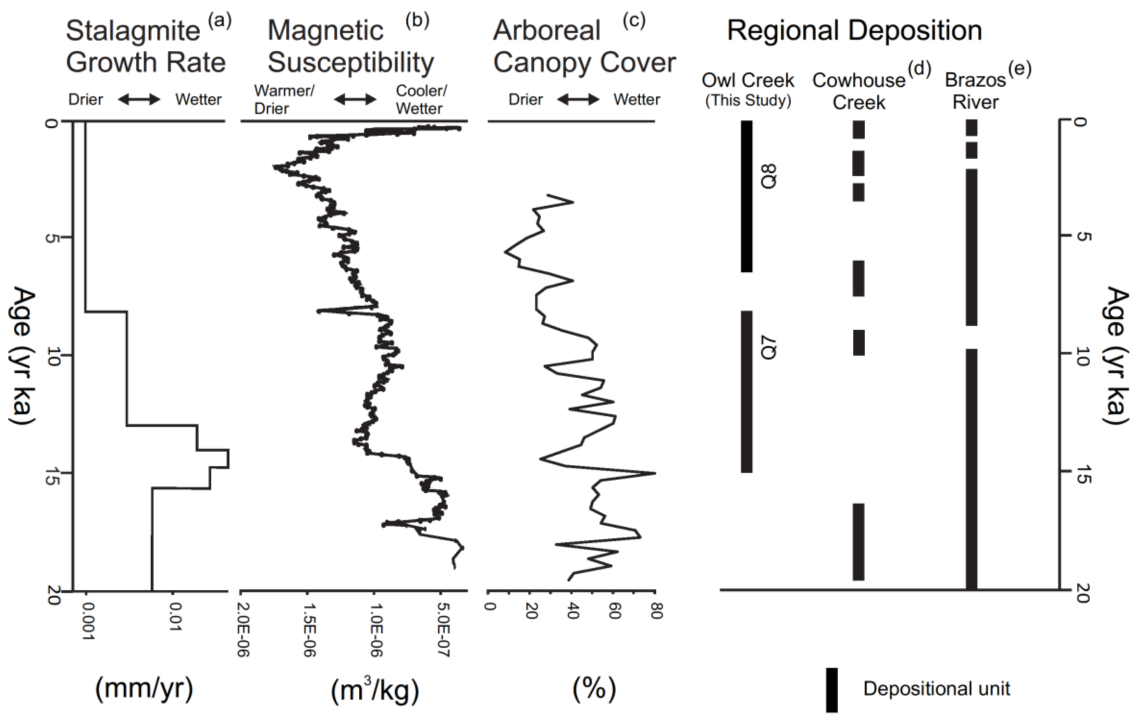

Fig. 2.6. Composite regional environmental and fluvial record for the past 20 ka compiled from (a) stalagmite growth rate (Musgrove et al., 2001); (b) magnetic susceptibility (Ellwood and Gose, 2006); (c) arboreal canopy cover (Bousman, 1998); this study; (d) Cowhouse Creek (Nordt, 2004); and (e) the Brazos River (Waters and Nordt, 1995).

A sequence of fine-grained overbank sediments associated with Buttermilk Creek, a first-order tributary of the Brazos River, shows nearly continuous deposition from ca. 33 ka to 1 ka, though there are increased rates of aggradation ca. 16-14 ka and 12.9-12.0 ka (Waters et al., 2011). Aggradation of the central Texas section of the Brazos River occurred sometime between ca. 20 and 9.4 ka, with the later age derived from a buried soil (Waters and Nordt, 1995). In contrast, the sedimentary records from Cowhouse and Owl creeks suggest periods of non-deposition or slight erosion ca. 15 ka. These erosional intervals occurred in Cowhouse Creek and Owl Creek sometime between ca. 18 and 10 ka and ca. 44 and 12 ka, respectively (Nordt, 2004). This variable response of lower order tributaries indicate at the sub-basin scale intrinsic variables such as sediment availability and runoff can yield various threshold responses for streams, yet more data is needed (cf. Bull, 1979). Interestingly, this variable response of tributaries between ca.16 and 12 ka is broadly coincident with substantial and variable meltwater input into the Gulf of Mexico with rapid northward retreat of the Laurentide ice sheet (Williams et al., 2010, 2012). Significant meltwater delivery ceased by 12.5 ka. However, high resolution marine sediment records from the Gulf of Mexico show no appreciable cooling during deglacial meltwater events (Williams et al., 2010, 2012), though broader scale cooling of the North Atlantic appears to suppress summer precipitation and temperatures into mid-continental N. America (cf. Bromwich et al., 2005). Ice sheet-climate modeling indicates that wetter and colder conditions prevailed in winter with the southerly position of the consolidated Jet Stream (Bromwich et al., 2004), which is consist with a variety of proxy climatic data from ca. 20 to 14 ka from the southwestern U.S. into Texas (Fig. 2.6) (Nordt et al., 1994; Bousman, 1998; Musgrove et al., 2001; Ellwood and Gose, 2006). The mean pathway of this Jet Stream migrates northward as the Laurentide ice sheet retreated (cf. Wang et al., 2012) with ensuing drying and warming in central Texas by ca. 10 ka (Nordt et al., 1994; Musgrove et al., 2001).

An ubiquitous stratigraphic marker in fluvial sequences in central Texas is a distinct zone of pedogenesis identified along the Brazos River (A&M soil), Cowhouse Creek (Royalty buried soil), Henson Creek (Royalty buried soil), and buried soils within unit Q7 from Owl Creek (Nordt, 1995, 2004; Waters and Nordt, 1995). These paleosols are associated with ameliorated climate conditions in the early Holocene, ca. 9.5e7 ka (Nordt et al., 1994; Musgrove et al., 2001). The Royalty paleosol developed incrementally preserving a single cumulic solum (Nordt, 1995, 2004). The P4, P5, and P6 buried soils may be coeval with the Royalty paleosol and reflect three brief periods of aggradation and subsequent stability. Fluvial aggradation resumed by ca. 7 ka for the Brazos River, Cowhouse, Henson and Owl creeks (Nordt, 1995, 2004; Waters and Nordt, 1995). The Owl Creek sequence indicates continuous aggradation through the late Holocene, based on the preservation of unit Q8 and recent down cutting in the past ca. 3 ka.

6. Conclusions

Integrated study of depositional facies in a low order drainage basin in central Texas, utilizing stratigraphy, sedimentology, soil morphology, and OSL chronology reveals a complex series of erosion, deposition, and soil-forming events during the past ca. 120 ka providing the first systematic glimpse into the late Pleistocene of central Texas. The trends in sedimentation, pedogenesis, and erosion at Owl Creek preserve an archive of valuable information about complex climate-stream basin history. Comparison of these records among streams within the Brazos River valley provides insight to regional-scale landscape development. At least six aggradation and degradation cycles assessed for Owl Creek during the late Pleistocene to Holocene indicates the importance of intrinsic factors, like sediment supply and local runoff, but broader scale climate change associated with the growth and decay of the Laurentide ice sheet are critical for fluvial erosion, deposition and preservation within central Texas.

The use of stratigraphy, soil characterization, and OSL chronology in the Owl Creek basin results in the following conclusions: (1) the preserved sequence of colluvial and fluvial deposits within the low-order tributary are evidence of an evolving sedimentary record, adding to the research potential of similar streams that may have similar, but unknown, environmental records; (2) the regional depositional record for central Texas is sparse during 120-~75 ka interval with Owl Creek strata (Q1-Q4) showing alternating colluvial and fluvial deposition with multiple erosional events; (3) Owl Creek deposits (Q5) during 75-50 ka interval are responding to a cool, wet climate, with high competency fluvial deposition (Q6) continuing at 44 ka; (4) noted periods of erosion at Owl Creek likely relate to intrinsic geomorphic instability from a wet climate; (5) aggradation and geomorphic stability (Q7) and subsequent pedogenesis in the warmer Holocene climate are likely responses to intrinsic mechanisms, as regional basins responded independently during this time; (6) Owl Creek deposition at 8 ka (Q8) was initiated by a regionally identified warming trend within the Holocene, with major subsequent incision associated with a warm, dry climate; (7) deposition at Owl Creek was affected by intrinsic factors, with climate acting as a driving mechanism based on the integration of regional fluvial systems, and (8) integrated with the records at Cowhouse Creek and the Brazos River, this study provides a sediment chronology from the Pleistocene into the Holocene with the regional systems responding independently to climate and intrinsic geomorphic thresholds.

Acknowledgments

Baylor University and the Luminescence Dating Research Laboratory at the University of Illinois at Chicago generously supported this research. Work at Owl Creek was undertaken with the permission of the Fort Hood Cultural Resource Management Team and generous assistance from Sunny Wood and Karl Kleinbach. The resources and support for Donna Prochaska and Dr. T. Hallmark from the Soil Characterization Lab at TAMU was invaluable. We also appreciate the field assistance from Will Torsch

(Louisiana State University), Gary Stinchcomb (Baylor University), Jason Mintz (Anardako Petroleum Corporation), Gordon Magenheim, and Lauren Michel (Baylor University). Dr. C. B. Bousman (Texas State University), Ryan S. Dhillon (Queen's University), and Aislyn Trendell (Anardako Petroleum Corporation) provided helpful comments on early drafts. We acknowledge the helpful reviews provided by R. Mandel, J. Wallinga, and N. Catto, which greatly improved the manuscript.

References

Abdullah, K.C., Anderson, J.A., Snow, J.N., Holdford-Jack, L., 2004. The late Quaternary Brazos and Colorado deltas, offshore Texas d their evolution and factors that controlled their development. In: Anderson, J.B., Fillon, R.H. (Eds.), 2004. Late Quaternary Stratigraphic Evolution of the Northern Gulf of Mexico Margin, vol. 64. SEPM Special Publication, pp. 237-269.

Anderson, J.B., Rodriguez, A., Abdulah, K.C., Fillon, R.H., Banfield, L.A., McKeown, H.A., Wellner, J.S., 2004. Late Quaternary stratigraphic evolution of the northern Gulf of Mexico margin: a synthesis. In: Anderson, J.B., Fillon, R.H. (Eds.), Late Quaternary Stratigraphic Evolution of the Northern Gulf of Mexico Margin, vol. 64. SEPM Special Publication, pp. 1-23.

Asmerom, Y., Polyak, V.J., Burns, S.J., 2010. Variable winter moisture in the south-western United States linked to rapid glacial climate shifts. Nature Geoscience 3, 114-117.

Barnes, V.E., 1970. Geologic Atlas of Texas: Waco Sheet. Bureau of Economic Geology, University of Texas, Austin.

Bettis, E.A., Muhs, D.R., Roberts, H.M., Wintle, A.G., 2003. Last Glacial loess in the continuous USA. Quaternary Science Reviews 22, 1907-1946.

Berger, G.W., 1990. Effectiveness of natural zeroing of the thermoluminescence of sediments. Journal of Geophysical Research 95, 12375-12397.

Blum, M.D., Aslan, A., 2006. Signatures of climate vs. sea-level change within incised valley-fill successions: Quaternary examples from the Texas Gulf Coast. Sedimentary Geology 190, 177-211.

Blair, T.C., McPherson, J.G., 1994. Alluvial fans and their natural distinction from rivers based on morphology, hydraulic processes, sedimentary processes, and facies assemblages. Journal of Sedimentary Research 64, 450-489.

Blikra, L.H., Nemec, W., 1998. Postglacial colluvium in western Norway: deposi- tional processes, facies and palaeoclimatic record. Sedimentology 45, 909-959.

Blum, M.D., Price, D.M., 1998. Quaternary alluvial plain construction in response to glacioeustatic and climatic controls, Texas Gulf Coastal Plain. In: Shanley, K.W., McCabe, P.J. (Eds.), Relative Role of Eustacy, Climate, and Tectonism in Continental Rocks. Special Publication Society of Economic Paleontologists and Mineralogists, pp. 31-48. http://dx.doi.org/10.2110/pec.98.59.0031.
Blum, M.D., Toomey III, R.S., Valastro Jr., S., 1994. Fluvial response to Late Quaternary climatic and environmental change, Edwards Plateau, Texas. Palaeogeography, Palaeoclimatology, Palaeoecology 108, 1-21. http://dx.doi.org/10.1016/0031-0182(94)90019-1.
Blum, M.D., Valastro, S., 1989. Response of the Pedernales River of Central Texas to late Holocene climatic change. Annals of the Association of American Geographers 79, 435-456. http://dx.doi.org/10.1111/j.1467-8306.1989.tb00271.x.
Blum, M.D., Valastro, S., 1992. Quaternary stratigraphy and geoarchaeology of the Colorado and Concho rivers, west Texas. Geoarchaeology 7, 419-448. http://dx.doi.org/10.1002/gea.3340070502.
Blum, M.D., Price, D.M., 1994. Glacioeustatic and climatic controls on Quaternary alluvial plain deposition, Texas coastal plain. Gulf Coast Association of Geological Societies Transactions 44, 85-92.
Blum, M.D., Valastro, S., 1994. Late quaternary sedimentation, lower Colorado River, Gulf Coastal Plain of Texas. Geological Society of America Bulletin 106, 1002-1016. http://dx.doi.org/10.1130/0016-7606(1994)106<1002:LQSLCR>2.3.CO;2.
Bomar, G.W., 1983. Texas Weather.University of Texas Press, Austin.
Bongino, J.D., Nordt, L.C., 2007. Late Quaternary History of the Waco Mammoth Site: Environmental Reconstruction and Interpreting the Cause of Death (MA thesis). Baylor University, Waco, Texas.
Botter-Jensen, L., Bulur, E., Duller, G.A.T., Murray, A.S., 2000. Advances in luminescence instrument systems. Radiation Measurements 32, 523-528.
Bousman, C., 1998. Paleoenvironmental change in central Texas: the palynological evidence. Plains Anthropologist 43, 201-219.
Breecker, D., Sharp, Z., McFadden, L., 2009. Seasonal bias in the formation and stable isotopic composition of pedogenic carbonate in modern soils from New Mexico, USA. Geological Society of America Bulletin 121 (3/4), 630-640.
Bromwich, D.H., Toracinta, E.R., Oglesby, R.J., Fastook, J.L., Hughes, T.J., 2004. Polar MM5 simulations of the winter climate of the Laurentide Ice Sheet at the LGM. Journal of Climate 17 (17), 3415-3433.
Bromwich, D.H., Toracinta, E.R., Oglesby, R.J., Fastook, J.L., Hughes, T.J., 2005. LGM summer climate on the southern margin of the Laurentide Ice Sheet: wet or dry? Journal of Climate 18 (16), 3317-3338.
Buck, B.J., Monger, H.C., 1999. Stable isotopes and soil-geomorphology as indicators of Holocene climate change, northern Chihuahuan Desert. Journal of Arid Environments 43, 357-373. http://dx.doi.org/10.1006/jare.1999.0584.
Bryan, K., 1940. Gully gravure e a method of slope retreat. Journal of Geo- morphology 3, 331-344.
Bull, W.B., 1979. Threshold of critical power in streams. Geological Society of America Bulletin 90, 453-464.

Candy, I., Black, S., Sellwood, B.W., 2004. Quantifying time scales of pedogenic calcrete formation using U-series disequilibria. Sedimentary Geology 170, 177-187. http://dx.doi.org/10.1016/j.sedgeo.2004.07.003.

Cleveland, D.M., Atchley, S.C., Nordt, L.C., 2007. Continental sequence stratigraphy of the Upper Triassic (Norian-Rhaetian) Chinle strata, northern New Mexico, USA: allocyclic and autocyclic origins of paleol-bearing alluvial successions. Journal of Sedimentary Research 77, 909-924. http://dx.doi.org/10.2110/jsr.2007.082.

Curry, B.B., Baker, R.G., 2000. Palaeohydrology, vegetation, and climate since the late Illinois episode (~130 ka) in south-central Illinois. Palaeogeography, Palaeoclimatology, Palaeoecology 155, 59-81.

Dietrich, W.E., Dunne, T., 1978. Sediment budget for a small catchment in mountainous terrain. Zeitschrift fur Geomorphologie Supplementband 29, 191-206.

Dorale, J.A., Edwards, R.L., Ito, M., González, L.A., 1998. Climate and vegetation history of the midcontinent from 75 to 25 ka: a speleothem record from Crevice Cave, Missouri, USA. Science 282, 1871-1874.

Dorale, J.A., Wozniak, L.A., Bettis III, E.A., Carpenter, S.J., Mandel, R.D., Hajic, E.R., Lopinot, N.H., Ray, J.H., 2010. Isotopic Evidence for Younger Dryas Aridity in the North American Midcontinent Geology, vol. 38, pp. 519-522.

Duller, G.S.T., Bøtter-Jensen, L., Murray, A.S., 2003. Combining infrared- and green-laser stimulation sources in single-grain luminescence measurements of feld- spar and quartz. Radiation Measurements 37, 543-550.

Duller, G.A.T., 2008. Single-grain optical dating of Quaternary sediments: why aliquot size matter in luminescence dating. Boreas 37, 589-612. http://dx.doi.org/10.1111/j.1502-3885.2008.00051.x.

Durbin, J.M., Blum, M.D., Price, D.M., 1997. Late Pleistocene stratigraphy of the Nueces River, Corpus Christi, Texas: climatic and glacio-eustatic control on valley fill architecture. Transactions of the Gulf Coast Association of Geological Societies 47, 119-130.

Ellwood, B.B., Gose, W.A., 2006. Heinrich H1 and 8200 yr B.P. climate events recorded in Hall's Cave, Texas. Geology 34, 753-756. http://dx.doi.org/10.1130/G22549.1.

Fain, J., Soumana, S., Montret, M., Miallier, D., Pilleyre, T., Sanzelle, S., 1999. Luminescence and ESR dating Beta-dose attenuation for various grain shapes calculated by a Monte-Carlo method. Quaternary Science Reviews 18, 231-234. http://dx.doi.org/10.1016/S0277-3791(98)00056-0.

Forman, S.L., 1990. Thermoluminescence properties of fiord sediments from Engelskbukta, western Spitsbergen, Svalbard: a new tool for deciphering depositional environment? Sedimentology 37, 377-384.

Galbraith, R.F., Roberts, R.G., Laslett, G.M., Yoshida, H., Olley, J.M., 1999. Optical dating of single and multiple grains of quartz from Jinmium rock shelter, northern Australia, part 1, experimental design and statistical models. Archaeometry 41, 339-364.

Galbraith, R.F., Roberts, R.G., 2012. Statistical aspects of equivalent dose and error calculation and display in OSL dating: an overview and some recommendations. Quaternary Geochronology 11, 1-27.

Germanoski, D., Schumm, S.A., 1993. Changes in braided river morphology resulting from aggradation and degradation. The Journal of Geology 101, 451-466.
Gile, L.H., Peterson, F.F., Grossman, R.B., 1966. Morphological and genetic sequences of carbonate accumulation in desert soils. Soil Science 101, 47-360.
Gile, L.H., Hawley, J.W., Grossman, R.B., 1981. Soils and Geomorphology in the Basin and Range Area of Southern New-Mexico. New Mexico Bur. Mines and Mineral Resources.
Hall, S.A., Boutton, T.W., Lintz, C.R., Baugh, T.G., 2012. New correlation of stable carbon isotopes with changing late-Holocene fluvial environments in the Trinity River Basin of Texas, USA. The Holocene 22, 541-549. http://dx.doi.org/10.1177/0959683611427338.
Harvey, A.M., 2012. The coupling status of alluvial fans and debris cones: a review and synthesis. Earth Surface Processes and Landforms 37, 64-76. http://dx.doi.org/10.1002/esp.2213.
Huckabee, J.W.J., Thompson, D.R., Wyrick, J.C., Pavlat, E.G., 1977. Soil Survey of Bell County, Texas. US Department of Agriculture, Natural Resources Conservation Service, Washington, D.C.
Johnsen, S.J., Clausen, S.J., Dansgaard, W., Gundestrup, N.S., Hammer, C.U., Andersen, U., Andersen, K.K., Hvidberg, C.S., Dahl-Jensen, D., Steffensen, J.P.,
Shoji, H., Sveinbjörnsdóttir, A.E., White, J.W.C., Jouzel, J., Fisher, D., 1997. The d180 record along the Greenland Ice Core Project deep ice core and the problem of possible Eemian climatic instability. Journal of Geophysical Research 102, 26471e26487. http://dx.doi.org/10.1029/97JC00167.
Joyce, J.E., Tjalsma, L.R.C., Prutzman, J.M., 1993. North American glacial meltwater history for the past 2.3 m.y.: oxygen isotope evidence from the Gulf of Mexico. Geology 21, 483-486.
Kraimer, R.A., Monger, H.C., 2009. Carbon isotopic subsets of soil carbonateda particle size comparison of limestone and igneous parent materials. Geoderma 150, 1-9. http://dx.doi.org/10.1016/j.geoderma.2008.11.042.
Kutzbach, J.E., Guetter, P.J., 1986. The influence of changing orbital parameters and surface boundary conditions on climate simulations for the past 18,000 years. Journal of Atmospheric Science 43 (16), 1726-1759.
Lambeck, K., Purcell, A., Dutton, A., 2012. The anatomy of interglacial sea levels: the relationship between sea levels and ice volumes during the Last Interglacial. Earth and Planetary Science Letters 315-316, 411.
Maasch, K.A., Oglesby, R.J., 1990. Meltwater cooling of the Gulf of Mexico: a GCM simulation of climatic conditions at 12 ka. Paleoceanography 5, 977-996.
Machette, M.N., 1985. Calcic soils of the southwestern United Stated. In: Weide, D.L. (Ed.), Soils and Quaternary Geology of the Southwestern United States, Special Paper 203. Geological Society of America, Boulder, pp. 1-21.
Mandel, R.D., Jacob, J.S., Nordt, L.C., 2007. Geoarchaeology of the Richard Beene Site. In: Thoms, A.V., Mandel, R.D. (Eds.), Archaeological and Paleoecological Investigations at the Richard Beene Site (41BX831), South Central Texas, Center for Ecological Archaeology, Reports of Investigations No. 8. Texas A&M Uni- versity, College Station, Texas, pp. 27-60.

Martinson, D.G., Pisias, N.G., Hays, J.D., Imbrie, J., Moore, T.C., Shackleton, N.J., 1987.Age dating and the orbital theory of the ice ages: development of a high-resolution 0 to 300,000-year chrono-stratigraphy. Quaternary Research 27, 1-29.

Mejdahl, V., Christiansen, H.H., 1994. Procedures used for luminescence dating of sediments. Boreas 13, 403-406.

Miall, A.D., 1978. Lithofacies types and vertical profile models in braided river deposits: a summary. In: Miall, A.D. (Ed.), 1978. Fluvial Sedimentology, vol. 5. Canadian Society of Petroleum Geologists, pp. 598-604.

Miall, A.D., 1992. Alluvial deposits. In: Walker, R.G. (Ed.), Facies Models: Response to Sea Level Change. Geological Association of Canada, St. John's, Newfoundland, pp. 119-142.

Miall, A.D., 2006. The Geology of Fluvial Deposits: Sedimentary Facies, Basin Analysis, and Petroleum Geology. Springer, New York, p. 582.

Mills, H.H., 1981. Boulder deposits and the retreat of mountain slopes, or "gully gravure" revised. Journal of Geology 89, 81-179. Murray, A.S., Wintle, A.G., 2003. The single aliquot regenerative dose protocol: potential for improvements in reliability. Radiation Measurements 37, 377-381.

Musgrove, M., Banner, J.L., Mack, L.E., Combs, D.M., James, E.W., Cheng, H., Edwards, R.L., 2001. Geochronology of late Pleistocene to Holocene speleothems from Central Texas: implications for regional paleoclimate. Geological Society of America Bulletin 113, 1532-1543. http://dx.doi.org/10.1130/0016-76006(2001) 113<1532:GOLPTH>2.0.CO;2.

Nordt, L.C., 1992. Archaeological Geology of the Fort Hood Military Reservation, Fort Hood, Texas. In: U.S. Army Fort Hood, Archaeological Resource Management Series. Research Report 25, Fort Hood.

Nordt, L., 1995. Geoarchaeology of Henson Creek: a low-order tributary in Central Texas. Geoarchaeology 10, 205-221.

Nordt, L., 2004. Late quaternary alluvial stratigraphy of a low-order tributary in central Texas, USA and its response to climate and sediment supply. Quaternary Research 62, 289-300. http://dx.doi.org/10.1016/j.yqres.2004.07.004.

Nordt, L.C., Boutton, T.W., Hallmark, C.T., Waters, M.R., 1994. Late Quaternary vegetation and climate changes in Central Texas based on the isotopic composition of organic carbon. Quaternary Research 4, 109-120.

Nordt, L.C., Boutton, T.W., Jacob, J.S., Mandel, R.D., 2002. C4 plant productivity and climate-CO2 variations in South-Central Texas during the Late Quaternary. Quaternary Research 58, 182-188.

Nordt, L.C., Hallmark, C.T., Wilding, L.P., Boutton, T.W., 1998. Quantifying pedogenic carbonate accumulations using stable carbon isotopes. Geoderma 82, 115-136. http://dx.doi.org/10.1016/S0016-7061(97)00099-2.

Olley, J.M., Pietsch, T., Roberts, R.G., 2004. Optical dating of Holocene sediments from a variety of geomorphic settings using single grains of quartz. Geo- morphology 60, 337-358. http://dx.doi.org/10.1016/j.geomorph.2003.09.020.

Prescott, J.R., Hutton, J.T., 1994. Cosmic ray contributions to dose rates for luminescence and ESR dating: large depths and long-term time variations. Radiation Measurements 23, 497-500.

Pu, B., Vizy, E.K., Cook, K.H., 2012. Warm season response over North America to a shutdown of the Atlantic meridional overturning circulation and CO2 in- creases. Journal of Climate 25, 6701-6720. http://dx.doi.org/10.1175/JCLI-D-11-00611.1.

Rittenour, T.M., Blum, M.D., Goble, R.J., 2007. Fluvial evolution of the lower Mississippi River valley during the last 100 k.y. glacial cycle: response to glaciations and sea-level change. Geological Society of America Bulletin 119, 586-608.

Schoeneberger, P.J., Wysocki, D.A., Benham, E.C., Broderson, W.D., 2002. Field Book for Describing and Sampling Soils, Version 2.0. Natural Resources Conservation Service, National Soil Survey Center, Lincoln, NE.

Schumm, S.A., 1999. Causes and controls of channel incision. In: Darby, S.E., Simon, A. (Eds.), Incised River Channels: Processes, Forms, Engineering, and Management. John Wiley and Sons. Inc., New York, pp. 19-33.

Siddall, M., Stocker, T.F., Clark, P.U., 2009. Constraints on future sea-level rise from past sea- level change. Nature Geoscience 2, 571-575.

Shen, Z., Törnqvist, T.E., Autin, W.J., Mateo, Z.R.P., Straub, K.M., Mauz, B., 2012. Rapid and widespread response of the Lower Mississippi River to eustatic forcing during the last glacial-interglacial cycle. Geological Society of America Bulletin 124 (5-6), 690-704. http://dx.doi.org/10.1130/b30449.1.

Soil Survey Staff, 1996. Soil Survey Laboratory Methods Manual. Soil Survey Investigations. Report No. 42. US Government Printing Office, Washington, D.C.. Version 3.0.

Soil Survey Staff, 2010. Keys to Soil Taxonomy, 11th ed. US Government Printing Office, Washington, D.C., p. 331

Soil Survey Staff, 2012. Natural Resources Conservation Service, United States Department of Agriculture. Web Soil Survey. Available online at: http://websoilsurvey.nrcs.usda.gov/ (accessed 16.03.12.).

Stanistreet, I.G., McCarthy, T.S., 1993. The Okavango fan and the classification of subaerial fan systems. Sedimentary Geology 85, 115-133. http://dx.doi.org/10.1016/0037-0738(93)90078-J.

Sylvia, D.A., Galloway, W.E., 2006. Morphology and stratigraphy of the late Quaternary lower Brazos valley: implications for paleo-climate, discharge and sediment delivery. Sedimentary Geology 190, 159-175. http://dx.doi.org/10.1016/j.sedgeo.2006.05.023.

Taha, Z.P., Anderson, J.B., 2008. The influence of valley aggradation and listric normal faulting on styles of river avulsion: a case study of the Brazos River, Texas, USA. Geomorphology 95, 429-448.

Thomas, A.I., Henderson, G.M., Deschamps, P., Yokoyama, Y., Mason, A.J., Bard, E., Hamelin Durand, N., Camoin, G., 2009. Penultimate deglacial sea- level timing from uranium/thorium dating of Tahitian corals. Science 324, 1186-1189.

Tripsanas, E.K., Bryant, W.R., Slowey, N.C., Bouma, A.H., Karageorgis, A.P., Berti, D., 2007. Sedimentological history of Bryant Canyon area, northwest Gulf of Mexico, during the last 135 kyr (Marine Isotope Stages 1e6): a proxy record of Mississippi River discharge. Palaeogeography, Palaeoclimatology, Palaeoecology 246, 137-161.

Waelbroeck, C., Labeyrie, L., Michel, E., Duplessy, J.C., Mcmanus, J.F., Lambeck, K., Balbon, E., Labracherie, M., 2002. Sea-level and deep water temperature changes derived from benthic foraminifera isotopic records. Quaternary Science Reviews 21, 295-305.
Wang, H., Stumpf, A.J., Miao, X., Lowell, T.V., 2012. Atmospheric changes in North America during the last deglaciation from dune-wetland records in the Mid- western United States. Quaternary Science Reviews 58, 124-134.
Waters, M.R., Forman, S.L., Jennings, T.A., Nordt, L.C., Driese, S.G., Feinberg, J.M., Keene, J.L., Halligan, J., Lindquist, A., Pierson, J., Hallmark, C.T., Collins, M.B., Wiederhold, J.E., 2011. The Debra L. Friedkin Site, Texas and the origins of Clovis. Science 331, 1599-1603.
Waters, M.R., Nordt, L.C., 1995. Late Quaternary floodplain history of the Brazos River in East-Central Texas. Quaternary Research 43, 311-319. http://dx.doi.org/10.1006/qres.1995.1037.
Williams, C., Flower, B.P., Hastings, D.W., Guilderson, T.P., Quinn, K., Goddard, E.A., 2010. Deglacial abrupt climate change in the Atlantic Warm Pool: a Gulf of Mexico perspective. Paleoceanography 115, PA4221. http://dx.doi.org/10.1029/2010PA001928.
Williams, C., Flower, B.P., Hastings, D.W., 2012. Seasonal Laurentide ice sheet melting during the "Mystery Interval" (17.5e14.5 ka). Geology 40, 955-958. http://dx.doi.org/10.1130/G33279.1.
Wintle, A.G., Murray, A.S., 2006. A review of quartz optically stimulated lumines- cence characteristics and their relevance in single-aliquot regeneration dating protocols. Radiation Measurements 41, 369-391.
Wood, J.R., Forman, S.L., Everton, D., Pierson, J., Gomez, J., 2010. Lacustrine sediments in Porter Cave, Central Indiana, USA and possible relation to Laurentide ice sheet marginal positions in the middle and late Wisconsinan. Palaeogeography, Palaeoclimatology, Palaeoecology 298 (3-4), 421-431.
Wright, V.P., 1990. Estimating rates of calcrete formation and sediment accretion in ancient alluvial deposits. Geological Magazine 127, 273-276.
Wright, D.K., Forman, S.L., Waters, M.R., Ravesloot, J.C., 2011. Holocene eolian activation as a proxy for broad-scale landscape change on the Gila River Indian Community, Arizona. Quaternary Research 76 (1), 10-21. http://dx.doi.org/10.1016/j.yqres.2011.04.008.

CHAPTER THREE

Interpretation of Late Quaternary climate and landscape variability based upon buried soil macro- and micromorphology, geochemistry, and stable isotopes of soil organic matter, Owl Creek, central Texas, USA

This chapter published as: Meier, H. A., Driese, S.G., Nordt, L.C., Forman, S.L., Dworkin, S.I., 2014. Interpretation of Late Quaternary climate and landscape variability based upon buried soil macro- and micromorphology, geochemistry, and stable isotopes of soil organic matter, Owl Creek, central Texas, USA. Catena, 114, 157-168.

Abstract

Small-basin floodplain buried soils formed in association with low-order tributary streams are valuable archives of past climates, but have not been studied extensively in central Texas, USA. Four buried soils exposed along Owl Creek, within the larger Brazos River drainage basin, were examined using soil morphology and micromorphology, optically stimulated luminescence (OSL) dating, soil characterization, whole-soil geochemical and stable isotope analyses of soil organic matter and pedogenic carbonate. These buried soils provide a record of changes in paleoecological and paleo-alluvial conditions spanning ~ 14 ky. Morphological and geochemical differences between buried soils reflect changes in landscape attributable to climate, with a distinct 5‰ increase in $\delta^{13}C$ values of soil organic matter corresponding to the Holocene onset and drier conditions. Paleoecological reconstructions coupled with depth to Bk suggest possible amounts of erosion of ~ 1 m for each of the buried soils. Compilation of the proxies

presented shows evidence for a cooler and wetter late Pleistocene climate, followed by a warmer and drier climate dominating during the Holocene.

1. Introduction

Buried soils developed from alluvial deposits in south-central North America can provide valuable environmental data for interpreting Late Pleistocene and Holocene climate conditions, when there was apparently significant moisture variability (e.g., Forman et al., 2001; Nordt et al., 2007). Exposures of pedogenically altered alluvial deposits in central Texas dating to this period are typically buried and few have a continuous exposure (Blum and Valastro, 1994; Mandel et al., 2007; Nordt, 1992, 1995, 2004; Nordt et al., 1994; Waters and Nordt, 1995; Waters et al., 2011). Previous analyses of alluvial deposits in central Texas streams focused on Holocene stratigraphy, profile description, and archeological preservation (Nordt, 1992, 1995, 2004; Nordt et al., 1994), with little emphasis on the dating of Pleistocene deposits, geo- chemical, and micromorphological features to aid in understanding associated pedogenesis. Recent work has focused on numerically dating sediment to identifying a depositional sequence that spans ca. the past 120 ka and developed during times of climatic instability (Meier et al., 2013).

The multi-centennial paleoecologic changes of the study area have primarily been reconstructed using stable carbon isotopes of soil organic matter (SOM). Nordt et al. (1994) concluded that during the late Pleistocene the plant communities contributing to the SOM pool recorded a cooler and/or wetter climate than modern based on stable isotope evidence for an abundance of C_3 plants. A warmer and drier climatic shift then occurred at the beginning of the Holocene and continued until around 6000 yr BP, with a peak in establishment of C_4 grasslands corresponding to the middle Holocene "Altithermal Event". Warm-season C_4 grasslands then decreased to near modern levels around 4000 yr BP as temperatures cooled (Nordt et al., 1994).

Buried soils identified at the Red Bluff exposure on Owl Creek in central Texas offer a unique opportunity to examine paleoecological and paleo-alluvial conditions in the latest Pleistocene and Holocene. Previous research in the Brazos River valley (Waters and Nordt, 1995), Cowhouse Creek (Nordt, 2004), Henson Creek (Nordt, 1995), and the current study at Owl Creek illustrates small-stream responses to climatic events, particularly those related to landscape stability and associated pedogenesis.

This study investigates four buried soils at the Red Bluff locality along Owl Creek using both macro- and micro-scale analyses, and synthesizes regional pedogenic events occurring in related large and small fluvial systems in this region. These data will be used to supplement previous stratigraphy (Meier et al., 2013) and isotopic work in the region (Nordt et al., 1994). The goals are: (1) to analyze the buried soils at Red Bluff using soil morphology and micromorphology, in conjunction with standard soil characterization data and bulk geochemical data, 2) to use bulk soil organic matter (SOM) and stable carbon isotopes ($\delta^{13}C$) to interpret changes in paleovegetation, paleoclimate and paleo-alluvial conditions at the time, (3) to apply geochemical weathering indices to estimate weathering intensity, and (4) to explore the paleoecological changes using multiple proxies with implications for the late Quaternary geological history in the greater central Texas region. The application of these techniques will further understanding of the depositional processes, and the pedogenic response to climate and other regional forcing mechanisms, with potential application for interpreting climate and landscape records at other late Quaternary localities.

2. Location and setting

Owl Creek is a small stream in central Texas with a drainage area of 72 km^2 located on the Fort Hood Military Reservation and flows in an easterly direction before terminating at Lake Belton (Fig. 3.1). The creek is within the larger Brazos River drainage valley and is comprised of eight depositional units that span the past 120 ka that are unconformable with the underlying Cretaceous-aged Walnut Clay Formation (Barnes, 1970; Meier et al., 2013). Regional climate is subhumid with hot summers and short, dry winters and with mean annual precipitation of 86 cm/yr (Bomar, 1983; Huckabee et al., 1977). The study section focuses on a late Quaternary exposure (T1 terrace) along Owl Creek that is inset within a larger outcrop, locally called “Red Bluff”. The outcrop is approximately 7 m high and 20 m wide on the south bank of Owl Creek (Fig. 3.1).

Previous research of Owl Creek and other fluvial systems on Fort Hood focused on the identification and preservation of deposits with archeological remains (Carlson, 1997; Carlson et al., 1986; Kleinbach et al., 1999; Mehalchick and Kibler, 2002; Mehalchick et al., 2000, 2003; Nordt, 1992; Trierweiler, 1994, 1996). Investigations at Owl Creek, at the same location of this study, identified one regionally extensive buried soil, informally named the “Royalty paleosol,” which yielded a calendar-corrected14C age on a bulk humate fraction of 13,230 ± 150 cal yr BP (GX15763 (Nordt, 1992). Radiocarbon assays on a humate fraction of soil organic matter from this region are problematic and tend to return ages 300 to 1700 years older than ages on corresponding charcoal samples (Nordt, 1992). Charcoal returned a calendar corrected ^{14}C age of 9240 ±

220 cal yr BP (Nordt, 1992) from the regionally extensive Royalty paleosol, along Cowhouse Creek, and is consistent with the humate age-overestimation. Recent research has refined Owl Creek stratigraphy and details sedimentation for the past 120 ka (Meier et al., 2013). The research will focus on four buried soils corresponding to the previously identified Q7 and Q8 depositional units (Meier et al., 2013).

3. Methods

One 5.5 m vertical profile was cleaned and described from the natural exposure along Owl Creek using standard USDA-NRCS (U.S. Department of Agriculture-Natural Resources Conservation Service). The previously described profile corresponds to Q6, Q7, and Q8 depositional units (Meier et al., 2013). Age control is provided by optically-stimulated luminescence (OSL) and ^{14}C dating (Meier et al., 2013; Nordt, 1992), with an additional OSL age obtained from the Cowhouse Creek type section to constrain the Royalty paleosol. The OSL age (UIC2904) follows the previously published methodology, single aliquot regenerative (SAR) protocols (Meier et al., 2013). The OSL ages were obtained by averaging ~ 30 separate, equivalent doses from respective aliquots of quartz grains and statistical analyses applying the central age model (Galbraith et al., 1999). The OSL age (UIC 2904) has overdispersion values ≤ 20%, which are routinely assessed for quartz grains that are well solar reset, like eolian sands (e.g., Olley et al., 2004; Wright et al., 2011) and the values are considered a threshold metric for calculation of a De value using the central age model of Galbraith et al. (1999). Equivalent dose values for selected OSL ages are presented in the context of shine down and radial plots that show the associated precision and relative standard error of the sample UIC2904 (Fig. 3.2).

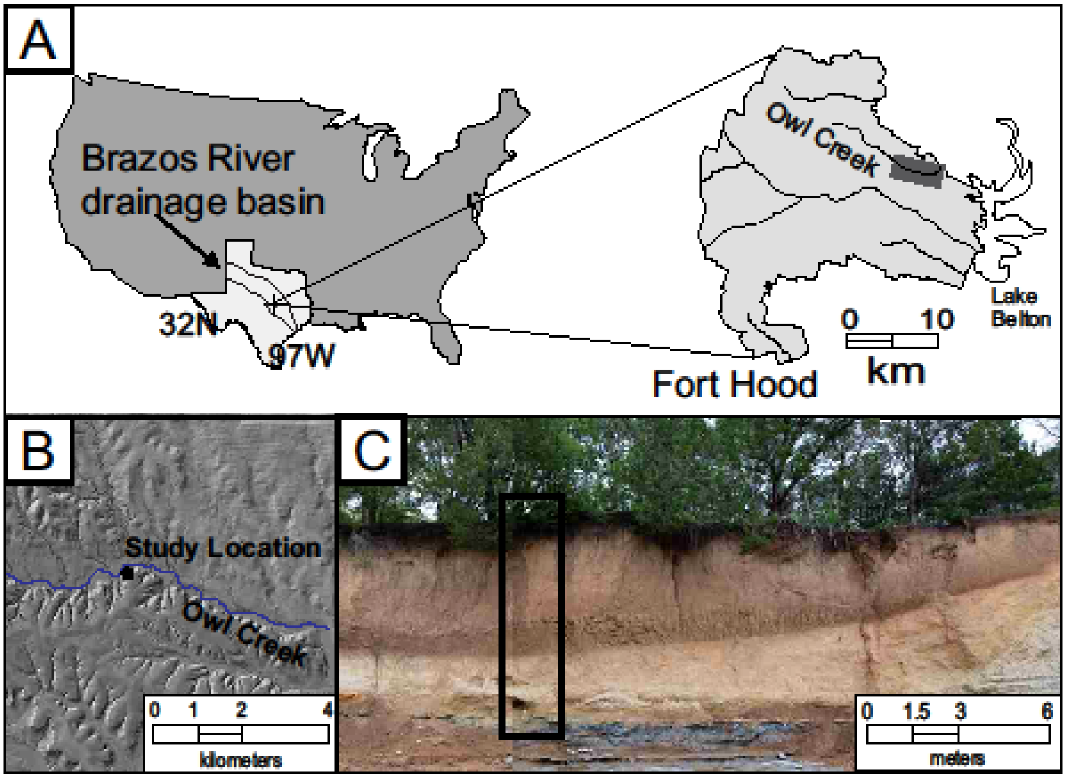

Fig. 3.1. Study area and outcrop location: (A) Map showing a portion of the Brazos River drainage basin and Owl Creek in central Texas, USA with a dark gray box to the right showing the location of the Digital Elevation Model (DEM) along Owl Creek; (B) DEM showing the location of study site along Owl Creek on the Fort Hood Military Reservation; (C) Pleistocene/Holocene outcrop with black box showing location of sampled buried soil profiles.

Oriented samples for thin sections were selected from the mid-point of major horizons, air-dried and then impregnated with epoxy, followed by commercial preparation for micromorphological analysis. Micromorphology was used to aid in paleoenvironmental interpretation based on the observed features indicating variations in soil- forming processes. Micromorphological descriptive terminology follows Brewer (1976), Fitzpatrick (1993), and Stoops (2003).

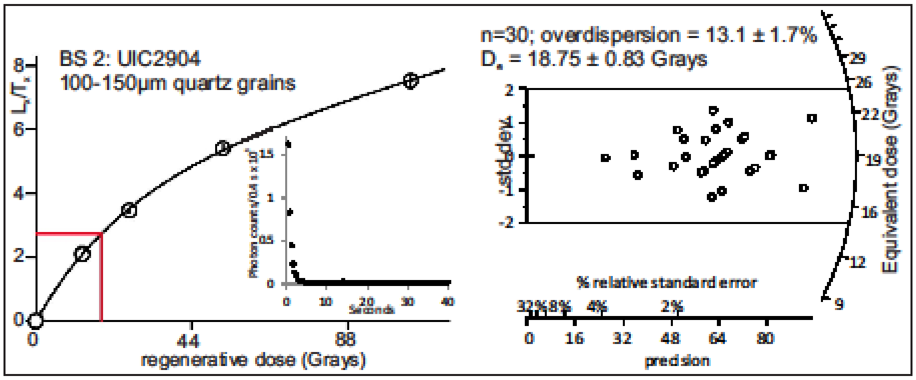

Fig. 3.2. Single aliquot regeneration (SAR) dose response curve, with inset figure showing representative shine down curve and radial plot of equivalent dose values for sample UIC2904.

Whole-soil and buried soil samples were oven-dried at 40 °C and milled in a shatterbox for commercial analysis by X-Ray fluorescence, ICP-AES, and ICP-MS at ALS-Chemex, Inc. Results were reported as element weight-percent, and oxide weight-percent were calculated from these data by normalizing to the molecular weight of each oxide for ratio analyses. Bulk geochemistry was examined to evaluate variable formation processes of the buried soils based on elemental proxies of base loss ($Al_2O_3/CaO + MgO + K_2O + Na_2O$), leaching (Ba/Sr), lessivage (Al_2O_3/SiO_2), calcification ($CaO + MgO/Al_2O_3$), salinization (Na_2O/K_2O), and parent material uniformity (Ti/Zr cross-plots) (Retallack, 2001). Base loss, leaching, lessivage, and salinization are indicators of soil drainage and chemical weathering, and can be used to infer relative changes in weathering attributable to climate change.

Bulk samples weighing approximately 200 g were collected from each genetic buried soil horizon for soil characterization, and for stable isotope analyses. In addition, smaller 20 g samples were collected from the buried soils at 10–20 cm intervals from 238 cm below the surface to the bedrock contact (Fig. 3.3) for bulk geochemical analyses. Oven-dried buried soil samples were prepared for stable carbon and oxygen isotopic analysis. The $\delta^{13}C$ values were measured from soil organic matter (SOM) prepared from the bulk geochemical samples. Pedogenic carbon- ate was removed from SOM $\delta^{13}C$ samples using a 2.5% HCl solution and following the aqueous method (Brodie et al., 2011; Komada et al., 2008). The samples were analyzed in the Baylor University stable isotope laboratory on a Thermo-Electron Delta V Advantage isotope ratio mass spectrometer configured with a combustion elemental analyzer (EA) for SOM $\delta^{13}C$. The $\delta^{13}C$ results were expressed as the standard per mil (‰) versus the Vienna PeeDee Belemnite (V-PDB) standard to deter- mine the relative contributions of C3 and C4 plants using a simple mixing model in which the isotope mixing line was calculated as:

$$\delta^{13}C_{soil} = (\delta^{13}C_{\ C4})\ (x) + (\delta^{13}C_{\ C3})\ (1\text{-}x) \qquad (1)$$

where δ^{13}Csoil is the SOM $\delta^{13}C$ of the buried soil samples, $\delta^{13}C$ C_4 is average $\delta^{13}C$ of C_4 plants (− 13‰), $\delta^{13}C$ C_3 is average $\delta^{13}C$ of C3 plants (− 27‰), x is fraction of vegetation that utilizes the C_4 photosynthetic pathway, and 1-x is the relative proportion of carbon derived from C_3 plants (Boutton, 1996). Modern C_4 communities are typically warm-season grasses, whereas C_3 plant communities are dominated by cool-season grasses, and by tree and desert shrubs that thrive in moist, cooler climates. The isotope mixing line was used to determine plant communities (the relative contributions of C_3 and C_4 plants) and to interpret paleoclimate, whereby greater contributions of C_4 plants to the soil biomass indicate drier conditions (Baker et al., 2001; Boutton, 1996; Driese et al., 2005; Nordt, 2004; Nordt et al., 1994, 2007). SOM $\delta^{13}C$ values have been found to correlate to paleo-temperatures (Nordt et al., 2007; Eq. (2)). Hall and Penner (2013) later adapted this paleo-temperature equation to the American Southwest determining mean annual temperature (MAT; Eq. (3)) and mean annual precipitation (MAP; Eq. (4)).

$$T\ (°C) = 0.685(\delta^{13}C)+34.9;\ r^2=0.67 \qquad (2)$$

$$MAT\ (°\ C) = -6.751+(0.809 \times \text{mean July temperature});\ r^2=0.94 \qquad (3)$$

$$MAP\ (mm) = 1208.220-(38.76 \times \text{mean July temperature});\ r^2=-0.81 \qquad (4)$$

The linkage of central Texas climate to southwestern U.S. has been noted by researchers (Bousman, 1998; Ellwood and Gose, 2006; Meier et al., 2013; Musgrove et al., 2001; Nordt et al., 1994) with the paleoecological approach proposed by Hall and Penner (2013) to semiarid grasslands. Pedogenic carbonate formation is a function of precipitation (cf. Jenny, 1941a; Jenny and Leonard, 1934) with Retallack developing a climofunction based on this relationship.

$$P = 137.24 + 6.54D + 0.013D^2;\ R^2 = 0.52\ \text{(Retallack, 2005)} \qquad (6)$$

The equation is based on the preservation of a complete soil profile with buried soil/paleosol preservation of a minimum of an A- over Bk- horizonation. In dynamic fluvial settings, soil truncation is common often preserving less erosive zones, such as Bk horizons. The selected study site, Owl Creek, shows preferential preservation of calcic horizons within the truncated soils, making “depth to Bk” soil measurements impossible. Yet reconfiguring the equation to solve to “depth to Bk” will allow for the estimation of soil truncation (D), when mean annual precipitation (MAP) can be determined. Here we have estimated MAP (Hall and Penner, 2013) (see Table 3.1) to evaluate potential erosion (E). The second degree polynomial equation (Eq. (6)) can be solved as:

$$E = -251.5385 + 38.4615(\sqrt{0.052P+35.6351}) \qquad (7)$$

$$E = -251.5385 - 38.4615(\sqrt{0.052P+35.6351})\ ) \qquad (8)$$

where E refers to the amount of potential erosion (cm) and P to MAP (mm). A cursory assessment of the proposed method was done using modern precipitation data with values of 860 mm/yr (Huckabee et al., 1977) and from weather data proximal to the study site (NOAA ID: 419419). The MAP values used in Eqs. (7) and (8) produce average erosion estimate values of 83.65 cm and − 600.5 cm respectively (See Appendix 3A). The negative value is a product of the second degree polynomial and will not be considered as a viable value. The potential erosion, E-value, should correlate to Bk horizons in modern soils. The calcic horizon depths from McLennan County soils (Miller, 2001) were recorded to have an average depth to Bk of 91.5 cm and appear correlated to the depth to Bk concept. This concept should be used with caution and provides a potential of erosion and may have less correlation in MAP values N 760 mm (Royer, 1999).

4. Results

The profile from Owl Creek consists of a surface soil and four buried soils, all of which overlie Cretaceous-aged Walnut Clay bedrock. The surface soil at the study area is mapped as the Topsey series (Schoeneberger et al., 2002; Soil Survey Staff, 2010). These strongly calcareous, alluvial soils are classified as fine-loamy, carbonatic, thermic Udic Calciustolls. At the study site the surface soil is a 300 cm thick, A-Bw1-Bw2-Bw3-C profile. The soil is unconformable with the underlying buried soil succession. The surface soil, and the stratigraphic interval in which it formed, were not examined for this study. The buried soils are ordered from oldest (BS 4) to youngest (BS 1) and span the late Pleistocene (~ 14 ka) to the Holocene (~ 8 ka), with the chronology based on previous OSL ages (Meier et al., 2013; Fig. 3.3A; Table 3.1). An additional OSL ages was taken to supplement the chronology for the study site along Owl Creek. The preserved buried soils have AB surface horizons, with characteristics of both horizons, and have been likely truncated by fluvial activity (Meier et al., 2013). Erosion of surface horizons impedes the classification of buried soils, yet the incorporation of techniques used in this study will assist in soil taxonomic classification.

Buried soil 4 (BS 4) developed in fine-grained alluvium and was in unconformable contact with coarse-grained alluvium (Fig. 3.3D; Table 3.1). Buried soil 4 is a yellowish brown (10YR 5/6) silty clay loam with pedogenic carbonate filaments and nodules (AB horizon) that increase at depth (Bk horizon, silty loam). The AB horizon was truncated by deposition of the overlying alluvium (Buried soil 3). An OSL age and interpreted deposition suggest that deposition was ongoing at ~ 14 ka (Meier et al., 2013; Fig. 3.4 and Table 3.2).

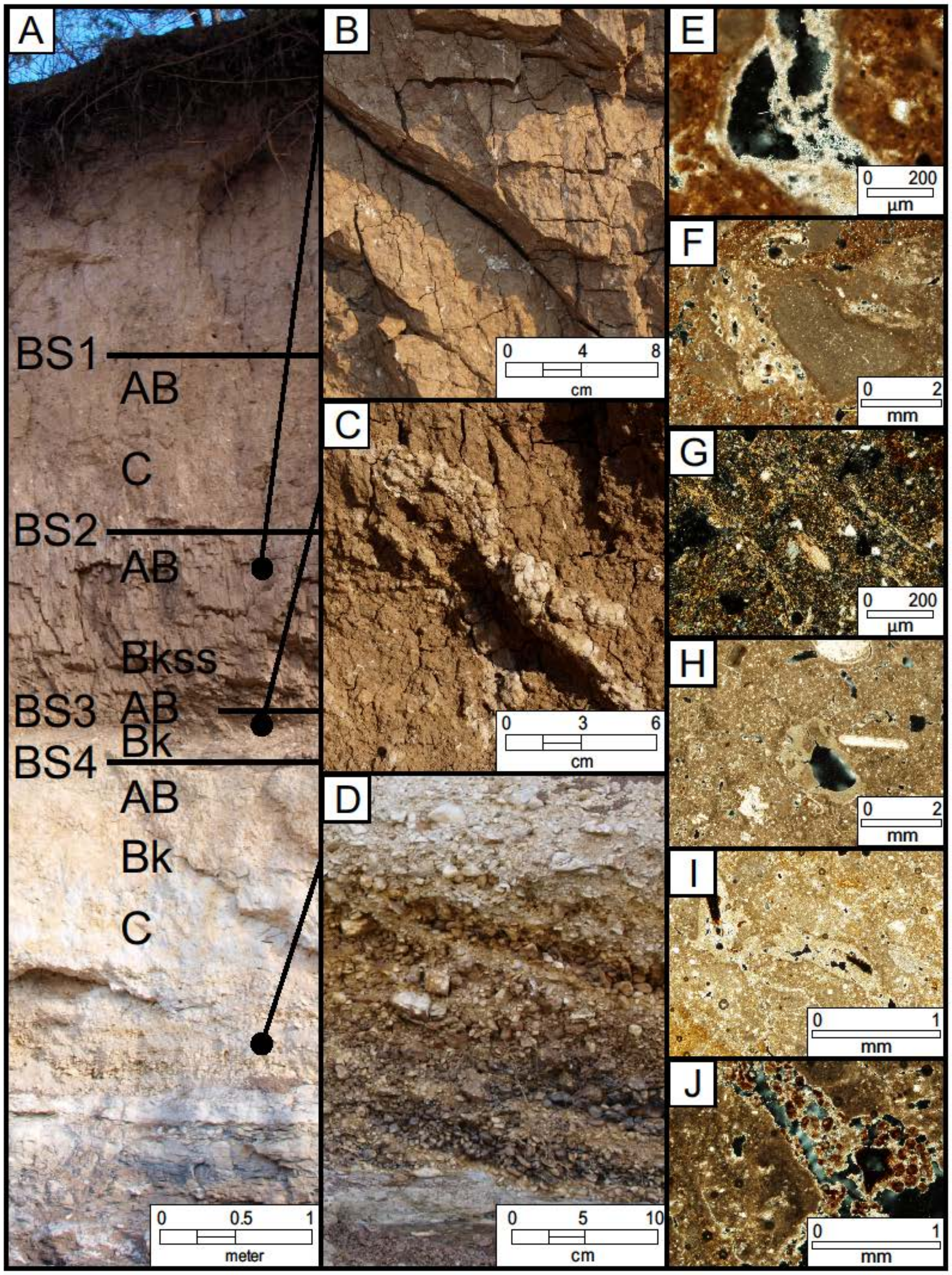

Fig. 3.3. Outcrop and photomicrograph images of the sampled profile along Owl Creek. (A) Interval shown in Fig. 3.1C, with horizon features described in Table 3.1. (B) Slickensides and peds from Buried soil 2. (C) Typical rhizocretion observed in Buried soil 3. (D) Basal stratigraphic interval in contact with the Walnut Clay (Cretaceous). (E–J) Photomicrographs of the buried soils along Owl Creek, all images in cross-polarized light (XPL). (E) Needle-fiber calcite forming in pore within Buried soil 1 (AB). (F) Multi-phase (microspar and micrite) of pedogenic and nonpedogenic carbonate from Buried soil 1 (AB) and commonly observed throughout the profile. (G) Masepic–plasmic fabric within Buried soil 2 (AB). (H) Hypocoating of carbonate biopore in Buried soil 3 (Bk). (I) Rhizocretion with organic matter preserved as inclusions within Buried soil 4 (AB). (J) Oribatid mite fecal pellets from Buried soil 4 (AB).

Table 3.1
Soil and buried soil field descriptions along Owl Creek, central Texas. Descriptions are from Meier et al., 2013 and the additional identification of Buried soil 1 is from this study.

	Horizon	Description
Surface soil	A	0-43 cm; dark grayish brown (10YR 4/2) gravelly clay loam; strong fine subangular blocky structure; slightly hard; common fine to coarse roots; common (20%) coarse to very coarse fragments, matrix supported, well sorted (rounded to subrounded) limestone and cherts; strongly effervescent; clear wavy boundary.
	Bw1	43-81 cm; brown (10YR 4/3) silty clay loam; moderate medium subangular blocky structure; moderately common medium roots; common coarse snail shells; few calcium carbonate filaments (stage I); common coarse fragments, matrix supported well sorted (rounded to subrounded, 0.5 mm to 3 cm) limestone and cherts; strongly effervescent; gradual wavy boundary.
	Bw2	81-132 cm; grayish brown (10YR 5/2) gravelly silty clay loam; weak coarse prismatic structure; very few coarse sediment in-filled burrows (10YR 6/2); few calcium carbonate filaments (stage I); common coarse fragments, matrix supported, poorly sorted (platy to rounded to angular, 1 to 8 cm diameter) limestone and cherts; strongly effervescent; gradual wavy boundary.
	Bw3	132-202 cm; brown (7.5YR 5/3) gravelly silty clay loam; massive structure; common coarse snail shells; many coarse fragments, matrix supported, poorly sorted, (subrounded to angular 0.5 to 8 cm diameter) limestone and cherts; strongly effervescent; clear smooth boundary associated with stone line.
Buried soil 1	AB	202-248 cm; brown (7.5YR 5/3) gravelly silty clay loam; weak coarse subangular blocky structure; few coarse snail shell fragments; few calcium carbonate filaments (stage I); many coarse fragments, matrix supported, poorly sorted (subangular to platy 2 mm to 5 cm diameter) limestone and few cherts; strongly effervescent; diffuse smooth boundary.
	C	248-300 cm; brown (7.5YR 5/3) gravelly silty clay loam; common mm snail shell fragments; few fine calcium carbonate filaments (stage I); many coarse fragments, matrix supported, poorly sorted (subangular to platy, 2 mm to 5 cm diameter) limestone and cherts; strongly effervescent; gradual smooth boundary.
Buried soil 2	AB	300-343 cm; dark yellowish brown (10YR 3/4) silty clay; strong coarse prismatic structure; extremely hard; common coarse granular infilled burrows; common distinct dark brown (7.5YR 3/3) masses of iron accumulation; common medium calcium carbonate filaments (stage I); common coarse calcium carbonate nodules (stage II); strongly effervescent; gradual smooth boundary.
	Bkss	343-393 cm; brown (10YR 4/3) silty clay; strong medium wedge structure; very hard; common distinct brown (7.5YR 4/4) masses of iron accumulation; common fine faint calcium carbonate filaments (stage I); common coarse calcium carbonate nodules (stage II); strongly effervescent; clear wavy boundary.
Buried soil 3	AB	393- 423 cm; brown (10YR 4/3) silty clay; strong fine subangular blocky structure; slightly hard; common faint dark brown (10YR 3/2) nodules of iron accumulation; few coarse calcium carbonate rhizoliths; few fine calcium carbonate filaments (stage I); common medium calcium carbonate nodules (stage II); common coarse fragments, matrix supported, well sorted (subangular, 1 to 2 cm diameter) limestone and cherts; strongly effervescent; gradual smooth boundary.
	Bk	423-453 cm; dark yellowish brown (10YR 4/4) silty clay loam; strong fine subangular structure; slightly hard; calcium carbonate granular calcium carbonate rhizoliths within horizon; common fine calcium carbonate filaments (stage I); common fine calcium carbonate nodules (stage II); few coarse fragments, matrix supported, well sorted (rounded, 1 cm to 2 cm diameter) limestone and cherts; strongly effervescent; clear smooth boundary.
Buried soil 4	AB	453-510 cm; yellowish brown (10YR 5/6) silty clay loam; strong medium subangular blocky structure; slightly hard; common fine black (10YR 2/1) nodules of iron accumulation; common fine calcium carbonate filaments (stage I); common calcium carbonate nodules globular (stage II); strongly effervescent; gradual smooth boundary.
	Bk	510-540 cm; very pale brown (10YR 7/4) silty loam; strong fine subangular blocky structure; soft; few fine calcium carbonate filaments (stage I); few coarse fragments, matrix supported, well sorted (rounded, 1 cm to 2 cm diameter) limestone and cherts; strongly effervescent; diffuse smooth boundary.
	C	540-560 cm; white (10YR 8/1) loam; strong medium subangular blocky structure; hard; very few very fine to fine rootlets; common coarse clasts, clast supported, well sorted (rounded, 1 cm to 2 cm diameter) limestone and cherts; finer and sandier facies within horizon; strongly effervescent; clear smooth boundary.
Strat	C1	560-624 cm; gravels; chaotic fill; common calcium carbonate pendants (stage I); many coarse clasts, clast supported, poorly sorted (rounded, 6 cm to 12 cm diameter) limestone and cherts; strongly effervescent; abrupt wavy boundary.
	C2	624-694 cm; gravels; cross stratified (20 to 30˚ dip upstream to modern channel flow); common calcium carbonate pendants (stage I); common coarse clasts, clast supported, poorly sorted (rounded, 6 cm to 12 cm diameter) limestone and cherts; strongly effervescent; very abrupt wavy boundary.

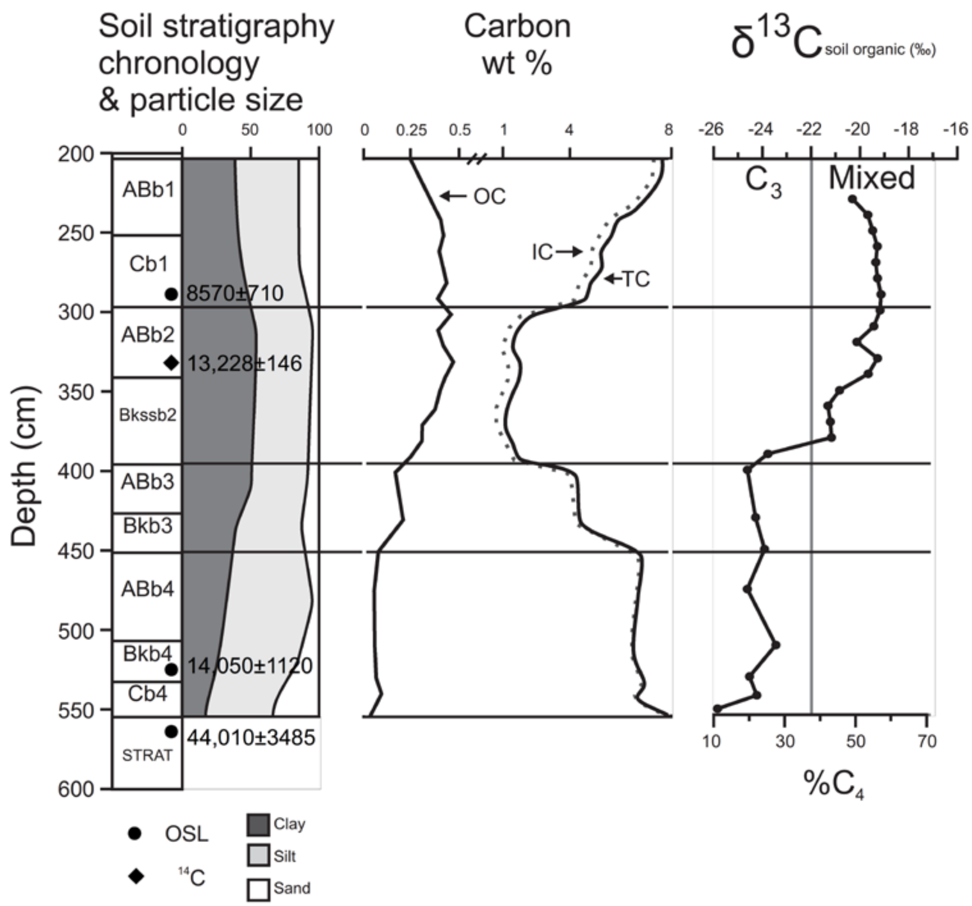

Fig. 3.4. Profile horizons, particle size distribution, sediment chronology, carbon weight percent (TC, OC, & IC), and $\delta^{13}C$ values of bulk soil organic matter. The C3 plant production is estimated by mixing model calculations discussed in the text. Summary of samples used for the chronology is given in Table 3.2.

Buried soil 3 (BS 3) formed in a modified fine-grained alluvial material that was distal to the active channel (Fig. 3.3C). This soil is a silty clay with pedogenic carbonate (AB horizon), which has an increase in pedogenic carbonate and detrital gravels as compared to the underlying silty clay loam horizon (Bk horizon). The pedogenic carbonates include filaments (stage 1), nodules (stage 2) and rhizoliths. The rhizoliths have been attributed to biological activity during pedogenesis, either from encrusted roots or preserved burrows (Klappa, 1980). Truncation of BS 3 likely occurred during deposition of the overlying alluvium associated with the Buried soil 2 (BS 2). Buried soil

3 was not directly dated, however, the soil age is constrained by the ages of BS 4 and BS 2 (Table 3.2).

Table 3.2
Optically stimulated luminescence (OSL) ages on quartz grains from fluvial sediments Owl Creek, Texas.

Sample #	Depth (m)	Laboratory number	Aliquots	Grain size (μm)	Equivalent dose (Gray) [a]	Over-dispersion (%) [b]	U (ppm) [c]	Th (ppm) [c]	K_2O (%) [c]	H_2O (%)	Cosmic dose (mGray/yr) [d]	Dose rate (mGray/yr)	OSL age (yr) [e]
BS 1	1.9	UIC 2900	25	150-250	11.94 ± 0.46	86.5 ± 10.4	2.6 ± 0.1	3.7 ± 0.1	0.49 ± 0.01	5 ± 2	0.18 ± 0.02	1.39 ± 0.07	8570 ± 710 [f]
BS 2*	8.5	UIC 2904	30	100-150	18.75 ± 0.83	13.1 ± 1.7	2.4 ± 0.1	6.5 ±0.1	1.00 ± 0.01	5 ± 2	0.08 ± 0.01	1.85 ± 0.09	10,115 ± 685
BS 4	4.7	UIC 2901	30	150-250	13.95 ± 0.57	72.9 ± 9.5	2.6 ± 0.1	4.0 ± 0.1	0.30 ± 0.01	25 ± 5	0.12 ± 0.01	0.99 ± 0.05	14,050 ± 1120 [f]
Strat	5.0	UIC 2640	30	100-150	38.27 ± 1.43	10.2 ± 1.4	2.3 ± 0.1	3.5 ± 0.1	0.23 ± 0.01	25 ± 5	0.11 ± 0.01	0.97 ± 0.05	44,010 ± 3485

[a] Quartz fraction analyzed under blue-light excitation (470 ± 20 nm) by single aliquot regeneration protocols (Murray and Wintle, 2003). Each aliquot contained between 100 and 500 grains in a 2 mm plate diameter.
[b] Values reflect precision beyond instrumental errors; values of ≤ 25% indicate low dispersion in equivalent dose values. 11
[c] U, Th and K_20 content analyzed by inductively coupled plasma-mass spectrometry analyzed by Activation Laboratory LTD, Ontario, Canada.
[d] From Presott and Hutton (1994).
[e] Ages calculated using the central age model of Galbraith et al. (1999).
[f] Ages calculated using the minimum age model of Galbraith et al. (1999). All errors are at 1 sigma and include systematic and random errors.
Ages are from the reference year AD 2010.
* Sample from Cowhouse Creek Royalty paleosol that correlates to BS 2.
Samples UIC200, 2901, & 2640 are from Meier et al., 2013.

Buried soil 2 (BS 2) is a pedogenically modified fine-grained alluvium (Fig. 3.3). BS 2 is dominated by silty clay with pedogenic carbonate (AB horizon), and is underlain by a silty clay with pedogenic carbonate with prominent slickensides (Bkss horizon) and preserving hillslope topography. Stage 1 pedogenic carbonate filaments and stage 2 nodules persist throughout the buried soil. The buried soil was truncated and buried by the overlying alluvium (Buried soil 1). Buried soil 2 corresponds to the “Royalty paleosol” of Nordt, with the type section located nearby on Cowhouse Creek (Nordt, 1992). BS 2 likely dates to ~ 12 to 9.5 cal yr BP, with the age range attributed to the known error associated with humate age- overestimation and a charcoal age (Meier et al., 2013). An OSL age on alluvial sediment at the type section beneath the Royalty paleosol on Cowhouse Creek dates deposition to 10,115 ± 685 yr BP (UIC2904)(Fig. 3.4; Table 3.2).

Buried soil 1 (BS 1) corresponds to the base of the Q8 depositional unit (Meier et al., 2013). The buried soil is previously unidentified by Meier et al. and is the youngest buried soil, formed in gravel-rich, fine- grained deposits with a gravelly silty clay loam, texture (2013). The buried soil has pedogenic carbonate (stage 1) filaments (AB horizon) over a weakly developed (Bk) horizon with limestone and chert gravels throughout (Figs. 3A, 3; Table 3.1). The buried soil has an unconformable contact with the underlying Holocene BS 2 (AB horizon). The unit was likely deposited at ~ 8 ka based on an OSL age from the C horizon Meier et al., 2013; Fig. 3.4; Table 3.2).

4.1. Micromorphology

The micromorphology of BS 4 is strongly influenced by high carbonate content, likely contributing to the light-colored matrix. Pedogenic carbonate morphologies include rhizoliths, carbonate nodules with sparry calcite grading to microspar (10–50 μm) texture, dense micritic masses with gradational boundaries, and detrital carbonate engulfed by micrite rinds. Sparry calcite rhizoliths lack internal structure, but commonly have preserved organic matter, and range in thickness from 200 to 500 μm (Fig. 3.3I). Commonly the micrite to microspar and sparry calcite nodules have septarian voids lined with microspar (Fig. 3.3J). Oribatid mite fecal pellets were identified within a biopore associated with organic matter; this biological activity is typically associated with freely-drained soil conditions (Mestdagh et al., 1999) (Fig. 3.3J).

Buried soil 3 microfabric shows little evidence of clay orientation/ fabric, with abundant carbonate. Pedogenic carbonate nodules with micrite and sparry calcite texture are common. Dense, micritic masses with gradational boundaries with the surrounding matrix are common, in addition to rhizoliths. The rhizoliths have a micrite to sparry calcite porphyric texture, with 1 cm thick walls. The hypocoatings of biopores have smooth micrite texture and internal zonation suggesting multi- phase growth (Fig. 3.3H).

The micromorphology of BS 2 varies with depth. The dominant fabric is masepic–plasmic with secondary skelsepic orientation increasing at depth (Fig. 3.3G). Microstructure mirrors the macro- structure, with horizontal and vertical cracks in the AB and 60° inclined micro-slickensides in the Bkss horizon. Iron–manganese nodules are common and typically show multi-generational growth, with diffuse masses less common. Carbonate morphology ranges from micrite and sparry calcite-textured nodules to detrital carbonate.

The microfabric of BS 1 is homogenous, with the AB and C horizons being similar. The buried soil matrix shows evidence of bioturbation, with skelsepic fabric associated with wetting and drying cycles. Identified morphologies include needle-fiber calcite, single and multi-generational pedogenic carbonate nodules, and detrital carbonate. Needle-fiber calcite within pore voids was identified in the AB horizon (Fig. 3.3E). The randomly oriented monocrystalline rods are ~ 100 μm long and formed within a micrite-lined pore (hypocoat) (cf. Verrecchia and Verrecchia, 1994) suggestive of weak pedogenesis with well-drained conditions (Strong et al., 1992; Wright, 1984). The pedogenic nodules generally have discrete boundaries and are composed of micritic infill with detrital quartz grain inclusions (Fig. 3.3F). Large, microsparitic crystals and septarian voids are less common. Fossiliferous limestone clasts (detrital carbonate) are easily differentiated from pedogenic nodules in thin-section, have common pedogenic exterior micrite rinds, and show evidence of dissolution and reprecipitation of carbonate within the preserved structure (Fig. 3.3F).

4.2. Bulk geochemistry

Bulk geochemistry of the buried soils identified at the Owl Creek study site profile indicates that the four buried soils have experienced variable soil-forming processes based on depth trends in elemental proxies (Retallack, 2001; Sheldon et al., 2002). Geochemical trends for leaching (Ba/Sr) and base loss (Al_2O_3/(CaO + MgO + K_2O + Na_2O)) covary through the section and both reach a maximum for BS 2, indicating that it is the most mature of the four buried soils, assuming that they all had similar soil drainage and chemical weathering environments (Fig. 3.4A, B). Salinization (Na_2O/K_2O) attains a maximum in BS 3, whereas calcification ((CaO + MgO)/Al_2O_3) has a minimum value in BS 2 and increases in the other three buried soils (Fig. 3.4C, D). The lessivage (Al_2O_3/SiO_2) ratios are a measure of clay production and clay transportation, with the maximum attained at the base of BS 2 and corresponding to the Bkss horizon, which has the highest clay content and is the only buried soil with prominent vertic (shrink–swell) features (Fig. 3.5E). The Ti vs. Zr cross-plot for the pro- file yields an r^2 value of 0.96 (Fig. 3.5F) showing that the Zr and Ti concentrations are in constant proportions in the profile and that parent material source(s) did not change through time. Overall the variations through the profile, with decreased calcification and increased leaching and base loss, indicate that Buried soil 2 is unique because it is the best-developed of the four buried soils and it is the only one with conspicuous vertic properties. It therefore may record a period of greater geomorphic stability on a landscape at Owl Creek that was generally very unstable and highly dynamic.

4.3. Carbon (OC, IC, & TC) weight percent

The preservation of buried soil surface horizons was confirmed based on relative increase in organic carbon (OC) content in the surface as compared with underlying horizons and micromorphology (Figs. 3.3 & 3.4). The OC content through the study interval is low with values below 0.5 wt.%. Buried soil 4 OC values are even lower, ranging from 0.05 to 0.1 wt.% (Fig. 3.4). The inorganic carbon (IC) values are high, peaking at 7.8 wt.%, with total carbon (TC) values reflecting the large amounts of pedogenic carbonate and detrital carbonate in the fine-earth fraction.

The OC values for BS 3 are 0.21 wt.%, and IC values increase from 4.0 to 7.0 wt.% (Fig. 3.4). TC values are high due to high IC content associated with pedogenic and detrital carbonate. The OC values confirm the presence of a buried soil with values higher in the AB horizon at 0.45 wt.% and decreasing to 0.16 wt.% in the Bkss horizon (Fig. 3.4). The IC values are roughly unchanged in the profile with values averaging 1.3 wt.%. The TC is very high, reflecting the amount of IC in the buried soil.

The OC values in Holocene BS 1 range from 0.4 wt.% in the Bk horizon, decreasing to 0.4 wt.% in the C horizon. The IC values also decrease with depth from 6.5 to 4.1 wt.%, with the higher values corresponding to abundant pedogenic and detrital carbonate.

4.4. $\delta^{13}C$ of soil organic matter (SOM)

The $\delta^{13}C$ PDB values of soil organic matter (SOM) are consistent with a C3-dominated ecosystem during formation of Buried soils 4 and 3, based on the stable carbon isotope mixing model (Fig. 3.4). The SOM $\delta^{13}C$ values are smaller at the base of the profile, with values averaging − 24‰ in BS 4, and similar values around − 24.5‰ in

BS 3 (Fig. 3.4). The low (10%) estimated contribution of C4 plant communities suggests that these buried soils formed in a wet paleoenvironment. Buried soils 2 and 1 have SOM with larger $\delta^{13}C$ values of approximately −19‰ (Fig. 3.4). These $\delta^{13}C$ values suggest a shift to a mixed C3–C4 plant ecosystem that consisted of an estimated average of 50% C4 warm-season grasses, based on the stable carbon isotope mixing model.

The mean July temperature (Eq. (2)), MAT (Eq. (3)), and MAP (Eq. (4)) (Hall and Penner, 2013; Nordt et al., 2007) show similar trends with BS 4 and 3 preserving cool July and mean annual temperatures, approximately 18 °C and 8 °C respectively (Table 3.3). MAP values range from 897 mm (BS 4) to 893 mm (BS 3). The younger BS 2 and 1 have values consistent with warmer temperatures at21 °C (mean annual July) and approximately 10 °C (MAT). MAP suggest drier conditions with values ranging from 814 to 791 mm/yr (Table 3.3).

Potential erosion rates (E) vary within the buried soils. BS 4 and 3 again have similar values, with 97 cm of potential erosion (Table 3.3). BS 2 shows less truncation and values suggestive of 88 cm of erosion. BS 1 was not evaluated for erosion rates because the unit does not have a preserved Bk horizon.

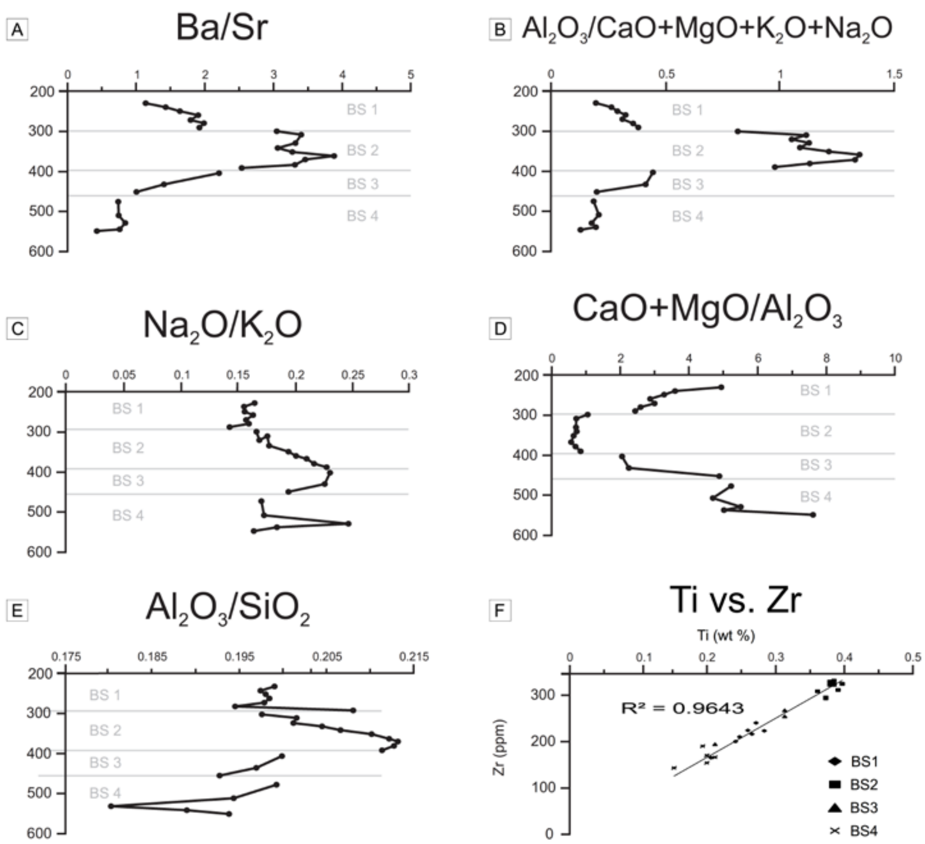

Fig. 3.5. Elemental proxies of (A) leaching (Ba/Sr), (B) base loss (Al2O3/CaO + MgO + K2O + Na2O), (C) salinization (Na2O/K2O), (D) calcification (CaO + MgO/Al2O3), (E) lessivage (Al2O3/SiO2), and (F) parent material (Ti vs. Zr cross-plots) for the Owl Creek profile.

5. Discussion

5.1. Owl Creek depositional history

The four late Pleistocene to Holocene buried soils exposed at Owl Creek, in central Texas, were likely proximal to an active channel and later truncated because of the dynamic nature of this small fluvial system. The buried soils have been interpreted as floodplain deposits formed from similar parent materials with a similar time of pedogenesis, with differences in profile characteristics mainly attributable to changes in climate and plant community (c.f. Jenny, 1941b).

The four buried soils examined in this study are each distinctive based upon differences in the soil characterization data, micromorphological features, carbon pools (TC, OC, IC), bulk geochemical weathering proxies, and $\delta^{13}C$ values of SOM. Measurements of $\delta^{13}C$ values of soil organic matter (SOM) show a pattern of negative values (Buried soils 4 and 3) shifting to less negative values (Buried soils 2 and 1) (Fig. 3.4). The observed isotopic shift to an increased mixed-C3/C4 plant com- munity at Owl Creek is attributed to regionally extensive warming period occurring at the Pleistocene–Holocene boundary (Bousman, 1998; Hall and Penner, 2013; Holliday et al., 1996, 2011; Mandel et al., 2007; Musgrove et al., Nordt, 2004; Nordt et al., 1994, 1998; Toomey et al., 1993). The regional warming event and $\delta^{13}C$ values refine the formation for Buried soils 4 & 3 deposition to between 12 and 14 ka, where previous chronologies constrained the Buried soils 9 to 14 ka range (Meier et al., 2013).

All buried soils are highly calcareous, because of detrital calcium carbonate inherited from the Cretaceous limestone parent material; in addition, all show evidence of well-drained conditions, as evidenced by various forms of pedogenic carbonates and general absence of gley or redoximorphic features. Such drainage would have been promoted by the abundance of coarse-textured, carbonatic sands and gravels being delivered by the high-energy alluvial system and a general absence of fines, especially clays. The abundance of stage 1 and 2 pedogenic carbonates reflects relatively shorter periods of soil formation that allowed only incipient translocation of carbonate translocation, reflecting an unstable, and geomorphically dynamic landscape.

Table 3.3
Paleoecological data from the buried soils at Owl Creek.

	Classification (Meier et al., 2013)	Horizon	Sample depth (cm)	$\delta^{13}C_{SOM}$	July T (°C)[a]	MAT (°C)[b]	MAP (mm)[c]	Possible Erosion (cm)[d]
Buried soil 1	Q8*	Ab1	230	-20.15	21.65	10.76	791.14	-
		Cb1	240	-19.53				
		Cb1	250	-19.33				
		Cb1	260	-19.13				
		Cb1	270	-19.20				
		Cb1	280	-19.13				
		Cb1	290	-18.98				
Buried soil 2	Q7c	AB	300	-19.01	20.90	10.16	814.53	88.12
	P6	AB	310	-19.27				
		AB	320	-19.97				
		AB	330	-19.12				
		Bkss	340	-19.50				
		Bkss	350	-20.67				
		Bkss	360	-21.16				
		Bkss	370	-21.05				
		Bkss	380	-21.00				
		Bkss	390	-23.63				
Buried soil 3	Q7b	AB	400	-24.46	18.39	8.12	893.37	96.94
	P5	Bk	430	-24.12				
		Bk	450	-23.75				
Buried soil 4	Q7a	AB	475	-24.46	18.26	8.02	897.27	97.37
	P4	AB	510	-23.31				
		Bk	530	-24.38				
		Cb	540	-23.78				
		Cb	550	-25.52				

[a] Mean July temperature calculated from $\delta^{13}C$ values, (eq 2) T (°C) = 0.685($\delta^{13}C$)+34.9; r^2=0.67 (Nordt et al., 2007)
[b] Mean temperature, (eq 3) MAT (°C) = -6.751+(0.809 x mean July temperature); r^2=0.94 (Hall and Penner, 2013)
[c] Mean annual precipitation, (eq 4) MAP (mm) = 1208.220-(38.76 x mean July temperature); r^2=-0.81 (Hall and Penner, 2013)
[d] Potential erosion, E-value, (eq 7) $E = -251.5385 + 38.4615(\sqrt{0.052P+35.6351})$
[*] Previously unidentified by Meier et al., 2013.

5.1.1. Depositional history of Owl Creek at ~ 14 ka (Buried soil 4)

The oldest depositional unit capped by a buried soil, BS4, developed in mixed fine-grained and coarse-grained alluvium (Meier et al., 2013). The facies of the fining-upward deposits at Owl Creek are consistent with deposition of a meandering, bedload-dominated fluvial system (Nordt, 1992).

The precipitation of pedogenic carbonate nodules, recrystallization of carbonate to microspar and sparry calcite, and other micro-features (Figs. 2J, 4D) suggest variable moisture regimes ranging from wet to dry, likely reflecting seasonal precipitation (Breecker et al., 2009; Machette, 1985; Nordt et al., 1994; Zhou and Chafetz, 2010). The more negative $\delta^{13}C$ SOM values reflect initial low contribution from C_4 plant ecosystems. The paleoecological data (see Table 3.3) suggest a climate cooler and wetter than modern conditions and is consistent with other late Pleistocene climate proxies (Fig. 3.4). The BS 4 profile (AB-Bk-C) is consistent with a calcic diagnostic horizon and later fluvial activity likely truncated ~ 1 m of the solum.

5.1.2. Depositional history of Owl Creek at ~ 12 ka (Buried soil 3)

Buried soil 3 formed from pedogenically modified, fine-grained alluvium that was deposited distal to the active channel. The deposits have characteristics that are suggestive of channel migration and/or a reduction in steam competency, with buried soil development occurring distal to the active channel.

The rhizolith features and other pedogenic carbonate forms are indicative of former root activity (Klappa, 1980) in a cool subhumid, but seasonally dry climate (Breecker et al., 2009; Machette, 1985; Nordt et al., 1994; Zhou and Chafetz, 2010). The persistence of more negative $\delta^{13}C$ SOM values with low estimated contribution from C4 plant ecosystems and paleoecological reconstruction that indicate continued cool and wet conditions are consistent with Pleistocene deposition ca. 14 to 12 ka (Table 3.3).

5.1.3. Depositional history of Owl Creek at ~ 10 ka (Buried soil 2)

Buried soil 2 formed from pedogenically modified, fine-grained alluvium deposited in association with a meandering, bedload-dominated stream (Meier et al., 2013; Nordt, 1992). Buried soil 2 has properties suggestive of variable moisture regimes, based on the presence of macro- and micro-slickensides and associated precipitation of pedogenic carbonate and iron manganese nodules. The preservation of Vertisol-like properties (wedge-shaped peds, pedogenic slickensides, sepic–plasmic microstructures), in a more C_4-dominated ecosystem, suggest variable drainage history and formation distal to the active channel, with repeated shrink–swell cycles driven by periods of soil-moisture surplus alternating with deficits during a drier mid- Holocene climate. The paleoecological proxies (mean July and mean annual temperatures & MAP) show warmer and drier conditions at Owl Creek (see Table 3.3). The sediments were deposited around ca. 10 ka (Fig. 3.4; Table 3.2), with pedogenesis occurring at some time afterward. The AB-Bkss profile is suggestive of 85 cm of potential erosion, with the preserved buried soil indicative of a mollic epipedon with a cambic diagnostic horizon, classify as Vertisol-like buried soil and likely a product of the warmer Holocene climate (Coulombe et al., 1996; Nordt, 2004; Southard et al., 2011).

5.1.4. Depositional history of Owl Creek at ~ 8 ka (Buried soil 1)

Buried soil1 formed from pedogenically altered fluvial deposits that began to aggrade at ca. 8 ka, by which time Owl Creek was a dominantly fine-grained meandering stream (Nordt, 1992). Carbonate precipitation (Fig. 3.2E) indicates variable soil moisture conditions (Breecker et al., 2009; Machette, 1985; Nordt et al., 1994; Zhou and Chafetz, 2010). The micromorphology of BS 1 is consistent with evidence suggesting limited pedogenesis and SOM $\delta^{13}C$ isotopic values indicate a mixed- C3/C4 plant community, with the added component of C4 plant ecosystem suggesting continuation of a warmer and drier, late Holocene cli- mate (Fig. 3.4). Buried soil 1 has a Bk-C profile, and has cambic-like properties, with no evidence of clay accumulation and increased organic carbon content, which suggests that an Inceptisol-like assignment is appropriate.

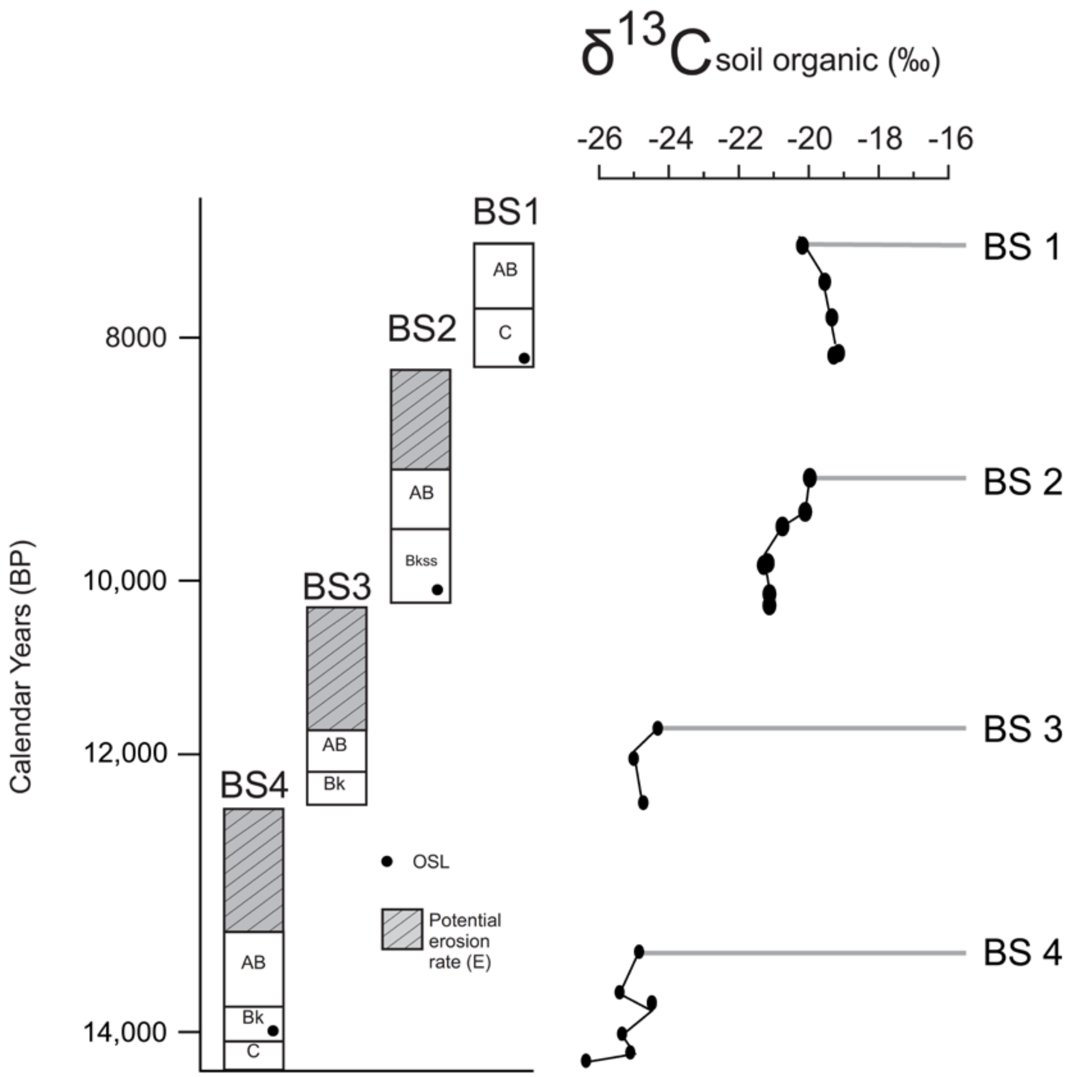

Fig. 3.6. Schematic of the Owl Creek Pleistocene/Holocene section with potential erosion rate (E) for each buried soil. The Owl Creek soil organic matter (SOM) stable carbonisotopic record shows the paleoecological trends for the preserved soils.

5.2. Regional paleoecological conditions and erosion rates

A variety of paleoclimate proxies, such as speleothem calcite records (Musgrove et al., 2001) and magnetic susceptibilities in cave sediment (Ellwood and Gose, 2006), pollen records (Bousman, 1998), and faunal assemblages (Koch et al., 2004; Toomey et al, 1993) indicated that there was considerable cli- mate variability during the transition from the late Pleistocene into the Holocene in the central Texas region. Regional climate proxies collectively indicate a cooler and wetter late Pleistocene climate transitioning to modern, warmer and drier conditions in the Holocene (Hall et al., 2012a, 2012b, Holliday et al., 2008, Humphrey and Ferring, 1994; Mandel et al., 2007; Nordt et al., 1998). This drying regional trend, as shown by the $\delta^{13}C$ paleoecological reconstructions, is also preserved in Owl Creek. Recent research of Hall and Penner (2013) was applied to Owl Creek to determine mean annual precipitation (MAP) and was essential to the inference (Eqs. (7) & (8)) of the depth to Bk concept (Retallack, 2005). Eq. (7) evaluates the amount of truncation of fluvial buried soil at Owl Creek in an attempt to quantify erosion rates (Fig. 3.6; See Table 3.3).

Owl Creek erosion, coupled with the OSL ages, would suggest a minimum denudation rate of 50 cm/ky. This rate is higher than 11 cm/ky the paleo-denudation rates from central Texas sediment in cave and upland settings (Cooke et al., 2003) yet lower than the rates of modern cropland of erosion (~ 100 cm/ky) and fluvial erosion rates from Duck Creek (1000 cm/ky) (Brackenridge, 1985, Pimentel et al., 1995). Differences between the central Texas rates have been attributed to the dynamic nature of the fluvial system at Owl Creek.

6. Summary

Owl Creek validates the use of small streams to investigate regional climate change. Four buried soils exposed along Owl Creek were examined using soil morphology and micromorphology, soil characterization, whole-soil geochemical and stable isotope analyses of soil organic matter and pedogenic carbonate. These buried soils provide a record of changes in paleoecological, paleo-alluvial, and soil-forming conditions spanning 14 ky. Buried soils 4 and 3 (14,050– ~ 12,000 cal yr BP) have SOM with more negative $\delta^{13}C$ values with a C_3 plant-dominated ecosystem indicating a cooler/wetter late Pleistocene climate, whereas Buried soils 2 and 1 (10,115–8570 cal yr BP) record the transition to a warmer/drier Holocene climate with a mixed C_3–C_4 plant ecosystem. Buried soil 2, which is a Vertisol-like buried soil, thus records episodes of alternating soil moisture deficit and surplus and coincident geomorphically stable conditions. All buried soils contain pedogenic carbonates indicating a high degree of soil drainage in spite of changing moisture regimes. The use of paleoecological proxies to estimate MAP and MAT (Hall and Penner, 2013) has uniquely allowed for evaluation of potential erosion at Owl Creek. Analyses of these multi-proxies suggest that the Late Quaternary history of alluviation and pedogenesis in central Texas is in response to environmental changes that occurred across the Pleistocene–Holocene transition, and that these changes are consistent with floodplain, speleothem, pollen and other climate proxies in central Texas (Bousman, 1998; Ellwood and Gose, 2006; Koch et al., 2004; Musgrove et al., 2001; Toomey et al, 1993). These combined records demonstrate consistent responses to the major climatic changes known to have occurred at the end of the Pleistocene constrained for the first time using OSL dating.

Acknowledgments

Thanks are extended to Sunny Wood and the Fort Hood Cultural Resources Management team, for their help in securing site access and logistical support. We appreciate the efforts of Dr. Tom Hallmark and Donna Prochaska (TAMU-Soil Characterization Lab) for providing soil characterization data. We thank Dr. Ren Zhang (Baylor University) for the stable isotopic analyses, Will Torsch, Gordon Mangenheim, Lauren Nix, and Lauren Michel (Baylor University) for their field assistance, and Hope

Sepela for the sample preparation. This research was funded by student grants-in-aid of research provided by the Department of Geology at Baylor University. The helpful comments were from the anonymous reviewers of this manuscript.

Appendix 3A. Data used to evaluate the potential erosion (E) using depth to Bk.

		NOAA id: 419419		Eq. 7	Eq. 8
Soil Series Name McLennan County	Depth of Bk (mid point of horizon)(cm)	Year	MAP (mm/yr)	$E = -251.5385 + 38.4615(\sqrt{0.052P+35.6351})$	$E = -251.5385 - 38.4615(\sqrt{0.052P+35.6351})$
Queeny	40.64	2012	800.862	77.28	-589.65
Purves	30.48	2011	702.056	72.14	-578.22
Wilson	180.55	2010	1018.54	88.60	-613.57
Sanger	117.905	2009	953.262	85.20	-606.56
Real	24.77	2008	851.916	79.93	-595.41
Sunev	63.33	2007	1220.216	99.09	-634.39
San Saba	69.41	2006	606.044	67.15	-566.71
Slidell	99.665	2005	590.55	66.34	-564.81
Payne	93.225	2004	1510.792	114.20	-662.55
Ships	103.98	2003	710.692	72.59	-579.23
Lott	59.34	2002	926.338	83.80	-603.63
Ovan	180.55	2001	906.78	82.79	-601.49
McLennan	47.18	2000	1022.35	88.80	-613.97
Lewisville	89.1		860*	93.23	-596.30
Lamar	58.34	*Huckabee et al., 1977			
Krum	114.59				
Housotn Black	124.075				
Heiden	124.525				
Frio	81.93				
Fairlie	97.17				
Frio	72.04				
Crockett	113.095				
Chazos	83.29				
Burleson	174.2				
Bremond	75.805				
Branyon	169.12				
Bolar	39.74				
Axtell	108.195				
Aledo	19.78				
Min	19.78		Min	66.34	-662.55
Max	180.55		Max	114.20	-564.81
Average	92.14032		Average	83.65	-600.46

References

Baker, R.G., Bettis III, E.A., Denniston, R.F., Gonzalez, L.A., 2001. Plant remains, alluvial chronology, and cave speleothem isotopes indicate abrupt Holocene climatic change at 6 ka in midwestern USA. Global Planet. Change 28, 285–291.

Barnes, V.E., 1970. Geologic Atlas of Texas.

Blum, M.D., Valastro, S., 1994. Late Quaternary sedimentation, lower Colorado River, Gulf Coastal Plain of Texas. Geol. Soc. Am. Bull. 106, 1002–1016.

Bomar, G.W., 1983. Texas Weather. University of Texas, Austin.

Bousman, C.B., 1998. Paleoenvironmental change in central Texas: the palynological evidence. Plains Anthropol. 43, 201–219.

Boutton, T.W., 1996. Stable Carbon Isotope Ratios of Soil Organic Matter and their Use as Indicators of Vegetation and Climate Change. Marcel Dekker, New York 47–82.

Breecker, D., Sharp, Z.D., McFadden, L., 2009. Seasonal bias in the formation and stable isotope composition of pedogenic carbonate in modern soils from central New Mexico, USA. Geol. Soc. Am. Bull. 121, 630–640.

Brewer, R., 1976. Fabric and Mineral Analysis of Soils. Robert E. Krieger Pub. Co., Huntington, New York.

Brodie, C.R., Casford, J.S.L., Lloyd, J.M., Leng, M.J., Heaton, T.H.E., Kendrick, C.P., Yongqiang, Z., 2011. Evidence for bias in C/N, δ13C and δ15N values of bulk organic matter, and on environmental interpretation, from a lake sedimentary sequence by pre-analysis acid treatment methods. Quat. Sci. Rev. 30, 3076–3087.

Carlson, D.C. (Ed.), 1997. Archaeological investigations along Owl Creek: results of the 1992 summer archaeological field school. United States Army Fort Hood Archaeological Management Series, Research Report Number 29.

Carlson, D.L., Carlson, S.B., Briuer, F.L., Roemer Jr., E., Moore, W.E., 1986. Archaeological survey at Fort Hood, Texas: fiscal year 1983: the eastern training area. United States Army Fort Hood Archaeological Management Series, Research Report Number 11.

Cooke, M.J., Stern, L.A., Banner, J.L., Mack, L.E., 2003. Evidence for the silicate source of relict soils on the Edwards Plateau central Texas. Quat. Res. 67, 275–285.

Coulombe, C.E., Dixon, J.B., Wilding, L.P., 1996. Chapter 5 Mineralogy and chemistry of vertisols. In: Ahmad, N., Mermut, A. (Eds.), Developments in Soil Science. Elsevier, pp. 115–200.

Driese, S.G., Li, Z.-H., Horn, S.P., 2005. Late Pleistocene and Holocene climate and geomorphic histories as interpreted from a 23,000 14C yr B.P. paleosol and floodplain soils, southeastern West Virginia, USA. Quatern. Res. 63, 136–149.

Ellwood, B.B., Gose, W.A., 2006. Heinrich H1 and 8200 yr B.P. climate events recorded in Hall's Cave, Texas. Geology 34, 753–756.

Fitzpatrick, E.A., 1993. Soil Microscopy and Micromorphology. John Wiley & Sons, New York.

Forman, S.L., Oglesby, R., Webb, R., 2001. Patterns of Holocene dune activity on the Great Plains of North America: megadroughts and climate links. Global Planet. Change 29, 1–29.

Galbraith, R.F., Roberts, R.G., Laslett, G.M., Yoshida, H., Olley, J.M., 1999. Optical dating of single and multiple grains of quartz from Jinmium Rock Shelter, Northern Australia: Part I, experimental design and statistical models. Archaeometry 41, 339–364.
Hall, S.A., Penner, W.L., 2013. Stable carbon isotopes, C3–C4 vegetation, and 12,800 years of climate change in central New Mexico, USA. Palaeogeogr. Palaeoclimatol. Palaeoecol. 369, 272–281.
Hall, S.A., Boutton, T.W., Lintz, C.R., Baugh, T.G., 2012a. New correlation of stable carbon isotopes with changing late-Holocene fluvial environments in the Trinity River basin of Texas, USA. The Holocene 22, 541–549.
Hall, S.A., Penner, W.L., Palacios-Fest, M.R., Metcalf, A.J., Smith, S.J., 2012b. Cool, wet conditions late in the Younger Dryas in semi-arid New Mexico. Quatern. Res. 77, 87–95. http://dx.doi.org/10.1016/j.palaeo.2012.10.034.
Holliday, V.T., Hovorka, S.D., Gustavson, T.C., 1996. Lithostratigraphy and geochronology of fills in small playa basins on the Southern High Plains. Geological Society of America Bulletin 108, 953–965.
Holliday, V.T., Mayer, J.H., Fredlund, G.G., 2008. Late Quaternary sedimentology and geochronology of small playas on the Southern High Plains, Texas and New Mexico, U.S.A. Quat. Res. 70, 11–25.
Holliday, V.T., Meltzer, D.J., Mandel, R., 2011. Stratigraphy of the Younger Dryas Chronozone and paleoenvironmental implications: Central and Southern Great Plains. Quat. Intl. 520–533.
Huckabee, J.W.J., Thompson, D.R., Wyrick, J.C., Pavlat, E.G., 1977. Soil Survey of Bell County, Texas. US Department of Agriculture, Natural Resources Conservation Service, Washington, D.C.
Humphrey, J.D., Ferring, C.R., 1994. Stable isotopic evidence for latest Pleistocene and Holocene climatic change in north-central Texas. Quatern. Res. 41, 200–213.
Jenny, H., 1941a. Calcium in the soil: III. Pedologic relations. Soil Sci. Soc. Am. Proc. 6, 27–35.
Jenny, H., 1941b. Factors of Soil Formation: A System of Quantitative Pedology. McGraw- Hill, New York.
Jenny, H., Leonard, C.D., 1934. Functional relationships between soil properties and rainfall. Soil Sci. 38, 363–381.
Klappa, C.F., 1980. Rhizoliths in terrestrial carbonates: classification, recognition, zh-order tributary in central Texas, USA and its response to climate and sediment supply. Quatern. Res. 62, 289–300.
Kleinbach, K., Mehalchick, G., Boyd, D.K., Kibler, K.W., 1999. National register testing of 42 prehistoric archeological sites on Fort Hood, Texas: the 1996 season. United States Army Fort Hood Archaeological Management Series, Research Report Number 38.
Koch, P.L., Diffenbaugh, N.S., Hoppe, K.A., 2004. The effects of late Quaternary climate and pCO2 change on C4 plant abundance in the south-central United States. Palaeogeogr. Palaeoclimatol. Palaeoecol. 207, 331–357.

Komada, T., Anderson, M.R., Dorfmeier, C.L., 2008. Carbonate removal from coastal sediments for the determination of organic carbon and its isotopic signatures, δ13C and Δ14C: comparison of fumigation and direct acidification by hydrochloric acid. Limnol. Oceanogr. Methods 6, 254–262.
Machette, M.N., 1985. Calcic soils of the southwestern United States. In: Weide, D.L. (Ed.), Soils and Quaternary geology of the southwestern United States. Geological Society of America Special Paper, 203, pp. 1–21.
Mandel, R.D., Jacob, J.S., Nordt, L.C., 2007. Geoarchaeology of the Richard Beene Site. In: Thoms, A.V., Mandel, R.D. (Eds.), Archaeological and paleoecological investigations at the Richard Beene site (41BX831), South Central Texas. Center for Ecological Archaeology, Reports of Investigations No. 8. Texas A&M University, College Station, Texas.
Mehalchick, G., Kibler, K.W., 2002. National register testing of nine prehistoric sites on Fort Hood, Texas: the 2001–2002 season. United States Army Fort Hood Archaeological Resource Management Series Research Report Number 50.
Mehalchick, G., Kleinbach, K., Boyd, D.K., Kibler, K.W., 2000. Geoarcheological investigations and national register testing of 52 prehistoric archeological sites on Fort Hood, Texas: the 1997 season. United States Army Fort Hood Archaeological Management Series, Research Report Number 39.
Mehalchick, G., Killian, K., Caran, S.C., Kibler, K.W., 2003. Geoarchaeological investigations and national register testing of 57 prehistoric archaeological sites of Fort Hood, Texas: 1999 season. United States Army Fort Hood Archeological Resource Management Series, Research Report Number 44.
Meier, H.A., Nordt, L.C., Forman, S.L., Driese, S.G., 2013. Late Quaternary alluvial history of the middle Owl Creek drainage basin in central Texas: a record of geomorphic response to environmental change. Quat. Int. 306, 24–41. http://dx.doi.org/10.1016/j.quaint.2013.07.010.
Mestdagh, H., Haesaerts, P., Dodonov, A., Hus, J., 1999. Pedosedimentary and climatic reconstruction of the last interglacial and early glacial loess–paleosol sequence in Outh Tabzhikistan. Catena 35, 197–218.
Miller, G.B., 2001. Soil survey of McLennan County, Texas. United States Department of Agriculture, Natural Resources Conservation Services, Washington DC.
Murray, A.S., Wintle, A.G., 2003. The single aliquot regenerative dose protocol: potential for improvements in reliability. Radiation Measurements 37, 377–381.
Musgrove, M., Banner, J.L., Mack, L.E., Combs, D.M., James, E.W., Cheng, H., Edwards, R.L., 2001. Geochronology of Late Pleistocene to holocene speleothems from Central Texas: implications for regional paleoclimate. Geological Society of America Bulletin 113, 1532–1543.
Nordt, L.C., 1992. Additional geoarchaeology at the Fort Hood Military Reservation, Ft. Hood, Texas. Fort Hood (Tex.), Texas A & M University. Archeological Research Laboratory. United States Army, Fort Hood.
Nordt, L.C., 1995. Geoarchaeological investigations of Henson creek: a low-order tributary in Central Texas. Geoarchaeology 10, 205–221.
Nordt, L., 2004. Late Quaternary alluvial stratigraphy of a low-order tributary in central Texas, USA and its response to climate and sediment supply. Quatern. Res. 62, 289–300. http://dx.doi.org/10.1016/j.yqres.2004.07.004.

Nordt, L.C., Boutton, T.W., Hallmark, C.T., Waters, M.R., 1994. Late Quaternary vegetation and climate changes in Central Texas based on the isotopic composition of organic carbon. Quatern. Res. 41, 109–120.
Nordt, L.C., Hallmark, C.T., Wilding, L.P., Boutton, T.W., 1998. Quantifying pedogenic carbonate accumulations using stable carbon isotopes. Geoderma 82, 115–136.
Nordt, L., von Fischer, J., Tieszen, L., 2007. Late Quaternary temperature record from buried soils of the North American Great Plains. Geology 35, 159–162.
Oceanic, National, Atmospheric Administration (NOAA), 2010. Climatological Data, Annual Summary. New Mexico, 2010. National Climatic Data Center, Ashville, NC.
Olley, J.M., Pietsch, T., Roberts, R.G., 2004. Optical dating of Holocene sediments from a variety of geomorphic settings using single grains of quartz. Geomorphology 60, 337–358.
Pimentel, D., Harvey, C., Resosudarmo, P., Sinclair, D., Kurz, D., MnCair, M., Crist, S., Shpritz, L., Fitton, L., Saffouri, R., Blair, R., 1995. Environmental and economic costs of soil erosion and conservation benefits. Science 267, 1117–1123.
Prescott, J.R., Hutton, J.T., 1994. Cosmic ray contributions to dose rates for luminescence and ESR dating: large depths and long-term time variations. Radiation Measurements 23, 497–500.
Retallack, G.J., 2001. Soils of the Past, 2nd ed. Wiley-Blackwell.
Retallack, G.J., 2005. Pedogenic carbonate proxies for amount and seasonality of precipitation in paleosols. Geology 33, 333–336.
Royer, D.L., 1999. Depth to pedogenic carbonate horizon as a paleoprecipitation indicator? Geology 27, 1123–1126. http://dx.doi.org/10.1130/0091-7613(1999) 027b1123: DTPCHAN2.3.CO;2.
Schoeneberger, P.J., Wysocki, D.A., Benham, E.C., Broderson, W.D., 2002. Field book for describing and sampling soils, Version 2.0. ed. Natural Resources Conservation Service, National Soil Survey Center, Lincoln, NE.
Sheldon, N.D., Retallack, G.J., Tanaka, S., 2002. Geochemical climofunctions from North American soils and application to paleosols across the Eocene–Oligocene boundary in Oregon. J. Geol. 110, 687–696.
Soil Survey Staff, 2010. Keys to Soil Taxonomy. Keys to Soil Taxonomy. 2010 11th ed. US Government Printing Office, Washington, D.C. 331.
Southard, R.J., Driese, S.G., Nordt, L.C., 2011. Vertisols, In: Huang, P.M., Li, Y., Sumner, M.E. (Eds.), Handbook of Soil Science, 2nd edition. CRC Press, Boca Raton, Florida, pp. 33–82 (to 33-97).
Stoops, G., 2003. Guidelines for Analysis and Description of Soil and Regolith Thin Sections. Soil Science Society of America, Madison, WI.
Strong, G.E., Giles, J.R.A., Wright, V.P., 1992. A Holocene calcrete from North Yorkshire, England: implications for interpreting palaeoclimates using calcretes. Sedimentology 39, 333–347.
Toomey, R.S., Blum, M.D., Valastro, S., 1993. Late Quaternary climates and environments of the Edwards Plateau. Texas, Global and Planetary Change 7, 299–320.
Trierweiler, W.N., 1994. Archeological investigations on 571 prehistoric sites at Fort Hood, Bell and Coryell Counties, Texas. United States Army Fort Hood Archaeological Management Series, Research Report Number 31.

Trierweiler, W.N. (Ed.), 1996. Archaeological testing at Fort Hood: 1994–1995. United States Army Fort Hood Archaeological Management Series, Research Report Number 35, vols. I and II.
Verrecchia, E.P., Verrecchia, K.E., 1994. Needle-fiber calcite: a critical review and a proposed classification. J. Sediment. Res. 64.
Waters, M.R., Nordt, L.C., 1995. Late Quaternary floodplain history of the Brazos River in East-Central Texas. Quatern. Res. 43, 311–319.
Waters, M.R., Forman, S.L., Jennings, T.A., Nordt, L.C., Driese, S.G., Feinberg, J.M., Keene, J.L., Halligan, J., Lindquist, A., Pierson, J., Hallmark, C.T., Collins, M.B., Wiederhold, J.E., 2011. The Buttermilk Creek complex and the origins of Clovis at the Debra L. Friedkin site, Texas. Science 331, 1599–1603.
Wright, V.P., 1984. The significance of needle-fibre calcite in a Lower Carboniferous paleosol. Geol. J. 19, 23–32.
Wright, D.K., Forman, S.L., Waters, M.R., Ravesloot, J.C., 2011. Holocene eolian activation as a proxy for broad-scale landscape change on the Gila River Indian Community, Arizona. Quatern. Res. 76, 10–21.
Zhou, J., Chafetz, H.S., 2010. Pedogenic carbonates in Texas: stable-isotope distributions and their implications for reconstructing region-wide paleoenvironments. J. Sediment. Res. 80, 136–150.

CHAPTER FOUR

Late Quaternary alluvial history of Owl Creek, central Texas USA: Aggradation and degradation in the past 50 ka

This chapter submitted as: Meier, H.A., Nordt, L.C., Forman, S.L., Driese, S.G., 2014. Late Quaternary alluvial history of Owl Creek, central Texas USA: Aggradation and degradation in the past 50 ka. Geomorphology, submitted.

Abstract

New data and a synthesis of previous studies of Owl Creek define periods of fluvial erosion, deposition, and stability spanning the past ca. 50 ka. The use of well-dated stratigraphy provides new insights on the dynamic response of low-order streams to variable extrinsic and intrinsic factors with stadial, interstadial and Holocene climate variability. Eight periods of aggradation were identified and constrained using optically stimulated luminescence and radiocarbon ages to document the late Quaternary fluvial history of central Texas streams. The comparison of the composite Owl Creek record compared to regional paleo-climate proxies proxies compelling evidence for the sensitivity and research potential of low-order streams.

Introduction

Fluvial deposits are critical for deciphering late Quaternary environmental change in central North America where many studies have focused on the fluvial dynamics of large systems affected by meltwater discharge and/or sea-level fluctuations (e.g., Saucier, 1994; Aslan and Autin, 1998; Blum et al., 2000; Rittenour et al., 2007). These extrinsic controls, however, appear to have had limited influence on fluvial systems on the Southern Great Plains that are beyond direct meltwater input and the direct effects of eustatic variability. Rivers that drain the interior of central Texas appear to respond to changes related to broader stadial and interstadial conditions, such as variation in seasonal climate, ecology, and to intrinsic geomorphic thresholds (e.g., Blum and Velastro, 1989; Waters and Nordt, 1994; Hall and Valastro, 1995; Bettis and Mandel, 2002; Nordt, 2004). River system response in central North America is complex, though there is compelling evidence for net degradation since retreat of the Laurentide ice sheet ca. 15 ka (e.g., Licciardi et al., 1999; Rittenour et al., 2007; Sionneau et al., 2010).

Pleistocene fluvial deposits are preserved in isolated locations along the southern border of the Great Plains. A noticeable exception is the middle Brazos River Valley where stratigraphic exposures of terrace deposits abound (Waters and Nordt, 1995; Bongino and Nordt, 2007; Waters et al., 2011; Meier et al., 2013). Specifically, along Owl Creek the fluvial sequence spans the past ~120 ka (Meier et al., 2013). This study at the Red Bluff site within the Owl Creek Basin focused on the depositional history of this low-order stream through stratigraphic studies coupled with optically stimulated luminescence (OSL) dating (cf. Meier et al., 2013). Central Texas streams, similar to the Southwestern USA, are inferred to have responded to the expansion and presence of the Laurentide ice sheet ca. 30 to 15 ka with a cooler and wetter climate associated from the southward displacement of the Jet Stream, and with subsequent drying and warming to ice sheet retreat (Kutzbach and Guetter, 1986; Asmeron et al., 2010; Bromwich et al., 2004; Sionneau et al., 2013). Here we present new data, particularly from the Holocene, and a synthesis of previous studies of Owl Creek that better define periods of fluvial erosion, deposition, and stability spanning the past ca. 50 ka (Nordt, 1992, 1997; Meier et al., 2013). This paper presents a well-dated sequence of fluvial deposits that provides new insights on the dynamic response of low-order streams to variable extrinsic and intrinsic factors with stadial, interstadial and climate variability.

Background and Methods

Owl Creek, located on Fort Hood Military Reservation, is tributary to the Brazos River (Fig. 4.1a) with an approximately 72 km^2 drainage basin. The Owl Creek channel has a gradient of 3.4 m km^{-1} with a sinuosity of 1.1 (Fig. 4.1b; Nordt, 1992). The local uplands, the Manning surface, are comprised of Edward, Duck Creek, and Comanche Peak limestone at approximately 330 m elevation while the lower Killeen surface (approximately 320 m elevation) consists of the Cretaceous-aged Walnut Clay Formation (Barnes, 1979; Fig. 4.1b). Although these geomorphic surfaces are undated, they were presumably carved by ancestral fluvial systems (Hayward et al., 1990; Nordt, 1992; Fig. 4.1b). Three Quaternary alluvial landforms (T2, T1, T0) are the focus of this study along Owl Creek where Owl Creek has incised into the Cretaceous-aged Walnut Clay Formation with Edwards Limestone forming the uplands (Barnes, 1970). Modern vegetation is dominated by grasslands and altered historically by farm practices (Bomar, 1983; Lintz and Jackson, 1994). Regional soils are mapped as calcic-rich Mollisols and Inceptisols in the uplands and Mollisols, Inceptisols, and Entisols on the modern floodplain. Taxonomically-defined soil moisture and temperature regimes are Ustic (seasonal) and Thermic (warm), respectively (Soil Survey Staff, 2012). Owl Creek has seasonal flow that coincides with the increased rainfall during the early fall and late spring with a mean annual precipitation of 860 mm/yr (Huckabee et al., 1977).

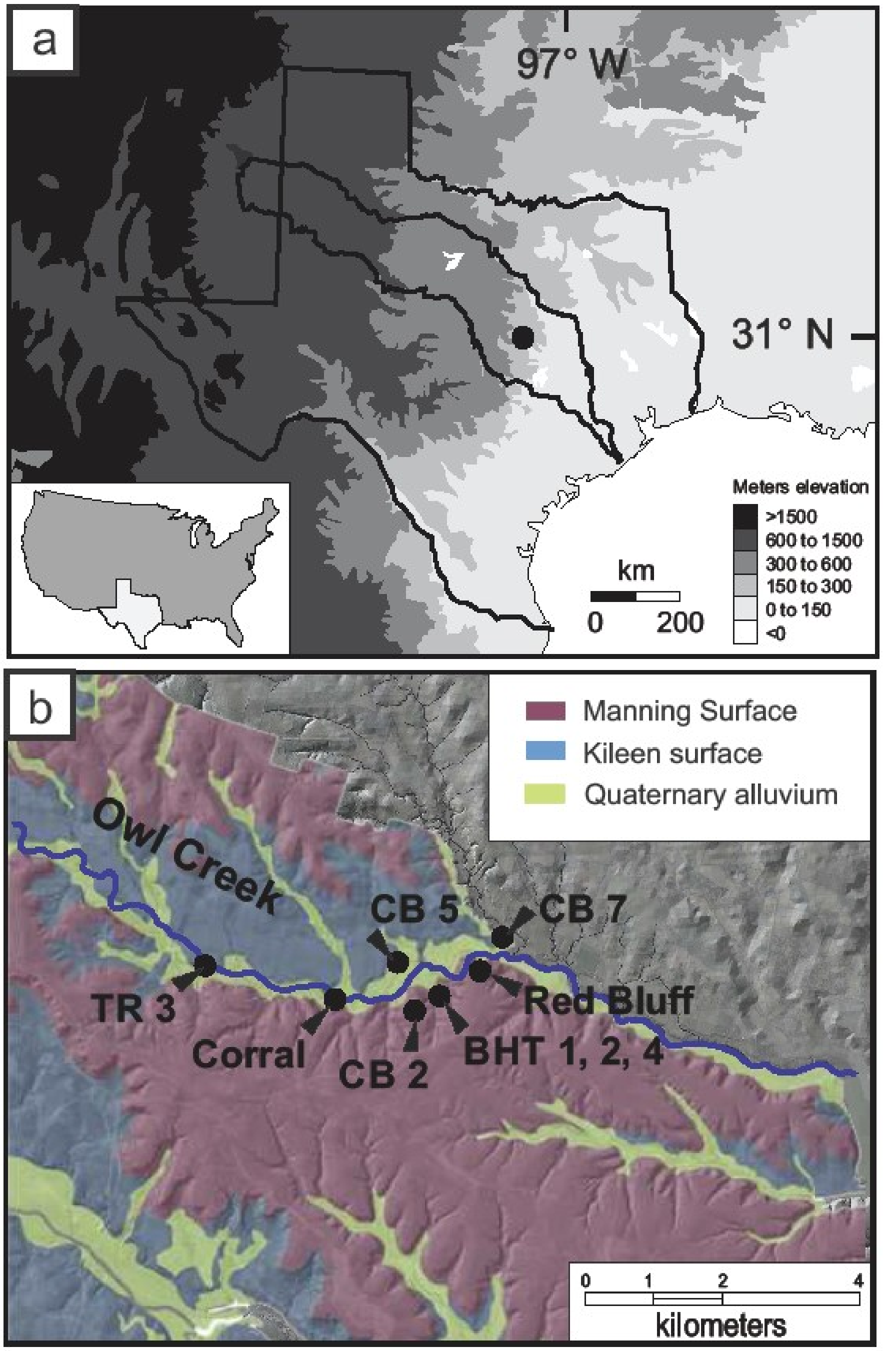

Fig. 4.1. Map of the study location (black dot) within the larger Brazos River valley (black line delineation). The lower image details Owl Creek geomorphology and study locations.

Three stratigraphic sections were studied at the Red Bluff locality, a natural exposure on the southern bank of Owl Creek (Fig. 4.1; Table 4.1; Meier et al., 2013).

Data from eight additional locations within the Owl Creek drainage basin are included in this investigation (CB 2, CB 5, CB 7, TR 3; Fig. 4.1; Table 4.1; Appendix 4A; Nordt, 1992). The BHT 1, 2, and 4 localities (Nordt, 1997) are from an archaeological site on the north-side of the catchment (Fig. 4.1; Table 4.1; Appendix 4A). The Corral locality is ~ 2 km upstream from Red Bluff (Fig. 4.1; Table 4.1; Appendix 4A).

Table 4.1.
Summary of units and chronology. All ^{14}C ages have been calibrated (Calib 7.0) and OSL ages are reported in years prior to AD 1950. Previous unit identification are from Nordt (1992) and Meier et al. (2013a).

Unit	Age (cal. yr B.P)	Lab Number	Previous unit identification
H	390±80	Beta37449[a, f]	Ford
G	710±60	Beta37016[a, f]	Upper West Range
	730±55	Beta63004[b, g]	
	770±30	GX15761[b, f]	
	950±55	Beta69870[b, g]	
	1445±80	Beta63003[b, g]	
F	2150±160	Beta38178[c, f]	Lower West Range
	4680±95	Beta42542[c, f]	
E	5700±60	Beta63000[d, g]	Q8, Fort Hood
	10,420±1060	UIC2900[e, h]	
D	10,055±685	UIC2904[e, h]	Q7, Georgetown
	12,635±1080	UIC2901[e, h]	
C	19,686±1610	UIC2648[e]	
	21,620±1340	UIC2644[e]	
B	43,050±3485	UIC2640[e, h]	Q6
A	~50 to 70 ka[h]		Q5

[a] ^{14}C age from dispersed charcoal
[b] ^{14}C age from hearth
[c] ^{14}C age from bulk humate
[d] ^{14}C age from charcoal
[e] OSL age
[f] Unit described by Nordt 1992
[g] Unit described by Nordt 1997
[h] Unit described by Meier et al., 2013

Topographic maps, soil survey manuals and digital elevation model (DEM) were analyzed to assess basin geomorphology, focusing on identification of alluvial terraces. The floodplain (T0) and alluvial terraces (T1-T3) are assigned based on relative elevation to the channel thalweg and to flood likelihood. For the seven backhoe trench and cutbank localities, lithological characteristics described in the field included grain size, sedimentary structure, stratal thickness, and boundary. These properties were used to interpret fluvial facies and environment of deposition. Field soil descriptions followed procedures of the USDA-NRCS (U.S. Department of Agriculture-Natural Resource Conservation Service) (Soil Survey Staff, 1996; Schoeneberger et al., 2002). These were used to interpret pedogenic processes and identify buried soils, or paleosols (Appendix 4A).

Age control of the fluvial history of Owl Creek was based on AMS^{14}C and OSL dating. The presented ^{14}C ages are from bulk humate, dispersed charcoal, and charcoal from an archaeological context (Nordt 1992, 1997; Table 4.1). The ages were calibrated using Calib 7.0 software (Stuiver ad Reimer, 1993). The OSL ages were obtained using single aliquots regenerative (SAR) protocols following the previously published methodology in Meier et al. (2013; Table 4.2). The OSL ages were obtained by averaging ~30 separate equivalent doses from respective aliquots of quartz grains and statistical analyses applying the central age model (Galbraith et al., 1999). Two OSL ages (UIC2900 & UIC2901) have overdispersion values ≥20% and have been recalculated using a finite mixture model, in lieu of the minimum age model (Galbraith and Roberts, 2012; Meier et al., 2014). Two additional OSL ages (UIC2648 & 2644) constrain the chronology at Corral site from quartz-rich sediments. The samples have overdispersion values ≤20%, have been assessed to be well solar rest (e.g. Olley et al., 2001; Wright et al., 2011) and are within the threshold of a D_e values using the central age model

(Galbraith et al., 1999). Optical ages are reported in years prior to AD 1950 to compare faithfully to ^{14}C ages (see Table 4.2).

TABLE 4.2.
Optically stimulated luminescence (OSL) ages on quartz grains from fluvial sediments of Owl Creek, Texas.

TABLE 2. Optically stimulated luminescence (OSL) ages on quartz grains from fluvial sediments Owl Creek, Texas

Unit	Depth (m)	Laboratory number	Aliquots	Grain size (µm)	Equivalent dose (Gray)[a]	Over-dispersion (%)[b]	U (ppm)[c]	Th (ppm)[c]	K_2O (%)[c]	H_2O (%)	Cosmic dose (mGray/yr)[d]	Dose rate (mGray/yr)	OSL age (yr)[e]
E	1.9	UIC2900	25	150-250	14.61 ± 1.26	86.5 ± 10.4	2.6 ± 0.1	3.7 ± 0.1	0.49 ± 0.01	5 ± 2	0.18 ± 0.02	1.39 ± 0.07	10,420 ± 1060[f]
D	8.5	UIC2904	30	100-150	18.75 ± 0.83	13.1 ± 1.7	2.4 ± 0.1	6.5 ±0.1	1.00 ± 0.01	5 ± 2	0.08 ± 0.01	1.85 ± 0.09	10,055 ± 685
D	4.7	UIC2901	30	150-250	12.61 ± 0.63	72.9 ± 9.5	2.6 ± 0.1	4.0 ± 0.1	0.30 ± 0.01	25 ± 5	0.12 ± 0.01	0.99 ± 0.05	12,635 ± 1080[f]
C	1.0	UIC2648	30	100-150	27.48 ± 1.01	6.9 ± 0.9	2.3 ± 0.1	4.8 ± 0.1	0.44 ± 0.01	5 ± 2	0.19 ± 0.02	1.40 ± 0.07	19,626 ± 1610
C	1.3	UIC2644	30	63-100	45.13 ± 1.61	8.3 ± 1.1	2.4 ± 0.1	7.9 ± 0.1	0.96 ± 0.01	5 ± 2	0.18 ± 0.02	2.08 ± 0.11	21,620 ± 1340
B	5.0	UIC2640	30	100-150	38.27 ± 1.43	10.2 ± 1.4	2.3 ± 0.1	3.5 ± 0.1	0.23 ± 0.01	25 ± 5	0.11 ± 0.01	0.97 ± 0.05	43,050 ± 3485

[a]Quartz fraction analyzed under blue-light excitation (470 ± 20 nm) by single aliquot regeneration protocols (Murray and Wintle, 2003). Each aliquot contained between 100 and 500 grains in a 2 mm plate diameter.
[b]Values reflect precision beyond instrumental errors; values of ≤ 25% indicate low dispersion in equivalent dose values. 11
[c]U, Th and K_20 content analyzed by inductively coupled plasma-mass spectrometry analyzed by Activation Laboratory LTD, Ontario, Canada.
[d]From Presott and Hutton (1994).
[e]Ages calculated using the central age model of Galbraith et al. (1999).
[f]Ages calculated using the finite mixture model of Galbraith and Roberts (2012). All errors are at 1 sigma and include systematic and random errors.
Ages are from the reference year AD 1950.

Owl Creek Fluvial Units

Terrace 2

Description

Terrace T2a is the oldest fluvial landform, which occurs ~9.5 m above the active channel. Remnants of this terrace are correlated based on similar physical characteristics and elevation with natural exposures on the north (See Fig. 4.1b; CB3; Nordt, 1992) and south side of the basin (Red Bluff; See Fig. 4.1b; Meier et al., 2013). Unit A is comprised of an ~2 to 3 m thick deposit of poorly-sorted, trough cross-bedded gravels that grade upward from a loam to a clay loam sediment (Table 4.1; Q6 of Meier et al., 2013; Jackson alluvium of Nordt, 1992). This sedimentologic succession is interpreted as a lateral accretion deposit capped by fine-grained overbank deposition (Fig. 4.2; Appendix 4A; Nordt, 1992; Meier et al., 2013). The fill sequence is underlain by the Walnut Clay Formation (Fig. 4.3). Although not directly dated, the cut and fill sequence of Unit A is constrained by associated OSL ages, which indicates aggradation sometime between ca. 75 and 50 ka (Meier et al., 2013).

The Corral location exposes the T2b terrace at ~5.5 m above the active channel, which is underlain by unit B (See Fig. 4.1). The basal, poorly-sorted coarse gravel rests unconformably on the Walnut Clay Formation (Fig. 4.2; Appendix 4A). These limestone and chert gravels fine upward into a pedogenically modified silty-clay loam deposit. The change in grain size through the lower part of this profile indicates a decrease in stream competency and/or a shift in source with terminated by surface stability. The thin, 40-cm-thick buried soil with A-Bw-C horizonation was later truncated and then buried by emplacement of a gravel-rich silty clay and silt clay loam. This deposit forms the constructional T2b terrace (Fig. 4.3). Quartz grains below and above the buried soil yielded OSL ages of 21,620 ± 1340 yr (UIC2644) and 19,626 ± 1610 yr (UIC2648), respectively (Table 4.2).

Interpretation

Owl Creek at this time was a meandering stream with unit A facies indicating channel migration with a fluctuating sediment supply, likely resulting from increased stream competency. Bedrock incision of approximately 4 m occurred before ca. 43 ka and was followed by deposition of Unit C (Fig. 4.3). These coarse-grained sediments may reflect a competent, but meandering stream that likely scoured the underlying Walnut Clay Formation in two phases (Meier et al., 2013). The coarse-grained gravels that underlie Unit B may be equivalent to the ca. 43 ka gravel unit, but correlation has not been assumed.

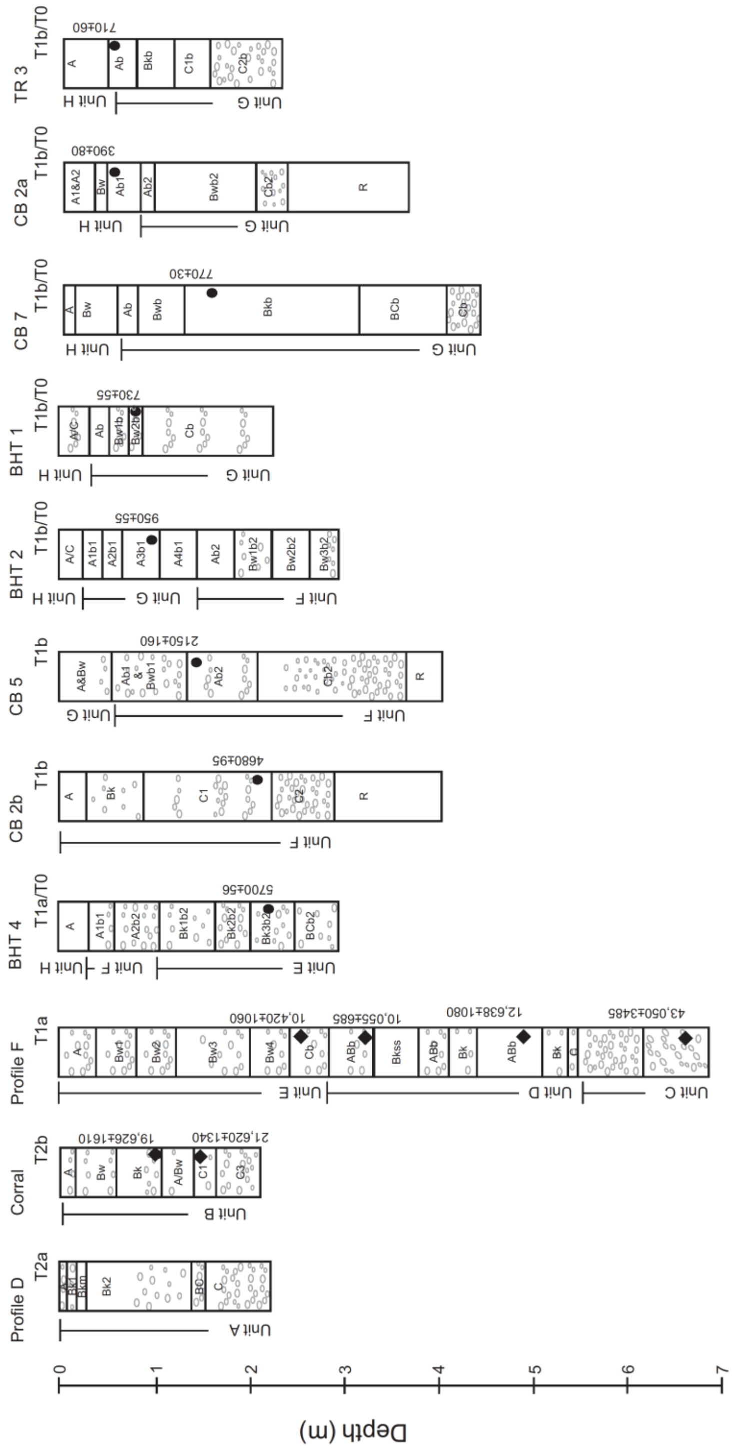

Fig. 4.2. Owl Creek soil-stratigraphic profiles from the study locations. Red Bluff profiles (Profile D & F) have been reconstructed from Meier et al. (2013). Refer to Tables 1 and 2 for radiocarbon and OSL samples, and Appendix 4A for soil stratigraphic descriptions.

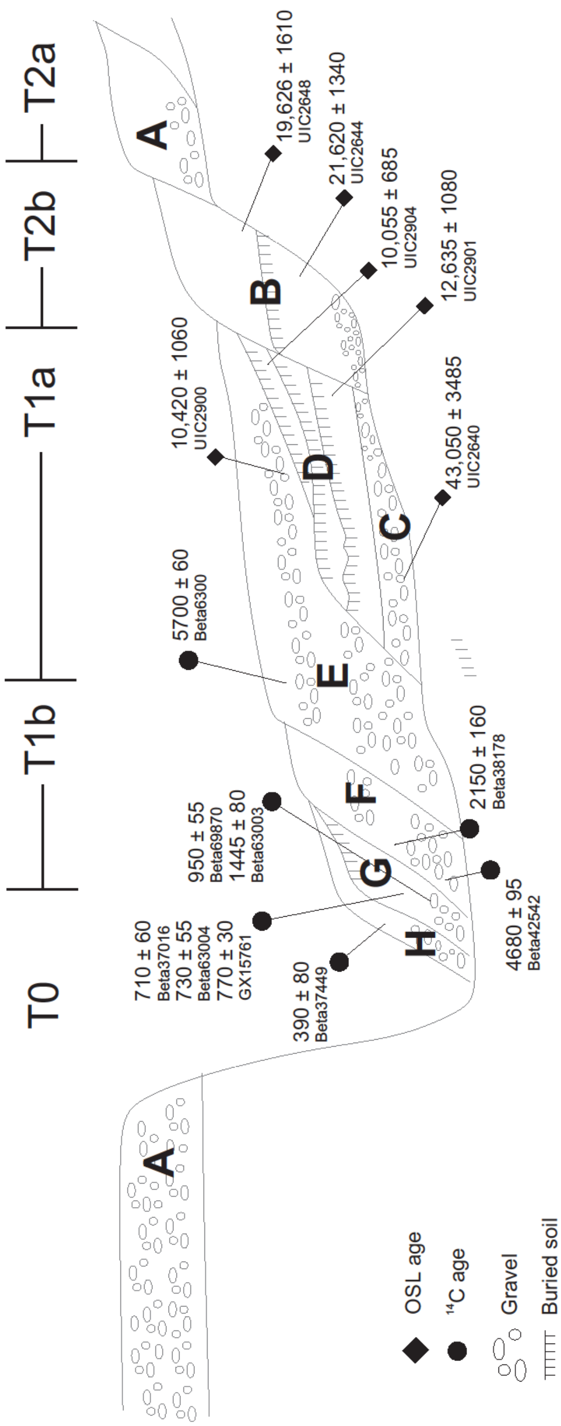

Fig. 4.3. Owl Creek composite stratigraphic cross-section with OSL and ^{14}C chronologies.

Terrace 1 (T1)

Description

Terrace 1 is comprised of fluvial sediments ~5 m above the modern Owl Creek channel. The terrace has been subdivided based on an approximately 1 m variation of topographic expression (T1a and T1b). The T1a terrace is underlain by Unit C, D, and E. Unit C from the stratigraphic composite corresponds to the previously described Q6 unit from Red Bluff (Fig. 4.2; Table 4.1; Meier et al., 2013). This unit is a 1.3-m-thick, coarse-grained, trough cross-bedded gravel that unconformably overlies the Walnut Clay Formation (Fig. 4.3; Meier et al., 2013). This facies is interpreted as a lateral accretion deposit and reflects stream competency with Owl Creek transitioning from a braided to a meandering system at ca. 43 ka, based on a previously reported OSL age (Table 4.2; Meier et al., 2013).

Unconformably overlying the Unit C gravels is a 2.6-m-thick, dominantly fine-grained deposit that has been pedogenically altered (Unit D). This unit corresponds to the Q7 and the equivalent Georgetown alluvium along Owl Creek (Table 4.1; Fig. 4.3; Meier et al., 2013; Nordt, 1992). Unit D, detailed by Meier et al. (2013), is a series of three buried soils, with AB-Bk or AB-Bkss horizonation (Fig. 4.3; Meier et al., 2014). The fine-grained alluvium of Unit D indicates distal deposition from a channel (Meier et al., 2013). Aggradation of this unit is inferred to between 13 and 10 ka based on OSL ages (Table 4.2).

Unit E is comprised predominately of fined-grained, silty-clay loam and loam deposits and forms the constructional T1a terrace (Fig. 4.1). Previously identified at Red Bluff (Q8 unit; Meier et al., 2013) and the Fort Hood alluvium (Fig. 4.2; BHT-4; Nordt, 1997), unit E overlies, in a few localities, partially truncates, Unit D and the Walnut Clay

(Fig. 4.3; Nordt, 1992; Meier et al., 2013). This silty clay and silty-clay loam deposit is interbedded with angular chert and limestone gravel indicating variable sediment supply and/or stream discharge (Meier et al., 2013). An OSL age from the base of the unit is 10,420 ± 1060 yr (UIC2900), accompanied by a ^{14}C age 5700 ± 60 cal. yr B.P. (Beta-6300) higher in the sequence. This indicates that Unit E was deposited in the early to middle Holocene.

Unit F was identified previously as the Lower West Range alluvium (Nordt, 1992, 1997) and was identified in BHT-2, BHT-4, CB2b, and CB5 (Fig. 4.2; Appendix 4A). This unit occurs beneath the T1b terrace. It ranges in thickness from ~1.5 m to ~3 m and is comprised of a clay loam interbedded with gravels (Nordt, 1992). The base of unit F is unconformable with the underlying Walnut Clay Formation, and is partially buried by unit G (Fig. 4.3). Radiocarbon ages on the bulk sediment humate fraction from unit F are 2150 ± 160 cal. yr B.P. (Beta38178) and 4680 ± 95 cal. yr B.P. (Beta42542).

Unit G is a fluvial deposit identified within the basin (Fig. 4.2; CB 5, BHT 2, BHT 1, CB7, CB 2 a, TR3). This unit, which corresponds to Upper West Range alluvium (Nordt, 1992), ranges in thickness from ~ 2 to 4 m and consists of sandy clay loam to a silty clay loams with isolated gravel lens (Fig. 4.2; Appendix 4A). The unit is erosionally inset into Unit F and scoured into underlying parent material (Fig. 4.3). It is chronologically constrained by a suite of radiocarbon ages-770 ± 30 cal. yr B.P. (GX15761), 730 ± 55 cal. yr B.P. (Beta63004), 950 ± 55 cal. yr B.P. (Beta69870), and 1445 ± 80 cal. yr B.P. (Beta63003)- also based on charcoal from an archaeological site and on one age from fluvial sediments of 710 ± 60 (Beta37016) on dispersed charcoal (Table 4.1).

Interpretation

Owl Creek deposition resumed by ca. 21 ka (Unit B) indicated by a fining upward succession, likely reflecting a decrease in stream competency or shift in sediment supply. After a brief interval of pedogenesis, deposition had resumed ended with construction of the T2b terrace after ca. 19 ka (Fig. 4.3). Unit D deposition began at ca. 12.6 and terminated by ca. 10 ka. The fine-grained overbank deposits with multiple buried soils forming together formed in approximately 2 ka (Meier et al., 2014). Deposition resumed from ca. 10 to 6 ka preserving fine-grained sediments, interbedded with gravels of unit E, and construction of the T1a terrace (Fig. 4.3). Lateral channel erosion with further bedrock incision occurred before Unit F deposition at ca. 5 ka and continued until ca. 2 ka. This fine-grained deposit interbedded with gravels is suggestive of variable stream flow or shift in sediment source, which constructs eventually the T1b terrace. Widespread fluvial deposition of Unit G occurs from ca. 1.5 ka to ca. 700 yr with deposition of a dominantly fined-grained facies (Fig. 4.3).

Floodplain (T0)

The thalweg of the modern Owl Creek flows on the Walnut Clay Formation incised ~1 to 3 m below the surface of the T1 terrace. The youngest depositional unit (H) occurs below the T0 terrace and corresponds to the Ford alluvium (Fig. 4.1; Nordt, 1992). The unit commonly has basal gravels that grade upward into interbedded sands to and silty-clay loams that in places bury Unit G (Fig. 4.2; Appendix 4A; BHT-4, BHT-2, BHT-1, CB7, CB2a, TR3). Unit H has aggraded to within 1 to 2 m of the T1b terrace surface. Deposition began sometime after 706 cal. yr B.P., and has continued until after 390 ± 80 cal. yr B.P. (Beta37449; Fig. 4.3; Table 4.1). Deposition of Unit H by ca. 400 yr is faintly laminated deposit and suggestive of overbank deposition that constructed the modern (T0) terrace.

Environmental and Regional Fluvial System Response

This research expands the previously known stratigraphic and chronologic record of Owl Creek during the late Quaternary. The correlation of these fluvial units to neighboring Cowhouse Creek (Nordt, 2004) offers greater insight to extrinsic and intrinsic geomorphic factors operating during the past ca. 50 ka. Fluvial records with direct numeric age control are sparse in central Texas and with only a few localities corresponding to the oldest units in Owl Creek (Blum and Valastro, 1989, 1994; Bongino and Nordt, 2007; Waters et al., 2011). Coincident records are more common during the early to middle Holocene when Owl Creek was dominated widespread valley filling of fine-grained over bank deposits (Nordt, 1995, 2004; Durbin et al., 1997; Blum and Price, 1998; Sylvia and Galloway, 2006; Mandel et al., 2007). The following discussion divides the depositional history of Owl Creek into two temporal stages in reference to marine isotope stages and the Last Glacial Maximum (Martinson et al., 1987).

MIS 4 to the LGM (ca. 71 to 26 ka)

This interval corresponds to glacial and interstadial periods with sea level most likely 30-120 m below present condition (Anderson et al., 2004; Siddall et al., 2009; Thomas et al., 2009; Lambeck et al., 2012). Lower sea level corresponds to increases in ice sheet volume when climate models show that this phenomemon perturbed atmospheric circulation resulting in the southward expansion of the Jet Stream and increased moisture during winter months (Kutzbach and Guetter, 1986, Bronwich et al., 2004; Asmerom et al., 2010; Sionneau et al., 2013). Speleothem records from the

Southwest and Midwest USA appear consistent with climate models, with the Southwest proxies showing wetter conditions when the Midwest is cooler and drier during times of increased continental ice volume (Fig. 4.4; Dorale et al., 1998; Musgrove et al., 2001; Forman and Pierson, 2002; Brooks et al., 2006).

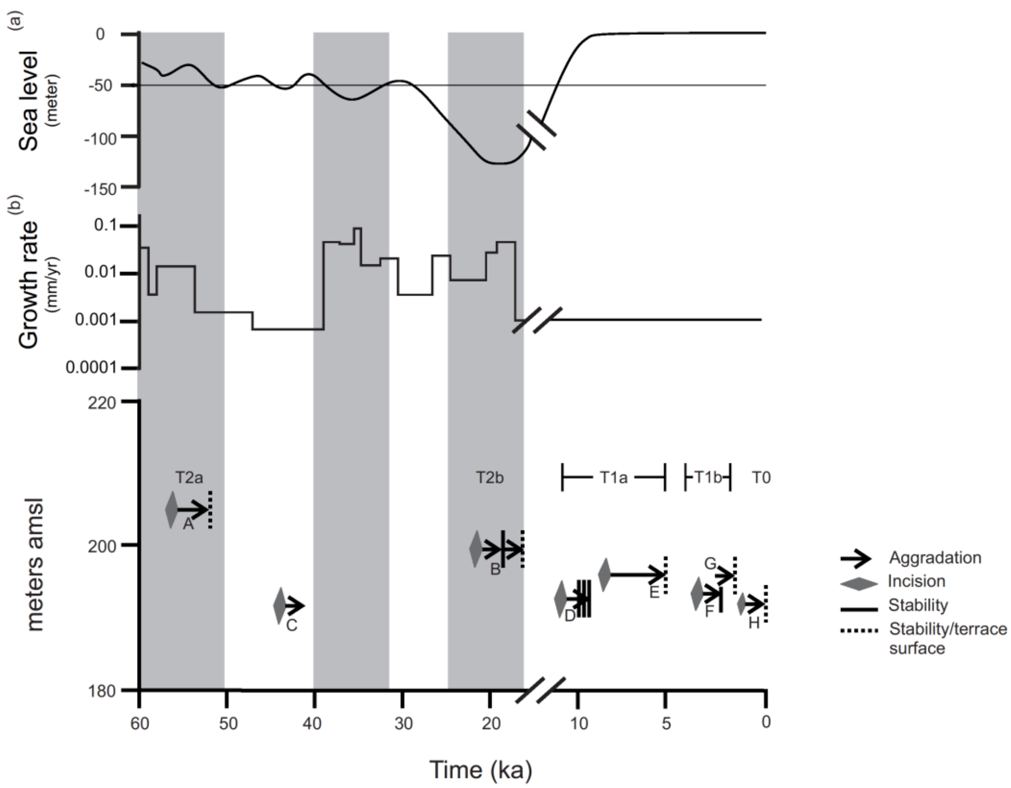

Fig. 4.4. Correlation of the alluvial stratigraphic record between Owl Creek and (a) global sea level (Chappell & Shackleon, 1986; Chappell et al., 1996) and the (b) speleothem growth rate from central Texas (Musgrove et al., 2001). The gray intervals correspond to greater wetness.

A speleothem record from central Texas indicates increased moisture at ca. 71-60 ka, 39-33 ka, and 24-12 ka (Fig. 4.4; Musgrove et al., 2001). These documented moist intervals are broadly equivalent with the deposition of units A, B, and C at Owl Creek (Fig. 4.4). Valley fill complexes for Cowhouse Creek correlate to Owl Creek (Nordt, 1992, 2004) and the Bosque River (Bongino and Nordt, 2007) are dated between ca.73 and 52 ka are suggestive of regional aggradation during a period of increased moisture (Fig. 4.4). Also, coastal fluvial sequences, such as the Deweyville Formation, span ca. 74 to 12 ka (Blum and Valastro, 1989; Blum and Price, 1998; Blum and Aslan, 2006). Buttermilk Creek in central Texas, the Perdernales River in central west Texas, and the Medina River in south central Texas (Blum and Valastro, 1989; Mandel et al., 2007; Waters et al., 2011) may be equivalent to deposition at Owl Creek at ca. 43 ka, which is roughly coeval to the documented increase in moisture at ca. 40 ka (Fig. 4.4; Unit C; Musgrove et al., 2001; Meier et al., 2013).

LGM to present (ca. 26 to present)

Owl Creek uniquely preserves fluvial deposits (Unit B) indicating aggradation spanning the Last Glacial Maximum (25- 15 ka), when sea level fell by ~120 m (Anderson et al., 2004) during a period of increased regional moisture (Fig. 4.4; Musgrove et al., 2001). In contrast, coastal reaches of rivers in central Texas incised and clastic sediments were transported into the Gulf of Mexico (Abdulah et al., 2004; Anderson et al., 2004; Wellner et al., 2004; Anderson et al, 2013), with the exception of aggradation along the Colorado and Brazos River at ca. 23 to 16 ka (Blum and Valastro, 1994; Blum and Aslan, 2006; Sylvia and Galloway, 2006). This inverse relation between degraded coastal reaches and aggraded systems may reflect a continental margin sea level response, with landward catchments receiving added precipitation with an enhanced North American summer monsoon (Lachniet et al., 2013).In turn the Gulf of Mexico was dominated by meltwater pulses from the Mississippi River between ca. 18 and 16 ka (Durbin et al., 1997; Blum and Price, 1998; Abdullah et al., 2004; Anderson et al., 2004; Taha and Anderson, 2008; Sionneau et al., 2010) though this input appears to have not significantly cooled surface waters (Williams et al., 2010, 2012) and thus the Gulf was a likely an advective source of moisture during summer (Musgrove et al., 2001; Koch et al., 2004). Deposits of this age are absent from Cowhouse Creek and may indicate degradation similar to the inferred response along the Brazos River (Waters and Nordt, 1995; Nordt, 2004).

Environmental and fluvial records are common post-LGM and are coincident with a rapid sea level rise and an increase in summer insolation (COHMAP, 1988; Anderson et al., 2004; Aharon, 2006; Nordt et al., 2002, 2008; Weight et al., 2011; Anderson et al., 2013). Climate models suggest that the Jet Stream migrated northward due to the retreating Laurentide ice sheet and resulted in a regional shift to more mesic conditions by 10 ka, potentially associated with a strengthened North American Monsoon (Fig. 4.5; Bousman, 1998; Musgrove et al., 2001; Nordt et al., 2002, 2008; Bromwich et al., 2004; Nordt, 2004; Ellwood and Gose, 2006; Williams et al., 2010, 2012; Hall and Penner, 2013; Lachniet et al., 2013). This climatic shift is preserved at Owl Creek, with carbon isotopes from bulk soil organic matter suggesting a paleoecological change at ca. 11 ka to warmer conditions (higher C4 plant biomass) during the deposition of Unit D (Fig. 4.5; Table 4.2; Meier et al., 2014). Coeval regional isotopic sedimentary records from the Abbo Arroyo from the Rio Grande basin (Fig. 4.5; Hall and Penner, 2013) and the Midwestern USA (Fig. 4.5; Nordt et al., 2008) parallel the record preserved at Cowhouse and Owl Creek (Fig. 4.5; Nordt et al., 1998; Meier et al., 2014). These records exhibit a shift to warmer conditions during reduced ENSO variability (Fig. 4.5; Waters and Nordt, 1995; Nordt, 2002; Hall and Penner, 2013 Nordt, 1998).

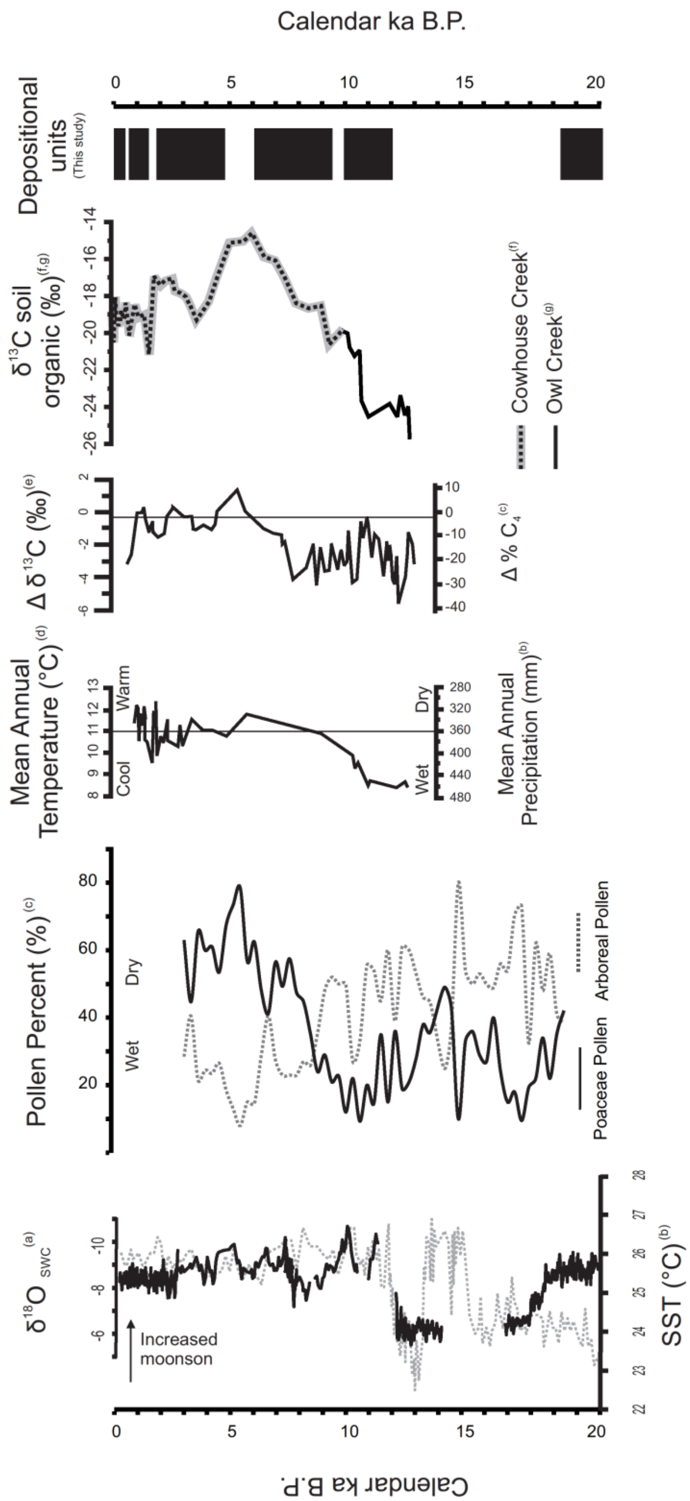

Fig 4.5 Composite regional environmental records for the past 20 ka compiled from (a) Lachniet et al., 2013; (b) Lea et al., 2003; (c) Bousman, 1998; (d) Hall and Penner (2013); (e) Nordt et al., 2008; (f) Nordt, 2004; (g) Meier et al., 2014.

Peak temperatures and summer drying are inferred post 7.5 ka, with disappearance of the Laurentide ice sheet and an increase in ENSO variability (Fig. 4.5; Bousman, 1998; Nordt et al., 1994; Nordt et al, 2002, 2008; Anderson et al., 2013; Lachniet et al., 2013). This interval marks a shift in depositional style at Owl Creek to widespread valley filling as documented by the T1b terrace and the associated units (Fig. 4.4). Incision to bedrock and aggradation of units D though H, from both Cowhouse and Owl Creek, suggests that these systems may be responding to extrinsic changes that control sediment flux, like changes in vegetation cover (cf. Nordt, 2004) that may have heightened climate sensitivity greater than that of the larger Brazos River (cf. Nordt, 2004). Upland erosion due to knickpoint migration after ca. 8 ka is suggestive of stream response to late Pleistocene erosion during an increasingly warming and drying climate (Fig. 4.5; Nordt, 2004). Climate proxies preserve a cool/wet interval at ca. 2.5 ka that correlates to Owl Creek and Cowhouse Creek incision (Fig. 4.5; Nordt et al., 2008; Bousman, 1998, Hall and Penner, 2013). The late Holocene is a period of multi-decadal to century scale drought variability with the valleys of the Brazos River and the Colorado River aggrading (Toomey et al., 1993; Nordt, 1995, 2002, 2004; Blum and Aslan, 2006; Anderson, 2008; Waters et al., 2011). The documented regional aggradation at ca. 1.5 ka and 400 yr, correlates to Owl Creek units G and H respectively , likely reflects continued erosion of the uplands and associated increase in temperatures and rainfall reduction associated with extreme drought (Fig. 4.5; Hall, 1988, 1990; Waters and Nordt, 1995; Grissino-Mayer etal., 1997; Holliday, 2001; Nordt, 1997, 2002; Nordt et al., 2002, 2008; Seifert et al., 2009).

Conclusion

The sedimentary record from Owl Creek details the late Quaternary depositional history of a low-order stream in central Texas. New data integrated with results from previous studies defines eight major aggradational events spanning the past ca. 50 ka. The well-dated sequence of fluvial deposits from Owl Creek results in the following conclusions: (1) the fluvial deposits confirm the research potential of small low-order stream as sediment catchments; (2) central Texas uniquely preserves climate variability linking the Southwestern and Midwestern proxies (3) the Owl Creek record from ca. 50 ka to ca. 19 ka is sparse (Unit A , B, & C) with wide spread valley filing during the Holocene (Units D to H); (4) Owl Creek shows evidence for aggradation during the last glacial maximum in contrast to the Brazos River and adjacent river reaches in coastal setting are incised reflecting changing controls on fluvial dynamics from sea level to an increase in precipitation up the catchment; (5) The Holocene units are suggestive of a change in depositional style, characteristic upland destabilization with drought conditions; and (6) noted periods of erosion likely relate to intrinsic periods of geomorphic instability that appear to be preserved at Owl and Cowhouse creeks.

Appendix 4A.
Soil descriptions from the Corral location. Soil descriptions for CB7, CB5, TR3; CB2a and CB2b have been reproduced from Nordt (1992). BHT1, BHT2, and BHT4 have been reproduced from Nordt (1997). All horizons are strongly effervescent and colors were taken from dry samples.

Abbreviations: Structure 1=weak, 2=moderate, 3=strong, f=fine, m=medium, co=coarse, sbk=subangular blocky, pr=prismatic, w=wedge; M=massive
Texture Si=silt, C=clay, L=loam, GR=gravelly, VGR=very gravelly, G=gravel, C=cobbles
Boundary V=very abrupt, A=abrupt, C=clear, G=gradual, D=diffuse, S=smooth, W=wavy

Corral Location -

A	0 – 15 cm	1fgr; C, S; SiCL; very dark grayish brown (10Y 3/2); common modern roots; common coarse fragments, matrix supported, well sorted limestone and cherts.
Bw	15 – 60 cm	2fsbk; C, S; SiCL; brown (7.5YR 4/3); few modern roots; common coarse fragments, matrix supported, well sorted limestone and cherts.
Bk	60 – 104 cm	1csbk; D, W; SiCL; brown (7.5YR 3/4); very few medium burrows; few fine calcium carbonate filaments; very few medium calcium carbonate nodules; isolate zone of coarse fragments, matirx supported well sorted limestone and cherts. Corresponds to UIC2648.
A/Bw	104 – 126 cm	2cpr; D, S; SiCL; very dark grayish brown (10YR 3/2); very few coarse burrows; very few fine calcium carbonate filaments; very few calcium carbonate nodules; few coarse fragments, matrix supported, well sorted limestone and cherts. Corresponds to UIC2644.
C1	126 – 142 cm	M; D, S; SiCL; brown (10YR 5/3); few fine burrows; very few modern snail shells; few coarse fragments, matrix supported, well sorted limestone and cherts.
C2	142 – 212 cm	C, W; G C; trough cross-bedded, matrix supported, poorly sorted limestone and cherts; few calcium carbonate pendants.
C3	212 to 280+	G C; matrix supported, poorly sorted limestone and cherts; few calcium carbonate pendants.

CB7

A	0 to 10 cm	very dark grayish brown (19YR 3/2) sand clay

		loam; abrupt boundary.
Bw	10 to 24 cm	dark brown (10YR 3/3) gravelly sandy clay loam to sandy clay loam; abrupt boundary.
Ab	24 to 76 cm	very dark grayish brown (10YR 3/1.5) silty clay loam; gradual boundary.
Bwb	76 to 129 cm	very dark grayish brown (10YR 3/2) silty clay loam; gradual boundary.
Bkb	129 to 310 cm	dark brown (10YR 3/3) to brown (10YR 4/3) clay loam; mycelial carbonate increases from 2 to 8% with depth; a charcoal hearth age (GX15761) at 157 cm; gradual boundary.
BCb	310 to 435 cm	mottled grayish brown (10YR 5/2) and yellowish brown (10YR 5/6) sandy clay loam; abrupt boundary.
Cb	435 to 465 cm	50% fine gravels in a sandy clay loan matrix like above.

CB2a

A1 & A2	0 to 35 cm	very dark grayish brown (10YR 3/2) sandy clay loam; clear boundary.
Bw	35 to 46 cm	very dark grayish brown (10YR 3/2) sandy clay loam with common brownish yellow (10YR 6/6) sand patches.
Ab1	46 to 81 cm	very dark grayish brown (10YR 3/2) clay loam; clear boundary; dispersed charcoal age (Beta37449) at 52 cm.
Bwb2	96 to 201 cm	dark brown (10YR 3/3) grading to brown (10YR 5/3) sandy clay loam; clear boundary.
Cb2	201 to 232 cm	mottled dark grayish brown (2.5 Y 4/2) and olive yellow (2.5Y 6/6) fine gravelly sandy clay loam.
R	232 to 362 cm	Walnut clay down to channel

CB2b

A	0 to 27 cm	dark brown (10YR 3/3) sandy clay loam; gradual boundary.
Bk	27 to 88 cm	dark brown (10YR 3/3) grading to brown (10YR 4/3) with 3 to 4% mycelial carbonates; 5 to 10% fine gravel; abrupt boundary.
C1	88 to 224 cm	alternating beds of brown (10YR 5/3) gravelly clay loam (horizontal) and mottled grayish brown (10YR 5/2) and yellowish brown (10YR 5/6) clay loam; channel and channel fill deposits; a bulk humate age (Beta42542) from channel fill at 210 cm; abrupt boundary.
C2	224 to 289	poorly sorted medium to coarse gravels in loamy grayish brown and brown matix.

R	289 to 400 cm	Walnut Clay down to waterline.

CB5

Road spoil	0 to 14 cm	
A & Bw	14 to 57 cm	dark brown (10YR 3/3) grading to light yellowish brown (10YR 6/4) sand clay loam; few fine gravels; abrupt boundary.
Ab1 & Bwb1	57 to 132 cm	very dark grayish brown (10YR 3/2) gravelly clay loam grading to dark brown (10YR 3/3) gravelly sandy clay loam; 2 to 3% mycelial carbonate; abrupt boundary.
Ab2	132 to 208 cm	multiple buried A horizons separated by thin gravel lines; very dark grayish brown (10YR 3/2) clay loam; 2% mycelial carbonate; bulk humate age (Beta38178) from 135 cm; clear boundary.
Cb2	208 to 367 cm	poorly sorted fine to coarse massive gravels in loamy brown matrix; coarsens downward; abrupt boundary.
R	367 to 410 cm	Walnut Clay down to channel.

TR3

A	0 to 49 cm	very dark grayish brown (10YR 3/2) clay loam; clear boundary.
Ab	49 to 78 cm	very dark grayish brown (10YR 3/2) sandy clay loam; gradual boundary; dispersed charcoal age (Beta37016).
Bkb	78 to 116 cm	dark brown (10YR 4/3) sandy clay loam with 3 to 4% mycelial carbonates; abrupt gravel line boundary.
C1b	116 to 152 cm	dark grayish brown (10YR 4/2) massive sandy clay loam; abrupt boundary.
C2b	152 to 230	medium and coarse moderately well sorted gravels in gray and tan matrix.

BHT-1

A/C	0 to 21 cm	dark brown (10YR 3/3) clay loam; moderate medium subangular blocky; firm; many roots; common carbonate sand grains; common biocasts; faintly laminated; clear smooth.
Ab	21 to 48 cm	vary dark grayish brown (10YR 3/3) clay loam; firm; few 2 to 4 mm coarse fragments; few snails; clear smooth.
Bw1b	48 to 72 cm	dark brown (10YR 3/3) loam; common very dark grayish brown (10YR 3/2) biocasts; weak coarse subangular blocky; friable; common carbonate sand

		grains; few pebble stringers (2 to 10 mm diameter) dipping towards modern channel; abrupt smooth.
Bw2b	72 to 87 cm	dark brown (10YR 3/3_ sandy clay loam; weak coarse subangular blocky; friable; 1% carbonate mycelia; 3 to5% coarse fragments 2 to 4 mm; horizon dipping to modern channel; abrupt smooth; hearth charcoal age (Beta6003).
Cb	87 to 223 cm	alternating beds (10 to 20 cm thick) of gravel-rich (0.2-2 cm diameter) and gravel-poor zones; brown (10YR 4/3) to pale brown (10YR 6/3) sandy clay loam matrix. Gravels become matrix-supported and moderately well sorted and coarsen downward.

BHT-2

A/C	0 to22 cm	very dark grayish brown (10YR 3/2) clay loam; 10 to 20% brown (10YR 5/3) biocasts; moderate medium subangular blocky; firm; faintly laminated; 2 to 3% carbonate fragments 3 to 5 mm; clear wavy.
A1b1	22 to 42 cm	very dark brown (10YR 2/2) silty clay loam; moderate medium subangular blocky; firm; few snails; clear wavy.
A2b1	42 to 61 cm	very dark grayish brown (10YR 3/2) clay loam; common brown (10YR 5/3) biocasts; moderate coarse subangular blocky; firm; few fine carbonate coarse fragments; few snails; clear wavy.
A3b1	61 to 105 cm	very dark grayish brown (10YR 3/2) silty clay loam; weak coarse prismatic to angular blocky; firm; dispersed charcoal, bone and burned limestone and chert; gradual wavy; hearth charcoal age (Beta69870).
A4b1	105 to 148 cm	very dark grayish brown (10YR 3/2) silty clay loam; weak coarse prismatic to angular blocky; very firm; 1% carbonate mycelia; few limestone fragments, dispersed charcoal and snails in upper part.
Bw2b2	222 to 262 cm	brown (10YR 5/3) loam; few loamy pockets and carbonate mycelia; gradual.
Bw3b2	262 to 292 cm	brown (10YR 5/3) loam; common medium faint yellowish brown (10YR 5/6) mottles; loamy pockets; dense gravel in lower 12 cm, waterworn and angular, 0.2 to 2 cm (auger).

BHT-4

A	0 to 30 cm	black (10YR 2.5/1) loam; moderate fine and medium subangular blocky; friable; few angular pebbles; clear smooth.

A1b1	30 to 52 cm	black (10YR 2/1) clay loam; moderate fine and medium subangular blocky; friable; 1 to 2% carbonate mycelia; few to common angular pebbles; clear wavy.
A2b1	52 to 104 cm	very dark brown (10YR 2/2) clay loam; weak coarse subangular blocky; firm; common burned limestone and chert; many shells; clear wavy.
Bk1b2	104 to 166 cm	yellowish brown (10YR 5/4) silty clay loam; weak coarse prismatic; firm; 5 to 8% angular pebbles 2 to 10 mm; 1 to 2% carbonate mycelia; few burned chert and limestone fragments; clear wavy.
Bk2b2	166 to 194 cm	yellowish brown (10YR 5/4) silty clay loam; weak coarse prismatic; firm; 4 to 5% carbonate mycelia; 10 to 15% angular pebbles 2 to 10 mm; gradual smooth.
Bk3b2	194 to 248 cm	yellowish brown (10YR 5/4) silty clay loam; weak coarse prismatic; firm; 4 to 5% carbonate filaments and threads; 10 to 15% angular pebbles 2 to 10 mm; charcoal age (Beta63000).
BCb2	248 to 288 cm	yellowish brown (10YR 5/4) loam; 1% carbonate mycelia; 5% angular pebbles (hand auger).

References

Abdullah, K.C., Anderson, J.A., Snow, J.N., Holdford-Jack, L., 2004. The late Quaternary Brazos and Colorado deltas, offshore Texas — their evolution and factors that controlled their development. In: Anderson, J.B., Fillon R.H. (Eds.), Late Quaternary Stratigraphic Evolution of the Northern Gulf of Mexico Margin, SEPM Special Publication, vol. 64, pp. 237–269.

Aharon, P., 2006. Entrainment of meltwaters in hyperycnal flows during deglaciation superfloods in the Gulf of Mexico. Earth and Planetary Science Letters 241, 260-270.

Anderson, J.B., Rodriguez, A., Abdulah, K.C., Fillon, R.H., Banfield, L.A., McKeown, H.A., Wellner J.S., 2004. Late Quaternary stratigraphic evolution of the northern Gulf of Mexico margin: a synthesis In: Anderson, J.B., Fillon R.H. (Eds.), Late Quaternary Stratigraphic Evolution of the Northern Gulf of Mexico Margin, SEPM Special Publication, vol. 64, pp.1-23.

Anderson, J.B., Wallace, D.J., Simms, A.R., Rodriguez, A.B., Milliken, K.T., 2013. Variable Response of Coastal Environments of the Northern Gulf of Mexico to Sea-Level rise and climate change: Implications for future change. Marine Geology, in press.

Aslan, A., Autin, W.J., 1998, Holocene flood-plain soil formation in the southern lower Mississippi Valley: implications for interpreting alluvial paleosols: Geological Society of America, Bulletin, v. 110, p. 433–449.

Asmerom, Y. Polyak, V.J., Burns S.J., 2010. Variable winter moisture in the southwestern United States linked to rapid glacial climate shifts. Nature Geoscience, 3, pp. 114–117.

Barnes, V.E., 1970. Geologic Atlas of Texas.

Bettis, E.A., Mandel, R.D., 2002. The effects of temporal and spatial patterns of Holocene erosion and alluviation on the archaeological record of the central and eastern Great Plains, USA. Geoarchaeology 17, 141-154.

Blum, M.D., Guccione, M.J., Wysocki, D., Robnett, P.C., 2000. Late Pleistocene evolution of the Mississippis valley, southern Missouri to Arkansas. Geological Society of America Bulletin 112, 221-235.

Blum, M.D., Aslan, A., 2006. Signatures of climate vs. sea-level change within incised valley-fill successions: Quaternary examples from the Texas Gulf Coast. Sedimentary Geology 190, 177-211.

Blum, M.D., Price, D.M., 1998. Quaternary alluvial plain construction in response to interacting glacio-eustatic and climate controls, Texas Gulf Coastal Plain, in Shanley, K.W., and McCabe, P.J., (Eds), Relative Role of Eustacy, Climate and Tectonism in Continental Rocks: SEPM Secial Publication 59, 31-48.

Blum, M.D., Velastro, S., 1989. Response of the Pedernales River of central Texas to late Holocene climate change. Annals of the Association of American Geographers 79, 435-456.

Blum, M.D. Velastro, S., 1994. Late Quaternary sedimentation, lower Colorado River, Gulf Coastal Plain of Texas. Geological Society of America 106, 1002-1016.

Bomar, G.W., 1983. Texas Weather. University of Texas Press, Austin.

Bongino, J.D., Nordt, L.C., 2007. Late quaternary history of the Waco Mammoth site: environmental reconstruction and interpreting the cause of death. MA Thesis, Baylor University. Waco, Texas.
Bousman, C.B., 1998. Paleoenvironmental change in central Texas: The palynological Evidence. Plains Anthopologist 43, 201–219.
Bromwich, D. H., Toracinta, E. R., Oglesby, R. J., Fastook, J. L., Hughes, T. J., 2004. Polar MM5 simulations of the winter climate of the Laurentide Ice Sheet at the LGM. Journal of Climate 17(17): 3415-3433.
Brooks, G.A., Ellwood, B.B., Railsback, B., Cowart, J.B., 2006. A 164 ka record of environmental change in the American Southwest from a Carlsbad Cavern speleothem. Palaeolgeography, Palaeoclimatology, Palaeoecology 237, 483-507.
COHMAP (Cooperative Holocene Mapping Project) Member, 1988, Climatic changes of the last 18,000 years: observations and model simulations: Science 241, 1043-1052.
Dorale, J.A., Edwards, R.L., Gonzalez, L., and Ito, E., 1998, Climate and vegetation history of the midcontinent from 75 to 25 ka: A speleothem record from Crevice Cave, Missouri, USA: Science, v. 282, p. 1871–1874, doi: 10.1126/science .282.5395.1871.
Durbin, J.M., Blum, M.D., Price, D.M., 1997. Late Pleistocene stratigraphy of the lower Nueces River Corpus Christi, Texas: glacio-eustatic influences on valley-fill architecture. Transactions of the Gulf Coast Association of Gological Societies 47, 119-129.
Ellwood, B.B., Gose, W.A., 2006. Heinrich H1 and 8200 yr B.P. climate events recorded in Hall's Cave, Texas. Geology 34, 753-756. http://dx.doi.org/10.1130/ G22549.1.
Forman, S.L., Pierson, J., 2002. Late Pleistocene luminescence chronology of loess deposition in the Missouri and Mississippi river valleys, United States. Palaeogeography, Palaeoclimatology, Palaeoecology 186, 25-46.
Galbraith, R.F., Roberts, R.G., Laslett, G.M., Yoshida, H., Olley, J.M., 1999. Optical Dating of single and multiple grains of quartz from Jinmium Rock Shelter, Northern Australia: Part I, experimental design and statistical models. Archaeometry 41, 339–364.
Galbraith, R.F. Roberts, R.G., 2012. Statistical aspects of equivalent dose and error calculation and display in OSL dating: An overview and some recommendations. Quaternary Geochronology 11, 1-27.
Grissino-Mayer, H.D., 1996. A 2129-year reconstruction of precipitation for northwestern New Mexico, U.S.A. In: Dean, J.S., Meko, D.M., Swetnam, T.W. (Eds.), Tree Rings, Environment, and Humanity. Arizona, Radiocarbon, Tucson, pp. 191–204.
Hall, S.A., 1988. Environment and archaeology of the central Osage Plains: Plains Anthropologist 33, 203-218.
Hall, S.A., 1990. Channel trenching and climatic change in the southern U.S. Great Plains. Geology 18, 342–345.
Hall, S.A., Boutton, T.W., Lintz, C.R., Baugh, T.G., 2012. New Correlation of Stable Carbon Isotopes with Changing Late-Holocene Fluvial Environments in the Trinity River Basin of Texas, USA. The Holocene 22, 541–549. doi: 10.1177/0959683611427338

Hall, S.A., Penner, W.I., 2013. Stable carbon isotopes, C3–C4 vegetation, and 12,800 years of climate change in central New Mexico, USA. Palaeogeography, Palaeoclimatology, Palaeoecology 369, 272–281.
Hall, S., Valastro, S., 1995. Grassland vegetation in the southern Great Plains during the last glacial maximum. Quaternary Research 44, 237– 245.
Holliday, V.T., 2001. Stratigraphy and geochronology of upper quaternary eolian sand on the Southern High Plains of Texas and New Mexico, United States. Geological Society of America Bulletin 113, 88–108.
Huckabee, J.W.J., Thompson, D.R.,Wyrick, J.C., Pavlat, E.G., 1977. Soil Survey of Bell County, Texas. US Department of Agriculture, Natural Resources Conservation Service, Washington, D.C.
Koch, P.L., Diffenbaugh, N.S., Hoppe, K.A., 2004. The effects of late Quaternary climate and pCO_2 change on C_4 plant abundance in the south-central United States. Paleogeography, Paleoclimatology, Paleoecology 207, 331-357.
Kutzbach, J.E., Guetter, P.J. 1986. The influence of changing orbital parameters and surface boundary conditions on climate simulations for the past 18,000 years. Journal of Atmospheric Science 43 (16), 1726-1759.
Lambeck, K., Purcell, A., Dutton, A., 2012. The anatomy of interglacial sea levels: The relationship between sea levels and ice volumes during the Last Interglacial. Earth and Planetary Science Letters 315-316, 4-11.
Licciardi, J.M., Teller, J.T., and Clark, P.U., 1999, Freshwater routing by the Laurentide ice sheet during the last deglaciation, *in* Clark, P.U., et al., eds., Mechanisms of global climate change at millennial time scales: American Geophysical Union Geophysical Monograph 112, 177–201.
Lintz and Jackson, 1994. In Significance for Prehistoric cultural resources: a case study from Fort Hood, Texas, USA CERL Technical Report, United States Arny Corps of Engineers, Construction Engineering Research Laboratories, Champaign, Illinois.
Mandel, R.D., Jacob, J.S., Nordt, L.C., 2007. Geoarchaeology of the Richard Beene Site. In: Thoms, A.V., Mandel, R.D. (Eds.), Archaeological and Paleoecological Investigations at the Richard Beene Site (41BX831), South Central Texas, Center for Ecological Archaeology, Reports of Investigations No. 8. Texas A&M University, College Station, Texas, pp. 27-60.
Martinson, D.G., Pisias, N.G., Hays, J.D., Imbrie, J., Moore, T.C., Shackleton, N.J., 1987. Age dating and the orbital theory of the ice ages: development of a highresolution 0 to 300,000-year chrono-stratigraphy. Quaternary Research 27, 1-29.
Meier, H.A., Nordt, L.C., Forman, S.L., Driese, S.G., 2013. Late Quaternary alluvial history of the middle Owl Creek drainage basin in central Texas: A record of geomorphic response to environmental change. Quaternary International 306, 24-41.
Meier, H.A., Driese, S.G., Nordt, L.C., Formna, S.L., Dworkin, S.I., 2014. Interpretation of Late Quaternary climate and landscape variability based upon buried soil macro- and micromorphology, geochemistry, and stable isotopes of soil orgainic matter, Owl Creek, central Texas, USA. Catena 114, 157-168.

Musgrove, M., Banner, J.L., Mack, L.E., Combs, D.M., James, E.W., Cheng, H., Edwards, R.L., 2001. Geochronology of Late Pleistocene to Holocene Speleothems from Central Texas: Implications for Regional Paleoclimate. Geological Society of America Bulletin 113, 1532–1543, doi: 10.1130/0016-76006(2001)113<1532:GOLPTH>2.0.CO;2

Nordt, L.C., 1992. Additional geoarchaeology at the Fort Hood Military Reservation, Ft. Hood, Texas. Fort Hood (Tex.), Texas A & M University. Archeological Research Laboratory. United States Army, Fort Hood.

Nordt, L.C., 1995. Geoarchaeological investigations of Henson creek: A low-order tributary in Central Texas. Geoarchaeology 10, 205–221.

Nordt, L.C., 1997. Geoarchaeology. In: Carlson, D.L. (Ed) Archaeological investigations along Owl Creek: Results of the 1992 summer archaeological field school. Fort Hood (Tex.), Texas A & M University. Archeological Research Laboratory. United States Army, Fort Hood.

Nordt, L.C., 2004. Late Quaternary alluvial stratigraphy of a low-order tributary in central Texas,USA and its response to climate and sediment supply. Quaternary Research 62, 289-300.

Nordt, L.C., Boutton, T.W., Hallmark, C.T., Waters, M.R., 1994. Late Quaternary vegetation and climate changes in Central Texas based on the isotopic composition of organic carbon. Quaternary Research 41, 109–120.

Nordt, L.C., Hallmark, C.T., Wilding, L.P., Boutton, T.W., 1998. Quantifying pedogenic carbonate accumulations using stable carbon isotopes. Geoderma 82, 115–136.

Nordt, L.C., Von Fisher, J., Tieszen, L., Tubbs, J., 2008. Coherent changes in relative C_4 plant productivity during the late Quaternary in the North American Great Plains. Quaternary Science Reviews 27: 1600-1611.

Olley, J.M., Pietsch, T., Roberts, R.G., 2004. Optical dating of Holocene sediments from a variety of geomorphic settings using single grains of quartz. Geomorphology 60, 337–358.

Rittenour, T.M., Blum, M.D., and Goble, R.J., 2007. Fluvial evolution of the lower Mississippi River valley during the last 100 k.y. glacial cycle: Response to glaciation and sea-level change. GSA Bulletin 119: 586-608. doi: 10.1130/B25934.1.

Saucier, R.T., 1994, Geomorphology and Quaternary geologic history of the lower Mississippi Valley. Waterways Experiment Station, US Army Corps of Engineers. 364 pp.

Schoeneberger, P.J., Wysocki, D.A., Benham, E.C., Broderson, W.D., 2002. Field book for describing and sampling soils, Version 2.0. ed. Natural Resources Conservation Service, National Soil Survey Center, Lincoln, NE.

Seifert, C.L., Cox, R.T, Forman, S.L., Foti, T.L., Wasklewicz, T.A., McColgan, A.T., 2009. Relict nebkhas (pimple mounds) record prolonged late Holocene drought in the forested region of south-central United States. Quaternary Researh 71: 329-339.

Siddall, M., Stocker, T.F., Clark, P.U., 2009. Constraints on future sea-level rise from past sea-level change. Nature Geoscience 2, 571-575.

Sionneau, T., Bou-Roumazeilles, V., Flower, B.P., Bory, A., Tribovillard, N., Kissel, C., 2010. Provenance of freshwater pulse in the Gulf of Mexico during the last deglaciation. Quaternary Research 74, 235-245.
Sionneau, T., Bout-Roumazeilles, V., Meunier, G., Kissel, C., Flower, B.P., Bory, A., Tribovillard, N., 2013. Atmospheric re-organization during Marine Isotope Stage 3 over the North American continent: sedimentological and mineralogical evidence from the Gulf of Mexico. Quaternary Science Reviews 81: 62-73.
Soil Survey Staff, 2010. Keys to Soil Taxonomy, 11th ed. US Government Printing Office, Washington, D.C., p. 331.
Stuiver, M., and Reimer, P. J., 1993, Extended 14C database and revised CALIB radiocarbon calibration program, Radiocarbon 35:215-230.
Sylvia, D.A., Galloway, W.E., 2006. Morphology and stratigraphy of the late Quaternary lower Brazos valley: implications for paleo-climate, discharge and sediment delivery. Sedimentary Geology 190, 159-175. http://dx.doi.org/10.1016/j.sedgeo.2006.05.023.
Taha, Z.P., Anderson, J.B., 2008. Sea-Level Controls on the Facies Architecture of the Trinity/Sabine Incised-Valley System, Texas Continental Shelf. In: Dalrymple, R., Boyd, R., Zaitlin, B.A., (Eds.), Incised Valley Systems: Origin and Sedimentary Sequences, Society for Sedimentary Researh Special Publication 51, 63-82.
Thomas, A.L., Henderson, G.M., Deschams, P., Yokoyama, Y., Mason, A.J., Bard, E., Hamelin, B., Durand, N., Camoin, G., 2009. Penultimate Deglacial Sea-leve timing from Uranium/Thorium dating of Tahitian corals. Science 324, 1186.
Toomey, R.S. Blum, M.D., Valastro, S., 1993. Late Quaternary climates and environments of the Edwards Plateau, Texas. Global Planetary Change 7, 299-320.
Waters, M.R., Nordt, L.C., 1995. Late Quaternary Floodplain History of the Brazos River in East-Central Texas. Quaternary Research 43, 311–319.
Waters, M.R., Forman, S.L., Jennings, T.A., Nordt, L.C., Driese, S.G., Feinberg, J.M., Keene, J.L., Halligan, J., Lindquist, A., Pierson, J., Hallmark, C.T., Collins, M.B., Wiederhold, J.E., 2011. The Buttermilk Creek complex and the origins of Clovis at the Debra L. Friedkin site, Texas. Science 331, 1599–1603.
Weight, R.W.R., Anderson, J.B., Fernandez, R., 2011. Rapid mud accumulation on the betral Texas shelf linked to climate change and sea-level rise. Journal of Sedimentary Research 81, 743-764. http://dx.doi.org/10.2110/jsr.2011.
Williams, C., Flower, B.P., Hastings, D.W., Guilderson, T.P., Quinn, K., Goddard, E.A., 2010. Deglacial abrupt climate change in the Atlantic Warm Pool: a Gulf of Mexico perspective. Paleoceanography 115, PA4221. http://dx.doi.org/10.1029/2010PA001928.
Williams, C., Flower, B.P., Hastings, D.W., 2012. Seasonal Laurentide ice sheet melting during the "Mystery Interval (17.5-14.5 ka). Geology 40, 955-958. http://dx.doi.org/10.1130/G33279.1.
57.

Wright, D.K., Forman, S.L., Waters, M.R., Ravesloot, J.C., 2011. Holocene eolian activation as a proxy for broad-scale landscape change on the Gila River Indian Community, Arizona. Quaternary Research 76 (1), 10-21. http://dx.doi.org/10.1016/j.yqres.2011.04.008.

CHAPTER FIVE

Conclusion

The integrated study of depositional facies at Owl Creek, a low order drainage basin in central Texas, utilizing stratigraphy, sedimentology, soil morphology, and OSL chronology reveals a complex series of erosion, deposition, and soil-forming events during the past ca. 120 ka. This research provides the first systematic glimpse into the late Pleistocene of central Texas. The trends in sedimentation, pedogenesis, and erosion at Owl Creek preserve an archive of valuable information about complex climate-stream basin history and indicates the importance of intrinsic factors, like sediment supply and local runoff, however broader scale climate change associated with the growth and decay of the Laurentide ice sheet is critical for governing periods of fluvial erosion, deposition and preservation within central Texas. Comparison of these records among streams within the Brazos River valley provides insight to regional-scale landscape development based on diachronic sediment preservation. At least six aggradation and degradation cycles assessed for Owl Creek during the late Pleistocene to Holocene and suggests that the stream was responding to extrinsic environmental factors and intrinsic geomorphic thresholds.

Owl Creek validates the use of small streams to investigate regional climate change. Four buried soils exposed along Owl Creek were examined using soil morphology and micromorphology, soil characterization, whole-soil geochemical and stable isotope analyses of soil organic matter and pedogenic carbonate. These buried soils provide a record of changes in paleoecological, paleo-alluvial, and soil-forming conditions spanning ca. 14 ky. The novel use of existing paleo-climate proxies allows estimates for erosion within the Owl Creek basin. These combined records demonstrate consistent responses to the major climatic changes known to have occurred at the end of the Pleistocene constrained for the first time using OSL dating. Environmental warming associated with the Holocene is preserved in the stable carob isotopes with the buried soils of the study interval.

The syntheses of previous studies along Owl Creek provide a chronology of depositional history spanning the past 50 ka. The addition of the Corral Site provides insight from ca. 21 to 19 ka, a period known as the LGM and regionally mesic conditions. This is evidence for aggradation during the last glacial maximum in contrast to the Brazos River and adjacent river reaches in coastal setting are incised reflecting changing controls on fluvial dynamics from sea level to an increase in precipitation up the catchment. Later Holocene deposition at Owl is characterized of dominantly fine-grained units suggestive of upland destabilization with drought conditions.

REFRENCES

Abdullah, K.C., Anderson, J.A., Snow, J.N., Holdford-Jack, L., 2004. The late Quaternary Brazos and Colorado deltas, offshore Texas d their evolution and factors that controlled their development. In: Anderson, J.B., Fillon, R.H. (Eds.), 2004. Late Quaternary Stratigraphic Evolution of the Northern Gulf of Mexico Margin, vol. 64. SEPM Special Publication, pp. 237-269.

Aharon, P., 2006. Entrainment of meltwaters in hyperycnal flows during deglaciation superfloods in the Gulf of Mexico. Earth and Planetary Science Letters 241, 260-270.

Anderson, J.B., Rodriguez, A., Abdulah, K.C., Fillon, R.H., Banfield, L.A., McKeown, H.A., Wellner, J.S., 2004. Late Quaternary stratigraphic evolution of the northern Gulf of Mexico margin: a synthesis. In: Anderson, J.B., Fillon, R.H. (Eds.), Late Quaternary Stratigraphic Evolution of the Northern Gulf of Mexico Margin, vol. 64. SEPM Special Publication, pp. 1-23.

Anderson, J.B., Wallace, D.J., Simms, A.R., Rodriguez, A.B., Milliken, K.T., 2013. Variable Response of Coastal Environments of the Northern Gulf of Mexico to Sea-Level rise and climate change: Implications for future change. Marine Geology, in press.

Asmerom, Y., Polyak, V.J., Burns, S.J., 2010. Variable winter moisture in the south-western United States linked to rapid glacial climate shifts. Nature Geoscience 3, 114-117.

Baker, R.G., Bettis III, E.A., Denniston, R.F., Gonzalez, L.A., 2001. Plant remains, alluvial chronology, and cave speleothem isotopes indicate abrupt Holocene climatic change at 6 ka in midwestern USA. Global Planet. Change 28, 285–291.

Barnes, V.E., 1970. Geologic Atlas of Texas: Waco Sheet. Bureau of Economic Geology, University of Texas, Austin.

Bettis, E.A. III and R.D. Mandel, 2002. The effects of temporal and spatial patterns of Holocene erosion and alluviation on the archaeological record of the Central and Eastern Great Plains, U.S.A. Geoarchaeology 17, 141-154.

Bettis, E.A., Muhs, D.R., Roberts, H.M., Wintle, A.G., 2003. Last Glacial loess in the continuous USA. Quaternary Science Reviews 22, 1907-1946.

Berger, G.W., 1990. Effectiveness of natural zeroing of the thermoluminescence of sediments. Journal of Geophysical Research 95, 12375-12397.

Blair, T.C., McPherson, J.G., 1994. Alluvial fans and their natural distinction from rivers based on morphology, hydraulic processes, sedimentary processes, and facies assemblages. Journal of Sedimentary Research 64, 450-489.

Blikra, L.H., Nemec, W., 1998. Postglacial colluvium in western Norway: depositional processes, facies and palaeoclimatic record. Sedimentology 45, 909-959.

Blum, M.D., Aslan, A., 2006. Signatures of climate vs. sea-level change within incised valley-fill successions: Quaternary examples from the Texas Gulf Coast. Sedimentary Geology 190, 177-211.

Blum, M.D., Guccione, M.J., Wysocki, D., Robnett, P.C., 2000. Late Pleistocene evolution of the Mississippi valley, southern Missouri to Arkansas. Geological Society of America Bulletin 112, 221-235.

Blum, M.D., Price, D.M., 1998. Quaternary alluvial plain construction in response to glacioeustatic and climatic controls, Texas Gulf Coastal Plain. In: Shanley, K.W., McCabe, P.J. (Eds.), Relative Role of Eustacy, Climate, and Tectonism in Continental Rocks. Special Publication Society of Economic Paleontologists and Mineralogists, pp. 31-48. http://dx.doi.org/10.2110/pec.98.59.0031

Blum, M.D., Price, D.M., 1994. Glacioeustatic and climatic controls on Quaternary alluvial plain deposition, Texas coastal plain. Gulf Coast Association of Geological Societies Transactions 44, 85-92.

Blum, M.D., Toomey III, R.S., Valastro Jr., S., 1994. Fluvial response to Late Quaternary climatic and environmental change, Edwards Plateau, Texas. Palaeogeography, Palaeoclimatology, Palaeoecology 108, 1-21. http://dx.doi.org/10.1016/0031-0182(94)90019-1.

Blum, M.D., Valastro, S., 1989. Response of the Pedernales River of Central Texas to late Holocene climatic change. Annals of the Association of American Geographers 79, 435-456. http://dx.doi.org/10.1111/j.1467-8306.1989.tb00271.x.

Blum, M.D., Valastro, S., 1992. Quaternary stratigraphy and geoarchaeology of the Colorado and Concho rivers, west Texas. Geoarchaeology 7, 419-448. http://dx.doi.org/10.1002/gea.3340070502.

Blum, M.D., Valastro, S., 1994. Late quaternary sedimentation, lower Colorado River, Gulf Coastal Plain of Texas. Geological Society of America Bulletin 106, 1002-1016. http://dx.doi.org/10.1130/0016-7606(1994)106<1002: LQSLCR>2.3.CO; 2.

Bomar, G.W., 1983. Texas Weather.University of Texas Press, Austin.

Bongino, J.D., Nordt, L.C., 2007. Late Quaternary History of the Waco Mammoth Site: Environmental Reconstruction and Interpreting the Cause of Death (MA thesis). Baylor University, Waco, Texas.

Botter-Jensen, L., Bulur, E., Duller, G.A.T., Murray, A.S., 2000. Advances in luminescence instrument systems. Radiation Measurements 32, 523-528.

Bousman, C., 1998. Paleoenvironmental change in central Texas: the palynological evidence. Plains Anthropologist 43, 201-219.

Boutton, T.W., 1996. Stable Carbon Isotope Ratios of Soil Organic Matter and their Use as Indicators of Vegetation and Climate Change. Marcel Dekker, New York 47–82.

Breecker, D., Sharp, Z.D., McFadden, L., 2009. Seasonal bias in the formation and stable isotope composition of pedogenic carbonate in modern soils from central New Mexico, USA. Geol. Soc. Am. Bull. 121, 630–640.

Brewer, R., 1976. Fabric and Mineral Analysis of Soils. Robert E. Krieger Pub. Co., Huntington, New York.

Brodie, C.R., Casford, J.S.L., Lloyd, J.M., Leng, M.J., Heaton, T.H.E., Kendrick, C.P., Yongqiang, Z., 2011. Evidence for bias in C/N, δ13C and δ15N values of bulk organic matter, and on environmental interpretation, from a lake sedimentary sequence by pre-analysis acid treatment methods. Quat. Sci. Rev. 30, 3076–3087.

Bromwich, D.H., Toracinta, E.R., Oglesby, R.J., Fastook, J.L., Hughes, T.J., 2004. Polar MM5 simulations of the winter climate of the Laurentide Ice Sheet at the LGM. Journal of Climate 17 (17), 3415-3433.

Bromwich, D.H., Toracinta, E.R., Oglesby, R.J., Fastook, J.L., Hughes, T.J., 2005. LGM summer climate on the southern margin of the Laurentide Ice Sheet: wet or dry? Journal of Climate 18 (16), 3317-3338.

Brooks, G.A., Ellwood, B.B., Railsback, B., Cowart, J.B., 2006. A 164 ka record of environmental change in the American Southwest from a Carlsbad Cavern speleothem. Palaeolgeography, Palaeoclimatology, Palaeoecology 237, 483-507.

Bryan, K., 1940. Gully gravure e a method of slope retreat. Journal of Geo- morphology 3, 331-344.

Buck, B.J., Monger, H.C., 1999. Stable isotopes and soil-geomorphology as indicators of Holocene climate change, northern Chihuahuan Desert. Journal of Arid Environments 43, 357-373. http://dx.doi.org/10.1006/jare.1999.0584.

Bull, W.B., 1979. Threshold of critical power in streams. Geological Society of America Bulletin 90, 453-464.

Carlson, D.C. (Ed.), 1997. Archaeological investigations along Owl Creek: results of the 1992 summer archaeological field school. United States Army Fort Hood Archaeological Management Series, Research Report Number 29.

Carlson, D.L., Carlson, S.B., Briuer, F.L., Roemer Jr., E., Moore, W.E., 1986. Archaeological survey at Fort Hood, Texas: fiscal year 1983: the eastern training area. United States Army Fort Hood Archaeological Management Series, Research Report Number 11.

Candy, I., Black, S., Sellwood, B.W., 2004. Quantifying time scales of pedogenic calcrete formation using U-series disequilibria. Sedimentary Geology 170, 177-187. http://dx.doi.org/10.1016/j.sedgeo.2004.07.003.

Cleveland, D.M., Atchley, S.C., Nordt, L.C., 2007. Continental sequence stratigraphy of the Upper Triassic (Norian-Rhaetian) Chinle strata, northern New Mexico, USA: allocyclic and autocyclic origins of paleol-bearing alluvial successions. Journal of Sedimentary Research 77, 909-924. http://dx.doi.org/10.2110/jsr.2007.082.

COHMAP (Cooperative Holocene Mapping Project) Member, 1988, Climatic changes of the last 18,000 years: observations and model simulations: Science 241, 1043-1052. Cooke, M.J., Stern, L.A., Banner, J.L., Mack, L.E., 2003. Evidence for the silicate source of relict soils on the Edwards Plateau central Texas. Quat. Res. 67, 275–285.

Coulombe, C.E., Dixon, J.B., Wilding, L.P., 1996. Chapter 5 Mineralogy and chemistry of vertisols. In: Ahmad, N., Mermut, A. (Eds.), Developments in Soil Science. Elsevier, pp. 115–200.

Curry, B.B., Baker, R.G., 2000. Palaeohydrology, vegetation, and climate since the late Illinois episode (~130 ka) in south-central Illinois. Palaeogeography, Palaeoclimatology, Palaeoecology 155, 59-81.

Dietrich, W.E., Dunne, T., 1978. Sediment budget for a small catchment in mountainous terrain. Zeitschrift fur Geomorphologie Supplementband 29, 191-206.

Dorale, J.A., Edwards, R.L., Ito, M., González, L.A., 1998. Climate and vegetation history of the midcontinent from 75 to 25 ka: a speleothem record from Crevice Cave, Missouri, USA. Science 282, 1871-1874.

Dorale, J.A., Wozniak, L.A., Bettis III, E.A., Carpenter, S.J., Mandel, R.D., Hajic, E.R., Lopinot, N.H., Ray, J.H., 2010. Isotopic Evidence for Younger Dryas Aridity in the North American Midcontinent Geology, vol. 38, pp. 519-522.

Driese, S.G., Li, Z.-H., Horn, S.P., 2005. Late Pleistocene and Holocene climate and geomorphic histories as interpreted from a 23,000 14C yr B.P. paleosol and floodplain soils, southeastern West Virginia, USA. Quatern. Res. 63, 136–149Holliday, V.T. 1989a, The Blackwater Draw Formation (Quaternary): A 1.4- plus m.y. record of eolian sedimentation and soil formation on the Southern High Plains. Geological Society of America Bulletin 101:1598-1607.

Duller, G.S.T., Bøtter-Jensen, L., Murray, A.S., 2003. Combining infrared- and green-laser stimulation sources in single-grain luminescence measurements of feldspar and quartz. Radiation Measurements 37, 543-550.

Duller, G.A.T., 2008. Single-grain optical dating of Quaternary sediments: why aliquot size matter in luminescence dating. Boreas 37, 589-612. http://dx.doi.org/10.1111/j.1502-3885.2008.00051.x.

Durbin, J.M., Blum, M.D., Price, D.M., 1997. Late Pleistocene stratigraphy of the Nueces River, Corpus Christi, Texas: climatic and glacio-eustatic control on valley fill architecture. Transactions of the Gulf Coast Association of Geological Societies 47, 119-130.

Ellwood, B.B., Gose, W.A., 2006. Heinrich H1 and 8200 yr B.P. climate events recorded in Hall's Cave, Texas. Geology 34, 753-756. http://dx.doi.org/10.1130/ G22549.1.

Fain, J., Soumana, S., Montret, M., Miallier, D., Pilleyre, T., Sanzelle, S., 1999. Luminescence and ESR dating Beta-dose attenuation for various grain shapes calculated by a Monte-Carlo method. Quaternary Science Reviews 18, 231-234. http://dx.doi.org/10.1016/S0277-3791(98)00056-0.

Fitzpatrick, E.A., 1993. Soil Microscopy and Micromorphology. John Wiley & Sons, New York.

Forman, S.L., 1990. Thermoluminescence properties of fiord sediments from Engelskbukta, western Spitsbergen, Svalbard: a new tool for deciphering depositional environment? Sedimentology 37, 377-384.

Forman, S.L., Oglesby, R., Webb, R., 2001. Patterns of Holocene dune activity on the Great Plains of North America: megadroughts and climate links. Global Planet. Change 29, 1–29.

Forman, S.L., Pierson, J., 2002. Late Pleistocene luminescence chronology of loess deposition in the Missouri and Mississippi river valleys, United States. Palaeogeography, Palaeoclimatology, Palaeoecology 186, 25-46.

Galbraith, R.F., Roberts, R.G., 2012. Statistical aspects of equivalent dose and error calculation and display in OSL dating: an overview and some recommendations. Quaternary Geochronology 11, 1-27.

Galbraith, R.F., Roberts, R.G., Laslett, G.M., Yoshida, H., Olley, J.M., 1999. Optical dating of single and multiple grains of quartz from Jinmium rock shelter, northern Australia, part 1, experimental design and statistical models. Archaeometry 41, 339-364.

Germanoski, D., Schumm, S.A., 1993. Changes in braided river morphology resulting from aggradation and degradation. The Journal of Geology 101, 451-466.

Gile, L.H., Peterson, F.F., Grossman, R.B., 1966. Morphological and genetic sequences of carbonate accumulation in desert soils. Soil Science 101, 47-360.

Gile, L.H., Hawley, J.W., Grossman, R.B., 1981. Soils and Geomorphology in the Basin and Range Area of Southern New-Mexico. New Mexico Bur. Mines and Mineral Resources.

Grissino-Mayer, H.D., 1996. A 2129-year reconstruction of precipitation for northwestern New Mexico, U.S.A. In: Dean, J.S., Meko, D.M., Swetnam, T.W. (Eds.), Tree Rings, Environment, and Humanity. Arizona, Radiocarbon, Tucson, pp. 191–204.

Hall, S.A., 1988. Environment and archaeology of the central Osage Plains: Plains Anthropologist 33, 203-218.

Hall, S.A., 1990. Channel trenching and climatic change in the southern U.S. Great Plains. Geology 18, 342–345.

Hall, S.A., Boutton, T.W., Lintz, C.R., Baugh, T.G., 2012a. New correlation of stable carbon isotopes with changing late-Holocene fluvial environments in the Trinity River basin of Texas, USA. The Holocene 22, 541–549.

Hall, S.A., Penner, W.L., Palacios-Fest, M.R., Metcalf, A.J., Smith, S.J., 2012b. Cool, wet conditions late in the Younger Dryas in semi-arid New Mexico. Quatern. Res. 77, 87–95. http://dx.doi.org/10.1016/j.palaeo.2012.10.034.

Hall, S.A., Penner, W.L., 2013. Stable carbon isotopes, C3–C4 vegetation, and 12,800 years of climate change in central New Mexico, USA. Palaeogeogr. Palaeoclimatol. Palaeoecol. 369, 272–281.

Hall, S., Valastro, S., 1995. Grassland vegetation in the southern Great Plains during the last glacial maximum. Quaternary Research 44, 237– 245.

Harvey, A.M., 2012. The coupling status of alluvial fans and debris cones: a review and synthesis. Earth Surface Processes and Landforms 37, 64-76. http://dx.doi.org/10.1002/esp.2213.

Holliday, V.T. 1989b, Middle Holocene drought on the Southern High Plains. Quaternary Research 31: 74-82.

Holliday, V.T., Hovorka, S.D., Gustavson, T.C., 1996. Lithostratigraphy and geochronology of fills in small playa basins on the Southern High Plains. Geological Society of America Bulletin 108, 953–965.

Holliday, V.T., Mayer, J.H., Fredlund, G.G., 2008. Late Quaternary sedimentology and geochronology of small playas on the Southern High Plains, Texas and New Mexico, U.S.A. Quat. Res. 70, 11–25.

Holliday, V.T., Meltzer, D.J., Mandel, R., 2011. Stratigraphy of the Younger Dryas Chronozone and paleoenvironmental implications: Central and Southern Great Plains. Quat. Intl. 520–533.

Huckabee, J.W.J., Thompson, D.R., Wyrick, J.C., Pavlat, E.G., 1977. Soil Survey of Bell County, Texas. US Department of Agriculture, Natural Resources Conservation Service, Washington, D.C.

Humphrey, J.D., Ferring, C.R., 1994. Stable isotopic evidence for latest Pleistocene and Holocene climatic change in north-central Texas. Quatern. Res. 41, 200–213.

Jenny, H., Leonard, C.D., 1934. Functional relationships between soil properties and rainfall. Soil Sci. 38, 363–381.

Jenny, H., 1941a. Calcium in the soil: III. Pedologic relations. Soil Sci. Soc. Am. Proc. 6, 27–35.

Johnsen, S.J., Clausen, S.J., Dansgaard, W., Gundestrup, N.S., Hammer, C.U., Andersen, U., Andersen, K.K., Hvidberg, C.S., Dahl-Jensen, D., Steffensen, J.P.,

Joyce, J.E., Tjalsma, L.R.C., Prutzman, J.M., 1993. North American glacial meltwater history for the past 2.3 m.y.: oxygen isotope evidence from the Gulf of Mexico. Geology 21, 483-486.

Klappa, C.F., 1980. Rhizoliths in terrestrial carbonates: classification, recognition, zh-order tributary in central Texas, USA and its response to climate and sediment supply. Quatern. Res. 62, 289–300.

Kleinbach, K., Mehalchick, G., Boyd, D.K., Kibler, K.W., 1999. National register testing of 42 prehistoric archeological sites on Fort Hood, Texas: the 1996 season. United States Army Fort Hood Archaeological Management Series, Research Report Number 38.

Knox, J.C. 1996, Late Quaternary upper Mississippi River alluvial episodes and their significance to the lower Mississippi River systems. Engineering Geology, 45: 263-285.

Knox, J.C., 2000. Sensitivity of modern and Holocene floods to climate change. Quaternary Science Reviews. 19: 439-457.

Koch, P.L., Diffenbaugh, N.S., Hoppe, K.A., 2004. The effects of late Quaternary climate and pCO2 change on C4 plant abundance in the south-central United States. Palaeogeogr. Palaeoclimatol. Palaeoecol. 207, 331–357.

Komada, T., Anderson, M.R., Dorfmeier, C.L., 2008. Carbonate removal from coastal sediments for the determination of organic carbon and its isotopic signatures, δ13C and Δ14C: comparison of fumigation and direct acidification by hydrochloric acid. Limnol. Oceanogr. Methods 6, 254–262.

Kraimer, R.A., Monger, H.C., 2009. Carbon isotopic subsets of soil carbonateda particle size comparison of limestone and igneous parent materials. Geoderma 150, 1-9. http://dx.doi.org/10.1016/j.geoderma.2008.11.042.

Kutzbach, J.E., Guetter, P.J., 1986. The influence of changing orbital parameters and surface boundary conditions on climate simulations for the past 18,000 years. Journal of Atmospheric Science 43 (16), 1726-1759.

Lambeck, K., Purcell, A., Dutton, A., 2012. The anatomy of interglacial sea levels: the relationship between sea levels and ice volumes during the Last Interglacial. Earth and Planetary Science Letters 315-316, 411.

Licciardi, J.M., Teller, J.T., and Clark, P.U., 1999, Freshwater routing by the Laurentide ice sheet during the last deglaciation, *in* Clark, P.U., et al., eds., Mechanisms of global climate change at millennial time scales: American Geophysical Union Geophysical Monograph 112, 177–201.

Lintz and Jackson, 1994. In Significance for Prehistoric cultural resources: a case study from Fort Hood, Texas, USA CERL Technical Report, United States Arny Corps of Engineers, Construction Engineering Research Laboratories, Champaign, Illinois.

Maasch, K.A., Oglesby, R.J., 1990. Meltwater cooling of the Gulf of Mexico: a GCM simulation of climatic conditions at 12 ka. Paleoceanography 5, 977-996.

Machette, M.N., 1985. Calcic soils of the southwestern United Stated. In: Weide, D.L. (Ed.), Soils and Quaternary Geology of the Southwestern United States, Special Paper 203. Geological Society of America, Boulder, pp. 1-21.

Mandel, R.D. 1995, Geomorphic controls of the Archaic record in the Central Plains of the United States. In Bettis, E.A. III (Ed.), Archaeological geology of the archaic period in North America (pp. 37-66). Special Paper 297. Boulder Co: Geological Society of America.

Mandel, R.D., Jacob, J.S., Nordt, L.C., 2007. Geoarchaeology of the Richard Beene Site. In: Thoms, A.V., Mandel, R.D. (Eds.), Archaeological and Paleoecological Investigations at the Richard Beene Site (41BX831), South Central Texas, Center for Ecological Archaeology, Reports of Investigations No. 8. Texas A&M University, College Station, Texas, pp. 27-60.

Martinson, D.G., Pisias, N.G., Hays, J.D., Imbrie, J., Moore, T.C., Shackleton, N.J., 1987.Age dating and the orbital theory of the ice ages: development of a high-resolution 0 to 300,000-year chrono-stratigraphy. Quaternary Research 27, 1-29.

Mehalchick, G., Kibler, K.W., 2002. National register testing of nine prehistoric sites on Fort Hood, Texas: the 2001–2002 season. United States Army Fort Hood Archaeological Resource Management Series Research Report Number 50.

Mehalchick, G., Kleinbach, K., Boyd, D.K., Kibler, K.W., 2000. Geoarcheological investigations and national register testing of 52 prehistoric archeological sites on Fort Hood, Texas: the 1997 season. United States Army Fort Hood Archaeological Management Series, Research Report Number 39.

Mehalchick, G., Killian, K., Caran, S.C., Kibler, K.W., 2003. Geoarchaeological investigations and national register testing of 57 prehistoric archaeological sites of Fort Hood, Texas: 1999 season. United States Army Fort Hood Archeological Resource Management Series, Research Report Number 44.

Mejdahl, V., Christiansen, H.H., 1994. Procedures used for luminescence dating of sediments. Boreas 13, 403-406.

Meier, H.A., Nordt, L.C., Forman, S.L., Driese, S.G., 2013. Late Quaternary alluvial history of the middle Owl Creek drainage basin in central Texas: a record of geomorphic response to environmental change. Quat. Int. 306, 24–41. http://dx.doi.org/10.1016/j.quaint.2013.07.010.

Meier, H.A., Driese, S.G., Nordt, L.C., Formna, S.L., Dworkin, S.I., 2014. Interpretation of Late Quaternary climate and landscape variability based upon buried soil macro- and micromorphology, geochemistry, and stable isotopes of soil orgainic matter, Owl Creek, central Texas, USA. Catena 114, 157-168.

Mestdagh, H., Haesaerts, P., Dodonov, A., Hus, J., 1999. Pedosedimentary and climatic reconstruction of the last interglacial and early glacial loess–paleosol sequence in Outh Tabzhikistan. Catena 35, 197–218.

Miall, A.D., 1978. Lithofacies types and vertical profile models in braided river deposits: a summary. In: Miall, A.D. (Ed.), 1978. Fluvial Sedimentology, vol. 5. Canadian Society of Petroleum Geologists, pp. 598-604.

Miall, A.D., 1992. Alluvial deposits. In: Walker, R.G. (Ed.), Facies Models: Response to Sea Level Change. Geological Association of Canada, St. John's, Newfoundland, pp. 119-142.

Miall, A.D., 2006. The Geology of Fluvial Deposits: Sedimentary Facies, Basin Analysis, and Petroleum Geology. Springer, New York, p. 582.

Miller, G.B., 2001. Soil survey of McLennan County, Texas. United States Department of Agriculture, Natural Resources Conservation Services, Washington DC.

Mills, H.H., 1981. Boulder deposits and the retreat of mountain slopes, or "gully gravure" revised. Journal of Geology 89, 81-179. Murray, A.S., Wintle, A.G., 2003. The single aliquot regenerative dose protocol: potential for improvements in reliability. Radiation Measurements 37, 377-381.

Murray, A.S., Wintle, A.G., 2003. The single aliquot regenerative dose protocol: potential for improvements in reliability. Radiation Measurements 37, 377–381.

Musgrove, M., Banner, J.L., Mack, L.E., Combs, D.M., James, E.W., Cheng, H., Edwards, R.L., 2001. Geochronology of Late Pleistocene to holocene speleothems from Central Texas: implications for regional paleoclimate. Geological Society of America Bulletin 113, 1532–1543.

Nordt, L.C., 1992. Archaeological Geology of the Fort Hood Military Reservation, Texas. U.S. Army Fort Hood Archaeological Research Management Series, Research Report Number 25. Texas A&M University, College Station.

Nordt, L.C., 1993. Additional Geoarchaeology at Fort Hood. U.S. Army Fort Hood. U.S. Army Fort Hood Archaeological Resource Management Series, Research Report Number 28. Texas A&M University, College Station.

Nordt, L., 1995. Geoarchaeology of Henson Creek: a low-order tributary in Central Texas. Geoarchaeology 10, 205-221.

Nordt, L.C., 1997. Geoarchaeology. In: Carlson, D.L. (Ed) Archaeological investigations along Owl Creek: Results of the 1992 summer archaeological field school. Fort Hood (Tex.), Texas A & M University. Archeological Research Laboratory. United States Army, Fort Hood.

Nordt, L., 2004. Late quaternary alluvial stratigraphy of a low-order tributary in central Texas, USA and its response to climate and sediment supply. Quaternary Research 62, 289-300. http://dx.doi.org/10.1016/j.yqres.2004.07.004.

Nordt, L.C., Boutton, T.W., Hallmark, C.T., Waters, M.R., 1994. Late Quaternary vegetation and climate changes in Central Texas based on the isotopic composition of organic carbon. Quatern. Res. 41, 109–120.

Nordt, L.C., Boutton, T.W., Jacob, J.S., Mandel, R.D., 2002. C4 plant productivity and climate-CO2 variations in South-Central Texas during the Late Quaternary. Quaternary Research 58, 182-188.

Nordt, L.C., Hallmark, C.T., Wilding, L.P., Boutton, T.W., 1998. Quantifying pedogenic carbonate accumulations using stable carbon isotopes. Geoderma 82, 115-136. http://dx.doi.org/10.1016/S0016-7061(97)00099-2.

Nordt, L., von Fischer, J., Tieszen, L., 2007. Late Quaternary temperature record from buried soils of the North American Great Plains. Geology 35, 159–162.

Oceanic, National, Atmospheric Administration (NOAA), 2010. Climatological Data, Annual Summary. New Mexico, 2010. National Climatic Data Center, Ashville, NC.

Olley, J.M., Pietsch, T., Roberts, R.G., 2004. Optical dating of Holocene sediments from a variety of geomorphic settings using single grains of quartz. Geo- morphology 60, 337-358. http://dx.doi.org/10.1016/j.geomorph.2003.09.020.

Pimentel, D., Harvey, C., Resosudarmo, P., Sinclair, D., Kurz, D., MnCair, M., Crist, S., Shpritz, L., Fitton, L., Saffouri, R., Blair, R., 1995. Environmental and economic costs of soil erosion and conservation benefits. Science 267, 1117–1123.

Prescott, J.R., Hutton, J.T., 1994. Cosmic ray contributions to dose rates for luminescence and ESR dating: large depths and long-term time variations. Radiation Measurements 23, 497–500.

Pu, B., Vizy, E.K., Cook, K.H., 2012. Warm season response over North America to a shutdown of the Atlantic meridional overturning circulation and CO2 in- creases. Journal of Climate 25, 6701-6720. http://dx.doi.org/10.1175/JCLI-D-11-00611.1.

Rittenour, T.M., Blum, M.D., Goble, R.J., 2007. Fluvial evolution of the lower Mississippi River valley during the last 100 k.y. glacial cycle: response to glacia- tions and sea-level change. Geological Society of America Bulletin 119, 586-608.

Retallack, G.J., 2001. Soils of the Past, 2nd ed. Wiley-Blackwell.

Retallack, G.J., 2005. Pedogenic carbonate proxies for amount and seasonality of precipitation in paleosols. Geology 33, 333–336.

Royer, D.L., 1999. Depth to pedogenic carbonate horizon as a paleoprecipitation indicator? Geology 27, 1123–1126. http://dx.doi.org/10.1130/0091-7613(1999) 027b1123: DTPCHAN2.3.CO;2.

Saucier, R.T., 1994, Geomorphology and Quaternary geologic history of the lower Mississippi Valley. Waterways Experiment Station, US Army Corps of Engineers. 364 pp.

Schoeneberger, P.J., Wysocki, D.A., Benham, E.C., Broderson, W.D., 2002. Field Book for Describing and Sampling Soils, Version 2.0. Natural Resources Conservation Service, National Soil Survey Center, Lincoln, NE.

Schumm, S.A., 1999. Causes and controls of channel incision. In: Darby, S.E., Simon, A. (Eds.), Incised River Channels: Processes, Forms, Engineering, and Management. John Wiley and Sons. Inc., New York, pp. 19-33.

Seifert, C.L., Cox, R.T, Forman, S.L., Foti, T.L., Wasklewicz, T.A., McColgan, A.T., 2009. Relict nebkhas (pimple mounds) record prolonged late Holocene drought in the forested region of south-central United States. Quaternary Researh 71: 329-339.

Sheldon, N.D., Retallack, G.J., Tanaka, S., 2002. Geochemical climofunctions from North American soils and application to paleosols across the Eocene–Oligocene boundary in Oregon. J. Geol. 110, 687–696.

Shen, Z., Törnqvist, T.E., Autin, W.J., Mateo, Z.R.P., Straub, K.M., Mauz, B., 2012. Rapid and widespread response of the Lower Mississippi River to eustatic forcing during the last glacial-interglacial cycle. Geological Society of America Bulletin 124 (5-6), 690-704. http://dx.doi.org/10.1130/b30449.1.

Shoji, H., Sveinbjörnsdóttir, A.E., White, J.W.C., Jouzel, J., Fisher, D., 1997. The d180 record along the Greenland Ice Core Project deep ice core and the problem of possible Eemian climatic instability. Journal of Geophysical Research 102, 26471e26487. http://dx.doi.org/10.1029/97JC00167.

Siddall, M., Stocker, T.F., Clark, P.U., 2009. Constraints on future sea-level rise from past sea- level change. Nature Geoscience 2, 571-575.

Sionneau, T., Bou-Roumazeilles, V., Flower, B.P., Bory, A., Tribovillard, N., Kissel, C., 2010. Provenance of freshwater pulse in the Gulf of Mexico during the last deglaciation. Quaternary Research 74, 235-245.

Sionneau, T., Bout-Roumazeilles, V., Meunier, G., Kissel, C., Flower, B.P., Bory, A., Tribovillard, N., 2013. Atmospheric re-organization during Marine Isotope Stage 3 over the North American continent: sedimentological and mineralogical evidence from the Gulf of Mexico. Quaternary Science Reviews 81: 62-73.

Soil Survey Staff, 1996. Soil Survey Laboratory Methods Manual. Soil Survey Investigations. Report No. 42. US Government Printing Office, Washington, D.C.. Version 3.0.

Soil Survey Staff, 2010. Keys to Soil Taxonomy, 11th ed. US Government Printing Office, Washington, D.C., p. 331

Soil Survey Staff, 2012. Natural Resources Conservation Service, United States Department of Agriculture. Web Soil Survey. Available online at: http://websoilsurvey.nrcs.usda.gov/ (accessed 16.03.12.).

Southard, R.J., Driese, S.G., Nordt, L.C., 2011. Vertisols, In: Huang, P.M., Li, Y., Sumner, M.E. (Eds.), Handbook of Soil Science, 2nd edition. CRC Press, Boca Raton, Florida, pp. 33–82 (to 33-97).

Stanistreet, I.G., McCarthy, T.S., 1993. The Okavango fan and the classification of subaerial fan systems. Sedimentary Geology 85, 115-133. http://dx.doi.org/10.1016/0037-0738(93)90078-J.

Stoops, G., 2003. Guidelines for Analysis and Description of Soil and Regolith Thin Sections. Soil Science Society of America, Madison, WI.

Strong, G.E., Giles, J.R.A., Wright, V.P., 1992. A Holocene calcrete from North Yorkshire, England: implications for interpreting palaeoclimates using calcretes. Sedimentology 39, 333–347.

Stuiver, M., and Reimer, P. J., 1993, Extended 14C database and revised CALIB radiocarbon calibration program, Radiocarbon 35:215-230.

Sylvia, D.A., Galloway, W.E., 2006. Morphology and stratigraphy of the late Quaternary lower Brazos valley: implications for paleo-climate, discharge and sediment delivery. Sedimentary Geology 190, 159-175. http://dx.doi.org/10.1016/j.sedgeo.2006.05.023.

Taha, Z.P., Anderson, J.B., 2008. The influence of valley aggradation and listric normal faulting on styles of river avulsion: a case study of the Brazos River, Texas, USA. Geomorphology 95, 429-448.

Thomas, A.I., Henderson, G.M., Deschamps, P., Yokoyama, Y., Mason, A.J., Bard, E., Hamelin Durand, N., Camoin, G., 2009. Penultimate deglacial sea- level timing from uranium/thorium dating of Tahitian corals. Science 324, 1186-1189.

Tripsanas, E.K., Bryant, W.R., Slowey, N.C., Bouma, A.H., Karageorgis, A.P., Berti, D., 2007. Sedimentological history of Bryant Canyon area, northwest Gulf of Mexico, during the last 135 kyr (Marine Isotope Stages 1e6): a proxy record of Mississippi River discharge. Palaeogeography, Palaeoclimatology, Palaeoecology 246, 137-161.

Toomey, R.S., Blum, M.D., Valastro, S., 1993. Late Quaternary climates and environments of the Edwards Plateau. Texas, Global and Planetary Change 7, 299–320.

Trierweiler, W.N., 1994. Archeological investigations on 571 prehistoric sites at Fort Hood, Bell and Coryell Counties, Texas. United States Army Fort Hood Archaeological Management Series, Research Report Number 31.

Trierweiler, W.N. (Ed.), 1996. Archaeological testing at Fort Hood: 1994–1995. United States Army Fort Hood Archaeological Management Series, Research Report Number 35, vols. I and II.

Verrecchia, E.P., Verrecchia, K.E., 1994. Needle-fiber calcite: a critical review and a proposed classification. J. Sediment. Res. 64.

Waelbroeck, C., Labeyrie, L., Michel, E., Duplessy, J.C., Mcmanus, J.F., Lambeck, K., Balbon, E., Labracherie, M., 2002. Sea-level and deep water temperature changes derived from benthic foraminifera isotopic records. Quaternary Science Reviews 21, 295-305.

Wang, H., Stumpf, A.J., Miao, X., Lowell, T.V., 2012. Atmospheric changes in North America during the last deglaciation from dune-wetland records in the Mid- western United States. Quaternary Science Reviews 58, 124-134.

Waters, M.R., Forman, S.L., Jennings, T.A., Nordt, L.C., Driese, S.G., Feinberg, J.M., Keene, J.L., Halligan, J., Lindquist, A., Pierson, J., Hallmark, C.T., Collins, M.B., Wiederhold, J.E., 2011. The Debra L. Friedkin Site, Texas and the origins of Clovis. Science 331, 1599-1603.

Waters, M.R., Nordt, L.C., 1995. Late Quaternary floodplain history of the Brazos River in East-Central Texas. Quaternary Research 43, 311-319. http://dx.doi.org/10.1006/qres.1995.1037.

Weight, R.W.R., Anderson, J.B., Fernandez, R., 2011. Rapid mud accumulation on the central Texas shelf linked to climate change and sea-level rise. Jousrnal of Sedimentary Research 81, 743-764. http://dx.doi.org/10.2110/jsr.2011.57.

Williams, C., Flower, B.P., Hastings, D.W., Guilderson, T.P., Quinn, K., Goddard, E.A., 2010. Deglacial abrupt climate change in the Atlantic Warm Pool: a Gulf of Mexico perspective. Paleoceanography 115, PA4221. http://dx.doi.org/10.1029/2010PA001928.

Williams, C., Flower, B.P., Hastings, D.W., 2012. Seasonal Laurentide ice sheet melting during the "Mystery Interval" (17.5e14.5 ka). Geology 40, 955-958. http://dx.doi.org/10.1130/G33279.1.

Wintle, A.G., Murray, A.S., 2006. A review of quartz optically stimulated lumines- cence characteristics and their relevance in single-aliquot regeneration dating protocols. Radiation Measurements 41, 369-391.

Wood, J.R., Forman, S.L., Everton, D., Pierson, J., Gomez, J., 2010. Lacustrine sediments in Porter Cave, Central Indiana, USA and possible relation to Laurentide ice sheet marginal positions in the middle and late Wisconsinan. Palaeogeography, Palaeoclimatology, Palaeoecology 298 (3-4), 421-431.

Wright, V.P., 1984. The significance of needle-fibre calcite in a Lower Carboniferous paleosol. Geol. J. 19, 23–32.

Wright, V.P., 1990. Estimating rates of calcrete formation and sediment accretion in ancient alluvial deposits. Geological Magazine 127, 273-276.

Wright, D.K., Forman, S.L., Waters, M.R., Ravesloot, J.C., 2011. Holocene eolian activation as a proxy for broad-scale landscape change on the Gila River Indian Community, Arizona. Quaternary Research 76 (1), 10-21. http://dx.doi.org/10.1016/j.yqres.2011.04.008.

Zhou, J., Chafetz, H.S., 2010. Pedogenic carbonates in Texas: stable-isotope distributions and their implications for reconstructing region-wide paleoenvironments. J. Sediment. Res. 80, 136–150.